M-Pos63 SOLUTION STRUCTURES OF CALMODULIN AND TROPONIN C STUDIED BY SMALL-ANGLE X-RAY SCATTERING AND CIRCULAR DICHROISM. Douglas B. Heidorn, Stephen P. Edmonson and Jill Trewhella, Life Sciences Division, Los Alamos National Laboratory, Los Alamos, New Mexico 87545.

Small-angle x-ray scattering (SAXS) data have been measured for the calcium regulating proteins calmodulin and troponin C in solution at physiological pH and ionic strength. Modelling studies based on the crystal structure coordinates show discrepencies between the SAXS data and the crystal structure. The experimental radius of gyration and maximum linear dimension for both troponin C and calmodulin are smaller than the values calculated from the crystal structures. Also, the experimental vector distribution (P(r)) functions of both proteins do not agree well with the P(r) functions calculated for models of the corresponding crystal structures.

Models have been developed that give good agreement with the solution scattering data. In each case the best model was derived from the crystal structures by placing a bend in the interconnecting helix region between the two calcium binding domains. The result of this rearrangement of the crystal structures was to bring the calcium binding domains closer together. Their centers of mass were closer by approximately 5 Å, while the distances of closest approach were smaller by approximately 10 Å.

Circular dichroism data have been measured for calmodulin in several solution conditions. It was found that adding calcium, lowering the pH and increasing the ionic strength each results in an increase in alpha-helix content, though to differing degrees. These factors may be important in stabilizing the crystal form. (This work is supported by DOE/OHER project # HA-02-02-03/B04664)

M-Pos64 PROTEIN CONFORMATIONAL DISTRIBUTIONS EXAMINED BY MULTIPLE TEMPERATURE STUDIES OF THE TIME DEPENDENT FLUORESCENCE OF SINGLE TRYPTOPHAN CONTAINING PROTEINS. Norberto Silva, Brett Feddersen, Martin vandeVen, Joseph Beechem, Enrico Gratton. Laboratory for Fluorescence Dynamics, Department of Physics, University of Illinois at Urbana-Champaign, Urbana, IL 61801.

Fluorescence decay of tryptophan in proteins have been described using discrete sets of lifetimes and/or distributions of lifetimes. Yet, besides being able to fit data, such analysis of any single experiment can provide little insight to the fluorescent system examined. In single tryptophan containing proteins, one possible explanation for the kinetically complex emission, is that the fluorescence lifetime of tryptophan is sensitive to various "micro-conformations" that the protein experiences during the excited state. To explore this possibility, experiments have been performed on single tryptophan containing proteins as a function of temperature. Such data can yield information concerning the energy barriers that the tryptophan (and hence protein) experiences during the picosecond to nanosecond time scales. The actual physical modeling of these multi-temperature studies is very difficult, and previously, a two-state excited state model with energy barriers between the two states has been used to fit the data. To obtain good fits to the data, a distribution of energy barriers was needed. We interpret the distribution of energy barriers to be a result of interconversion between multiple protein conformations during the lifetime of the excited state. A single distribution of energy barriers was sufficient for the global analysis of all the multi-temperature studies. Error analysis on the recovered energy barriers is performed. Various indole model systems are also examined as a function of temperature to assist in the modeling of the multi-temperature protein studies. Supported by NSF Minority Fellowship and NIH RR03155.

M-Pos65 TERTIARY STRUCTURE OF THE *E. COLI* HEAT-STABLE ENTEROTOXIN. Jean Gariepy[1], Armit K. Judd[2], and G.K. Schoolnik[3]. [1]Department of Medical Biophysics, University of Toronto, [2]SRI International and [3]Department of Medical Microbiology, Stanford University, California.

The *E. coli* heat-stable enterotoxin is a major cause of worldwide cases of diarrhea in humans and domestic animals. This toxin and the atrial natriuretic factors are the only peptides proven to activate membrane-bound guanylate cyclases. We (Gariepy & Schoolnik (1986) P.N.A.S. 83, 483) and others (Yoshimura *et al.* (1985) FEBS Lett. 181, 138) have mapped the receptor-binding domain and the enterotoxic property of ST I to 13 amino acids having the sequence;

```
6  7          10 11             15        18
Cys-Cys-Leu-Glu-Cys-Cys-Asn-Pro-Ala-Cys-Thr-Gly-Cys
```

This sequence includes six cysteines involved in three intramolecular bridges. Recently, our group has proposed a model for the folding of the peptide backbone in solution using results from NMR constraints and a proposed set of disulfide bridges (Gariepy *et al.* (1986) Biochemistry 25, 7854). We have now identified the correct pairing pattern for the three intramolecular disulfide bridges by chemically synthesizing fifteen analogues of this sequence, replacing all possible pairs of cysteine residues by alanines. Only two analogues cause diarrhea when given orally to infant mice and displace a radiolabeled analogue of ST I in our radiobinding assay. We concluded that at least two disulfide pairs were needed for both activities and that the pairing pattern was as follows; Cys-7 to Cys-15, Cys-6 to Cys-11 and Cys-10 to Cys-18 with the first disulfide pair listed being essential for activity. A recalculated structure based on the new disulfide pattern and the NMR constraints database will be presented. (Supported in part by MRC of Canada grant MA-9724).

M-Pos66 THE CONFORMATION OF THE INTERCHAIN DISULFIDE OF HUMAN IgG3/IgG4 IMMUNOGLOBULINS

Mark E. Snow and L. Mario Amzel, The Laboratory for Molecular Structure and Function, Department of Biophysics, The Johns Hopkins University School of Medicine, Baltimore, MD 21205 USA. BITNET address Mario@JHUIGF.

In most classes of immunoglobulins, the light and heavy chains are covalently linked by an interchain disulfide bridge. While this interchain disulfide always involves a cysteine at the C-terminus of the L chain, the residue from the H chain varies, depending on the immunoglobulin class. All Fab structures which have been determined crystallographically use the same residue from the H-chain, a cysteine at the C-terminal end of the C_H1. In most other immunoglobulin classes, however, the cysteine from the H-chain lies in a bend which, although distant in sequence, is spatially close to the C-terminal sequences of both C_H1 and C_L. In this paper, an exploration is made of the accessible conformations for the alternate disulfide arrangement. The study is based on the crystallographically determined structure of the human immunoglobulin fragment Fab New, the sequence of a human IgG4 and modeling procedures and energy equations which have previously been tested on immunoglobins (Snow and Amzel, 1986. Proteins 1, 267-279). By building the cysteines with different initial values of χ_1, and using different refinement schemes, twenty-two possible structures for the region were obtained. The observed conformations for the disulfide bridge in these structures fall into five distinct groups. The conformations that had the lowest energies were similar to those found only in the intrachain disulfide of immunoglobulins.

M-Pos67 VIBRATIONAL ANALYSIS OF PARALLEL- AND ANTIPARALLEL-CHAIN TRI-L-ALANINE.

Q. Weili, J. Bandekar, and S. Krimm,
Biophysics Research Division, University of Michigan, Ann Arbor, MI 48109

Tri-L-alanine,an inhibitor of elastase (1), is known to crystallize in an antiparallel-chain (AP) β structure (2). We have discovered a second crystal form, which is found to be a parallel-chain (P) structure (3). Using our vibrational force fields (4) and ab initio dipole derivatives (5), we have done complete normal mode analyses of these two structures and compared the predicted frequencies with observed infrared and Raman bands. The agreement for the amide modes is good. For example, the calculated [and observed] amide I and II frequencies (and infrared intensities) are as follows. AP: I - 1686(7.9)[1691ir,M], 1682(0.25), 1666(3.2)[1666ir,sh], 1665(0.4), 1656(0.1) [1658R,S], 1645(0.7), {1645(10.7), 1643(14.3)}[1640ir,VS]; II - 1571(1.5), 1567(1.4), 1566(0.2), 1557(7.5)[1550ir,MS], 1557(0.0)[1551R,W], 1533(0.3)[1536R,W], {1531(1.3), 1531(15.4)}[1532ir,S]. P: I - 1683(7.8)[1687ir,W], 1673(0.2), 1664(8.3)[1668ir,MW], 1663(0.2)[1662R,S], {1655(6.3), 1654(13.1)}[1649ir,VS], {[1651(0.5), 1651(0.0)}[1648R,sh]; II - 1567(0.3)[1568R,W], 1560(2.0) [1568ir,sh], 1561(0.9), 1549(2.5)[1550ir,sh], 1536(17.9)[1526ir,S], 1529(0.5), 1529(1.4), 1519(0.2) [1522R,W]. Comparably good agreement is obtained for the amide III and V modes. This research was supported by NSF grants DMB-8517812 and DMR-8303610.

1. D.M. Shotton, N.J. White, and H.C. Watson, Cold Spring Harbor Symp. Quant. Biol. 36, 91 (1971).
2. J.K. Fawcett, N. Camerman, and A. Camerman, Acta Cryst. B31, 658 (1975).
3. A. Hempel, N. Camerman, and A. Camerman, in preparation.
4. S. Krimm and J. Bandekar, Adv. Protein Chem. 38, 181 (1986).
5. T.C. Cheam and S. Krimm, J. Chem. Phys. 82, 1631 (1985).

M-Pos68 ANTIBODY Fab CONFIGURATION IS INFLUENCED BY pH AND BY INTER-HEAVY CHAIN DISULFIDE REDUCTION.

E. E. Uzgiris, Corporate Research & Development, General Electric, P.O. Box 8, Schenectady, NY 12301, and N. Mroczka and J. Newman, Physics Department, Union College, Schenectady, NY 12308.

Monoclonal antibodies crystallize in two dimensions in several different forms (Nature 301, 134 (1983); J. Cellular Biochem. 29, 239 (1985); Biochem. J. 242, 293 (1987)). One form, leading to highly ordered 2-D crystals, has a large unit cell (26 nm x 26 nm) with the antibodies in an extended T form, 120° between Fab arms. Another form, with a very much more compact lattice (5.5 nm x 5.5 nm unit cell), can be induced by dropping the pH below pH 7 or by the addition of a mild reductant (2 mM DTT). This compact form has been observed for mouse monoclonal IgE, IgG1, IgG2, and for rabbit anti-DNP and anti-FITC IgG. The compact lattice requires that the Fab arms be in a closed Y configuration with a 60° angle between the Fab arms. It thus appears that the Fab arm extension may be controlled in part by pH and by the oxidation/reduction of the hinge disulfides. We have endeavored to corroborate this effect for antibodies in free solution by dynamic light scattering measurements. For mouse IgG1 we find a decrease of hydrodynamic diameter from 10.9 nm to 10.3 nm at pH 7.4 upon the addition of 2 mM DTT. For rabbit anti-FITC the shift was from 10.8 nm to 10.35 nm. A pH trend was also observed for the rabbit antibody: 10.85 nm and 10.45 nm for pH 8 and pH 6.5, respectively. These measurements, taken together with the observations on 2-D crystal forms, support the view that the configuration of the Fab arms may swing in and out from an open to a closed configuration as a function of pH and inter-heavy chain disulfide linkage. Furthermore, we may compare these results with rotational relaxation measurements (V.T. Oi et al., Nature 307, 136 (1984)). The present work suggests that static conformational changes as well as flexibility may contribute to rotational relaxation of the antibody for different solution conditions.

M-Pos69 AGGREGATION OF INTERMEDIATES IN THE FOLDING OF BOVINE GROWTH HORMONE

David N. Brems (The Upjohn Company, Kalamazoo, MI 49001)

Recovery of active bovine growth hormone from transformed E. coli requires an in-vitro folding step. Precipitation of the protein during folding results in poor yields. We have studied this process and have found that the self-association of folding intermediates is the major cause of precipitation. If in-vitro folding occurs in conditions that solubilize the associated folding intermediate, then native protein is quantitatively obtained. However, if folding occurs in conditions that do not solubilize the associated intermediate, then most of the product results in an insoluble protein aggregate. Specific sites of interaction that lead to association have been identified. One of these interactive sites has been modified by oligonucleotide-directed mutagenesis. The result of this modification on the folding and aggregation of bovine growth hormone will be described.

M-Pos70 ESTIMATION OF PROTEIN CONFORMATION BY RESOLUTION-ENHANCED RAMAN SPECTROSCOPY.

D. Michael Byler and Heino Susi, US Department of Agriculture, Agricultural Research Service, Eastern Regional Research Center, 600 East Mermaid Lane, Philadelphia, PA 19118

The amide I (C=O stretching) Raman band of nine proteins found in bovine milk was Fourier deconvolved. This typically resolved the weak, broad band into several components. The overall shape of the original amide I band was found empirically to be nearly Gaussian or to be composed of Gaussian components. A Gaussian function was therefore used for deconvolution. Computer program #LI (National Research Council of Canada) was employed. More detailed results were obtained than with the Lorentzian approximation usually employed. The resolved band components were assigned to specific conformations such as the alpha-helix, beta-structure, reverse turns, and unordered segments. Characteristic frequencies were established for each type of sub-structure. The frequencies and assignments were in good agreement with results obtained by Berjot, Marx, and Alix [J. Raman Spectrosc., 1987, 18, 289] using a completely independent mathematical procedure. The areas of component bands were determined by the iterative curve-fitting program ABACUS written at this Research Center. The best fits of the resolved components to the deconvolved spectra were obtained when Gaussian contours were assumed. The relative component areas appear to reflect the fraction of any given substructure in a protein. Some structural information was obtained even on proteins, such as casein, which are usually classified as having undefined or aperiodic secondary structure. For crystalline proteins semi-quantitative estimates of conformational characteristics were in good agreement with information obtained through X-ray diffraction and deconvolved infrared spectra [D. M. Byler and H. Susi, Biopolymers, 1986, 25, 469].

M-Pos71 MAMMALIAN MYOGLOBINS HAVE VARIABLE HYDROPHOBIC STABILIZATION INTERACTIONS.

Leslie A. Holladay and Lenore Kelly, Dept. of Chemistry, Louisiana Tech University, Ruston, LA 71272. The temperature dependence of the equilibrium unfolding constant calculated from Soret absorbance data at pH 8 was examined for sperm whale, horse, rat, rabbit, opossum, and raccoon metmyoglobins in varying guanidinium chloride concentrations. At each denaturant concentration, van't Hoff data were analyzed by least squares fitting to estimate the equilibrium constant at 298 K, the change in heat capacity on unfolding (ΔC_p), and T_H, the temperature at which the unfolding enthalpy becomes zero. The value obtained for T_H for sperm whale metmyoglobin in 2.1-2.5 M denaturant (295.8±.4 K) is indistinguishable from that previously obtained (293.6±4.1 K) by calorimetry (Privalov et al., J. Mol. Biol. 190, 487 (1986)) in the absence of denaturant. For all metmyoglobins, the estimates for T_H were not dependent on denaturant concentration. Rat, rabbit, and raccoon metmyoglobins, previously shown to be more stable than sperm whale myoglobin (Kelly et al., Int. J. Pept. Prot, Res., in press), are characterized by T_H values near 298 K. Horse metmyoglobin has a T_H value close to sperm whale metmyoglobin, while the T_H value for opossum metmyoglobin is significantly lower at 293.9±.2 K. Analysis of model compound data (Gill and Wadso, P.N.A.S. 73, 2955 (1976)) suggest that each additional buried nonpolar hydrogen atom should increase ΔC_p by 8 cal/(mol K). Current data for compact globular proteins suggest for each 30 cal/(mol K) increase in ΔC_p that T_H for myoglobins should increase by 1 K. Thus, the burial of a few additional nonpolar hydrogen atoms would result in a significant increase in T_H. The hydrophobic model for protein folding (Baldwin, P.N.A.S. 83, 8069 (1986)) suggests that part of the variation in the stability of these myoglobins results from changes in the saturation of nonpolar contacts.

M-Pos72 FLUORESCENCE STUDIES OF SUBUNIT INTERACTIONS OF ENZYME I OF THE PTS.
Myun K. Han, The Biology Department, The Johns Hopkins University, Baltimore, MD 21218

Enzyme I of the bacterial phosphoenol pyruvate:glycose phosphotransferase system (PTS) exhibits a temperature-dependent monomer/dimer equilibrium. The enzyme contains 4 -SH groups/subunit. Rate measurements indicate that one of the -SH groups (fast) reacts ten times more rapidly with -SH specific reagents such as DTNB than the other three -SH groups (slow). Evidence will be presented that derivatization of only the "fast" -SH residue with probes such as pyrene maleimide results in an active enzyme capable of forming dimers at room temperature. Derivatization of the "slow" -SH groups results in an inactive enzyme that does not form dimers. The "fast" and "slow" -SH residues can be distinguished by unique fluorescence characteristics of pyrene bound to each type of residue. Direct evidence for the unique character of the "fast" -SH residue was also obtained by derivatization of only this group followed by HPLC peptide mapping. The kinetics of dimer formation of Enzyme I was measured in the following way: a derivatized Enzyme I sample was prepared with a pyrene moiety irreversibly attached to the "fast" -SH residue and DTNB reversibly attached to the "slow" -SH residues. This modified enzyme does not form dimers at room temperature. Addition of dithiothreitol results in total release of TNB anion within two minutes. Steady-state or nanosecond time-resolved emission anisotropy measurements (using the pyrene fluorescence) indicates that release of the TNB from the "slow" -SH residues results in dimer formation over a time period of 30 minutes. In a similar experiment, dimer formation is not observed at 3°C, a temperature at which the native enzyme also does not form dimers. These results suggest that dimer formation may be preceded by a conformational change following TNB release. The influence of solvent environment on dimerization will be discussed. Supported by NIH grant GM11632.

M-Pos73 SOLUTION CONFORMATIONS OF SYNTHETIC PEPTIDES CORRESPONDING TO THE LIGAND-BINDING SITE OF THE NICOTINIC ACETYLCHOLINE RECEPTOR (AChR) AND THE MODE OF PEPTIDE BINDING TO α-BUNGAROTOXIN (BGTX) AS REVEALED BY CD, FLUORESCENCE, AND NMR. Qing-luo Shi, K.L. Colson, T.L. Lentz*, I.M. Armitage+, and E. Hawrot. Depts. of Pharmacology, *Cell Biology, and +Molecular Biophysics and Biochemistry, Yale Univ. Sch. of Med., New Haven, CT 06510

The synthetic 12mer and 18mer peptides corresponding to residues 185-196 and 179-196 of the α-subunit of AChR from *Torpedo* bind BGTX with micromolar affinity. In an effort to describe the molecular interaction of BGTX with residues in the binding site of the AChR, several physico-chemical methods were employed to study the solution conformations of the peptides and the peptide-BGTX complex. For the 12mer in saline phosphate buffer at pH7, the CD profile in the far UV indicates a small amount of ordered structure, in agreement with the differential exchange of some peptide amide protons as detected by NMR. Methanolic and SDS solutions, in contrast, appear to stabilize β structure in the 12mer as indicated by the CD spectra in the near and far UV.

CD studies in the near UV and measurement of intrinsic fluorescence changes upon binding of the 12mer to BGTX reveal conformational changes involving aromatic residues, as well as a change in the environment of the disulfides in BGTX. In the far UV, CD studies indicate a distinct increase of β-structure content upon binding, presumably due to an increase in the ordered structure of the peptide. Fluorescence spectroscopy demonstrates that a tryptophan residue is involved in binding. The specific residue responsible for enhanced fluorescence was identified by NMR as Trp-28 of BGTX. NMR studies reveal that among other detectable shifts, the histidine residues in both the 12mer (His-186) and the toxin (His-4 and His-68) are affected by binding. Similar studies on the 18mer confirm the involvement of these histidine residues. We have observed several NMR peaks (C-2) corresponding to the bound state of His-186 in the 18mer, suggesting that this residue may serve as a sensitive probe of structural changes in the complex. Supported by the MDA, the AHA, NIH grants GM32629, NS21896, DK18778 and instrumentation grants from NIH and NSF (RR03475 & DMB-8610557)

M-Pos74 THE ORIENTATION OF MEMBRANE BOUND, SPIN-LABELED MELITTIN AS DETERMINED BY EPR SATURATION RECOVERY MEASUREMENTS. Christian Altenbach[1], Wojciech Froncisz[2,3], Wayne Hubbell[1], and James Hyde[2]. [1]Jules Stein Eye Institute and Department of Chemistry & Biochemistry, University of California, Los Angeles, CA 90024; [2]National Biomedical ESR Center, Department of Radiology, Medical College of Wisconsin, Milwaukee, WI 53226; [3]Department of Biophysics, Institute of Molecular Biology, Jagiellonian University, 31-120 Krakow, Poland.

Four different spin-labeled derivatives of the bee venom protein melittin have been prepared previously. Each of these derivatives covers a key part of the protein: N-terminus, Lys-7, -21, or -23. They behave normally with respect to tetramer formation and membrane binding (Altenbach et al., Biophys. J. 51:458a, 1987). Earlier results suggest that membrane bound melittin is monomeric. To extend these studies we performed EPR saturation recovery T_1 measurements of membrane bound, spin-labeled melittin in the presence of increasing amounts of chromium oxalate (Crox). Crox is a paramagnetic anion that reduces the T_1 of a spin label by direct collision with the spin-label but cannot penetrate the hydrophobic part of the membrane. From $d(1/T_1)/d[Crox]$ for Crox concentrations between 0 and 1 mM, it is therefore possible to directly determine the exposure of a spin-labeled site to the aqueous phase. Model compounds were used to calibrate the resolution of the method. The value of $d(1/T_1)/d[Crox]$ is largest for a spin-label free in solution; it drops by a factor of ≈6 at the membrane surface and is zero for spin-labeled androstane where the nitroxide group is buried ≈12 A in the hydrophobic part of the membrane. Monomeric melittin in solution has all labeled sites about equally accessible, but in membrane bound melittin they are clearly distinguishable. Lys-7 is most accessible, Lys-21 is intermediate and Lys-23 is more buried. The N-terminus shows two different populations: one similar to Lys-21 and one slightly more buried than Lys-23. A model for the conformation of membrane bound mellitin that is consistent with the data will be presented.

M-Pos75 INTEGRATION OF THE FOLDING TRANSITIONS OF RIBONUCLEASE. William Shalongo, M.V. Jaganadham, Christopher Flynn and Earle Stellwagen, Department of Biochemistry, University of Iowa, Iowa City, Iowa 52242.

We have utilized molecular sieve HPLC measurements to integrate the individual refolding reactions of guanidine hydrochloride (Gu) denatured bovine ribonuclease observed at pH 6.0 and 4°. Elution profiles were fit to a given mechanism using as many experimentally determined parameters as possible. All equilibrium and kinetic chromatographic measurements obtained using single and multimixing protocols can be fit to the illustrated minimal mechanism in which N represents the native protein, I a compact intermediate, U a denatured protein, F a fast folding form and S a slow folding form. The conformational transitions, N/IF, IF/UF, and IS/US have midpoints at 3.2, 3.5 and 1.8 M Gu, respectively. The configurational isomerizations UF/US and UF'/US' each have a concentration ratio of 20%/80%, UF/UF' and US/US' a ratio of 60%/40% and IF/IS a ratio of 99%/1%. US and UF' likely each contain a single but different nonnative proline peptide isomer while US' contains both nonnative proline peptide isomers. IS is a folded form containing a single nonnative isomer. Supported by PHS research grant GM22109.

N = IF = UF = UF'
‖ ‖ ‖
IS = US = US'

M-Pos76 DIFFERENTIAL SCANNING CALORIMETRY OF PROTEIN UNFOLDING ON SOLID SUPPORTS
Mark Sabat and John Shriver (Intro. by Michael Woodruff). Department of Chemistry and Biochemistry, Southern Illinois University, Carbondale, Illinois 62901.

Most informative studies of protein unfolding by differential scanning calorimetry have been of globular proteins which unfold reversibly in solution. As both the interest in DSC and the availability of excellent instruments increases, work has naturally been extended to more complicated proteins which quite often unfold irreversibly. Various strategies for treating irreversible systems as reversible have been proposed. These are primarily based on the assumption that the irreversibility is due to slow aggregation of the unfolded species. Irreversibility due to aggregation can be prevented by attachment of the protein to a solid support (Epstein and Anfinsen, J. Biol. Chem. 237, 2175 (1962)). We have begun a study of the feasibility of performing DSC studies of proteins attached to crosslinked agarose. Initial studies have been performed on ribonuclease A, a model protein which unfolds reversibly. Attachment is accomplished by reaction of protein primary amino groups with an N-hydroxysuccinimide ester derivative of agarose with a 10-atom spacer arm (Affi-Gel 10, Bio-Rad). Attachment via any of the ten lysine epsilon amino groups leads to a broad endotherm in the DSC scan, most likely due to heterogeneity in orientation of the protein on the gel. The unfolding is highly reversible with a T_m near to that observed for ribonuclease A in solution. We are attempting to reduce the heterogeneity by attachment via the N-terminus only, after specifically blocking the lysine epsilon amino groups with O-methylisourea. (Supported by NIH AR37174).

M-Pos77 POLYPEPTIDE FOLDING AND DIMERIZATION IN BACTERIAL LUCIFERASE. Jenny J. Waddle, Jun Sugihara, and Thomas O. Baldwin. Dept. of Biochemistry & Biophysics, Texas A&M Univ., College Station, TX 77843.

Bacterial luciferase is a heterodimeric bioluminescent enzyme comprised of two nonidentical but homologous subunits, α and β, which are inactive and do not self-associate. Therefore, it is possible to study the folding of individual subunits in the absence of association. *Vibrio harveyi* adjacent genes *luxA* and *luxB*, encoding α and β, were separated and expressed from separate plasmids in *Escherichia coli*. Cells carrying both plasmids accumulated active dimeric luciferase at levels similar to cells containing the intact *luxAB* genes. Cells carrying the individual plasmids accumulated large amounts of individual subunits. Mixing of a lysate of cells carrying the *luxA* gene with a lysate of cells carrying the *luxB* gene resulted in formation of very low levels of active heterodimeric luciferase. However, denaturation of the mixed lysates with urea followed by renaturation resulted in formation of large amounts of active luciferase. α and β, if allowed to fold independently *in vivo*, fold into structures that do not interact to form active heterodimeric luciferase. The complex formed between the two subunits must be an intermediate structure on the pathway to formation of active heterodimeric luciferase. To determine the role of the β subunit in the folding and stability of active heterodimeric luciferase, luciferases with normal α subunits and variant β subunits having deleted or changed amino acid residues in the 3' coding region were produced in *E. coli* cells carrying the recombinant plasmids. Deletion of amino acid residues from this region greatly reduced levels of accumulation of active luciferase, especially at higher temperatures, although the active luciferase that formed from the truncated β subunit had essentially normal activity and stability, but both impaired and temperature-sensitive refolding from urea *in vitro*. We conclude that the carboxyl terminal *ca.* 10-15 residues of the β subunit have little to do with the bioluminescence reaction or stability of the dimeric structure *per se*, but the region appears to have a critical function in the proper folding and/or assembly into the active heterodimeric structure.

M-Pos78 PREDICTIONS OF MEMBRANE PROTEIN SECONDARY STRUCTURES BASED ON BURIED RESIDUES IN GLOBULAR PROTEINS. D. L. Mielke[1,2], and B. A. Wallace[1], [1]Department of Chemistry and Center for Biophysics, Rensselaer Polytechnic Institute, Troy, New York 12180, [2]Department of Biochemistry, Columbia University, New York, New York 10032.

Empirical methods for predicting protein secondary structures from sequence information have been developed for soluble proteins, but these methods produce unsatisfactory results when applied to membrane-embedded proteins (Wallace et al., 1986, PNAS, 83, 9423-9427). Because the backbones of soluble proteins can hydrogen-bond with surrounding solvent, proteins fold differently in this environment than in a membrane environment where such interactions are not possible. As a result, a new basis for such predictions is needed. Ideally, this would be derived from membrane proteins with known structures, but there is presently a dearth of such information. An alternative is to derive such a data base from "buried" residues in soluble proteins, which also cannot hydrogen-bond with solvent.

We have compiled a data base from stretches of residues in which the backbone is buried in 51 large globular proteins found in the Brookhaven Protein Data Bank. The secondary structure for each of approximately 4000 buried residues was noted from the crystal structure. For each amino acid type, the conformational probabilities were found to differ from those in solvent-exposed residues. The relative helix-forming/breaking order differs dramatically for some amino acids, and five amino acids convert between beta-forming and breaking and six amino acids convert between helix-forming and breaking. The parameters calculated in this study may more closely reflect the condition confronting proteins embedded in a membrane, and should be useful in developing a data base for predictions of membrane protein structures. (Supported by NIH Grant GM27292).

M-Pos79 CONTRIBUTION OF AROMATIC SIDE-CHAINS TO THE CIRCULAR DICHROISM OF BOVINE PANCREATIC TRYPSIN INHIBITOR: A THEORETICAL STUDY. Mark C. Manning and Robert W. Woody, Department of Biochemistry, Colorado State University, Fort Collins, Colorado 80523

Bovine pancreatic trypsin inhibitor (BPTI) is a small globular protein containing four tyrosines, four phenylalanines, and three disulfide bridges. It provides an ideal test case for the study of tyrosine and phenylalanine side-chain contributions to the CD spectrum in the absence of tryptophan and histidine. Employing the matrix formulation, the model includes four transitions of each peptide chromophore ($n\pi^*$, $\pi_O\pi^*$, $n'\pi^*$, and $\pi_+\pi^*$) and four transitions on each aromatic side-chain (L_b, L_a, B_b, and B_a). Excited-state data were obtained from CNDO/S calculations on the model compounds, N-methylacetamide, p-cresol, and toluene. Calculated CD spectra for BPTI structures obtained from X-ray diffraction indicate that Tyr-23 and Tyr-21 account for most of the rotational strength of the 275 nm band, while neither Tyr-10 nor Tyr-35 contribute significantly. None of the four Phe groups possess significant rotational strengths in the near-UV CD spectrum. However, both tyrosine and phenylalanine chromophores contribute strongly to the far-UV CD spectrum. The strong negative band near 205 nm arises primarily from the L_a excited state of phenylalanine and from amide $\pi\pi^*$ transitions. In addition, the intense B_a and B_b transitions (~ 185-190 nm) of both phenylalanine and tyrosine have large rotational strengths. Rotation of tyrosine side-chains about χ_2 results in changes both in the near-UV and far-UV regions. This model suggests that both coupled-oscillator and "one-electron" contributions to the rotational strength are important for aromatic side-chains in proteins. Inclusion of both tyrosine and phenylalanine side-chains are necessary to obtain adequate agreement with experimantal data on BPTI. This work was supported by USPHS Grant GM-22994 and a grant of free computer time from the Colorado State University Computer Center).

M-Pos80 THE CIRCULAR DICHROISM OF TWO-CHAIN, COILED COILS IN THE TYROSINE/DISULFIDE SPECTRAL REGION. Marilyn Emerson Holtzer, Swatantar Kumar, and Alfred Holtzer, Department of Chemistry, Washington University, St. Louis, MO 63130.

Tropomyosin (Tm) in the coiled coil state not only shows a strong α-helical backbone CD spectrum in the region < 260 nm, but also shows bands near ~ 280 nm, where tyrosine and disulfide CD spectra lie. These higher-lying bands also have conformational significance, since they disappear on denaturation. Reduced αα Tm has no disulfide and at low temperature (~ 3°C) shows in this region only a single band of intensity ~ -23 deg·cm^2/mmol-of-tyrosine at ~ 280 nm with $\Delta^\circ \cong 12$ nm. The spectrum is the sum over six tyrosines/chain. Crosslinking at C190 yields in addition a positive maximum (23 deg·cm^2/mmol-of-disulfide) at ~ 300 nm and a slightly reduced negative band (-20 deg·cm^2/mmol-of-tyrosine). Subtracting the spectrum of the noncrosslinked species from that of the crosslinked one shows that the disulfide spectrum itself actually comprises two unresolved positive bands, each of intensity ~ 40-45 deg·cm^2/mmol-of-disulfide at, respectively, 250 and 280 nm. The existence of a chiral disulfide probably results from strains caused by the relatively rigid local α-helix. Experiments on N-terminal segments, $_8$Tm$_{125}$ or $_{11}$Tm$_{127}$, each with only one tyrosine (Y60) per chain reveal that not all tyrosines are alike. The spectra at low temperature show a small negative maximum at ~ 285 nm and a large positive one at ~ 270 nm. Heating (56°C) leaves only the negative band, now maximal at 280 nm. Reduced segments $_{142}$Tm$_{281}$ and $_{168}$Tm$_{284}$ do not show this extra positive band. Their negative bands have intensity -30 deg·cm^2/mmol-of-tyrosine, slightly larger than Tm, suggesting that Y60 in Tm also possesses this unusual positive feature. Crosslinked $_{142}$Tm$_{281}$ shows a chiral disulfide band similar to tropomyosin's while $_{168}$Tm$_{284}$ shows none.

M-Pos81 HELIX-COIL TRANSITION IN TWO-CHAIN, COILED COILS. A BACKBONE CD STUDY OF EQUILIBRIUM THERMAL UNFOLDING OF ISOLATED SEGMENTS OF THE TROPOMYOSIN MOLECULE. Swatantar Kumar, Marilyn Emerson Holtzer, and Alfred Holtzer, Department of Chemistry, Washington University, St. Louis, MO 63130.

The thermal unfolding of various isolated molecular segments of αα tropomyosin (Tm) has been measured by backbone CD. Data on two N-terminal-region segments, $_{11}Tm_{127}$ and $_{8}Tm_{125}$, and two C-terminal-region segments $_{142}Tm_{281}$ and $_{168}Tm_{284}$ were obtained in $NaCl_{500}NaPi_{50}(7.4)$ solvent. At low temperature (~ 3°C), all samples are > 90% helix, as is the parent Tm. All thermal unfolding curves are essentially reversible. Each N-terminal-region segment shows an apparently monophasic, cooperative transition with a melting temperature and concentration dependence appreciably greater than that for Tm. The C-terminal segments possess one cysteine per chain, allowing study on both a non- and C190-crosslinked species. Noncrosslinked $_{142}Tm_{281}$ and $_{168}Tm_{284}$ show very similar unfolding properties and substantial concentration dependence. The melting temperatures are appreciably lower than the parent Tm. The unfolding curves of the crosslinked segments, are different. Crosslinked parent Tm shows a biphasic curve with a smaller "pretransition" at lower T and a larger (70%) "posttransition" at higher T. Segment $_{142}Tm_{281}$ behaves as the parent Tm. In contrast, segment $_{168}Tm_{284}$ shows only a posttransition. Viewed naively, this would imply that the insertion of a crosslink at C190 in the coiled coil parent Tm has two effects: 1) it strengthens a formerly weak (168-284) part of the molecule, making it stronger than even the strong (8-127) part was formerly; and 2) it weakens a formerly strong, relatively remote portion (< 168), making it as weak as the weak (168-284) region was formerly. These results are difficult to rationalize using either the statistical-mechanical helix-coil theory or any other physical ideas so far proposed.

M-Pos82 AN INFLUENCE OF TERTIARY STRUCTURE ON PROTEIN INFRARED SPECTRA. John F. Hunt, Department of Molecular Biophysics and Biochemistry, Yale University.

The influence of tertiary structure on the infrared spectra of proteins has been analyzed using a transition dipole moment coupling model. Previously, this model has been used in conjunction with Miyazawa's perturbation treatment of vibrational interactions in polypeptides to explain the mode splittings and frequency shifts observed in the infrared spectra associated with particular kinds of protein secondary structure (e.g. the α-helix and the β-sheet). (These studies relied on an analytical diagonalization of the vibrational interaction matrix which limited their application to periodic arrays of localized vibrational modes such as those found in regular protein secondary structures.) In this study, an identical dynamic model is used to calculate the effect of transition dipole coupling between amide I vibrational modes in an array of anti-parallel α-helices. (Extension of the model to non-periodic structures necessitates numerical solution of the vibrational interaction matrix using Jacobi diagonalization.) It is shown that helix-helix interactions can lead to delocalized vibrational modes (i.e. exciton modes) involving individual amide I vibrations throughout the tertiary structure of the molecule. These delocalized modes have substantially different spectral properties from the equivalent modes in a single, isolated α-helix. In particular, given an array of anti-parallel α-helices with an arrangement equivalent to that of a monomer in the projected electron density map of the bacteriorhodopsin (BR) molecule, the calculations predict an increase of approximately $2cm^{-1}$ in the frequency of the amide I absorbtion maximum as well as changes in the polarization of individual components of that composite band. These results may explain the anomalously high amide I frequency previously observed for BR; they may also prove useful in interpreting effects observed in polarized FTIR studies on the folding of BR (see Hunt et al, this volume). Moreover, the results suggest that there may be limitations to the treatment of protein IR spectra as arising from the superposition of signals derived from individual secondary structural elements, especially in proteins containing a regular pattern in the higher-order organization of these elements. Supported by NIH Training Grant 5-T32-GM07223-13.

M-Pos83 AN FTIR STUDY OF INTEGRAL MEMBRANE PROTEIN FOLDING. John F. Hunt, Thomas N. Earnest*, Donald M. Engelman, and Kenneth J. Rothschild*, Department of Molecular Biophysics and Biochemistry, Yale University, and *Department of Physics, Boston University.

The folding of the integral membrane protein bacteriorhodopsin (BR) has been studied using polarized fourier transform infrared spectroscopy (FTIR). BR is isolated from cells in the form of a two-dimensional crystal called purple membrane (PM). Chymotrypsin cleaves BR into two fragments (called C1 and C2) which can be reconstituted separately into phospholipid vesicles. Fusion of independent vesicle populations containing these fragments followed by addition of the retinal cofactor regenerates the native tertiary structure of BR as assayed by the spectrum of its visible chromophore. In the current study, polarized FTIR spectra have been recorded for oriented protein / phospholipid multilayers containing a series of putative intermediates in the assembly of PM: each of the two chymotryptic fragments individually; a non-covalent complex between the two fragments both in the presence and absence of the retinal cofactor; and a number of samples in which the two-dimensional lattice of PM has been regenerated to a varying extent. Two salient conclusions emerge from these spectra: 1.) In both of the isolated fragments, the maximum of the amide I absorbance band occurs at $1657cm^{-1}$, a commonly observed frequency for α-helices. In the non-covalent complexes, the maximum of the amide I band is shifted to a frequency approximately midway between $1657cm^{-1}$ and the anomalously high value of $1661cm^{-1}$ observed in PM. Samples containing varying amounts of two-dimensional lattice exhibit absorbance maxima between those of native PM and the non-covalent complexes. These results suggest that the amide I frequency shift observed in PM may arise from helix - helix interactions. (A transition dipole moment coupling between localized vibrational modes in different α-helices could produce such a frequency shift; see Hunt, this volume.) 2.) There is a shoulder on the amide I band of PM which occurs at approximately $1634cm^{-1}$. This feature is observed to be enhanced in spectra of the C1 fragment and suppressed in spectra of the C2 fragment. These results may reflect the segregation of a structural subdomain of BR into one of the two chymotryptic fragments, although other explanations for this spectroscopic effect have not been excluded.

M-Pos84 CORRELATIONS BETWEEN AMINO ACID SEQUENCE AND PROTEIN SECONDARY STRUCTURE.

A. K. Dunker†, G. A. Arnold†, S. J. Johns†, and R. J. Douthart‡, †Chemistry Department and Biochemistry/Biophysics Program, Washington State University, Pullman, WA 99163-4660 and ‡Life Sciences Center, Battelle Pacific Northwest Laboratory, Richland, WA 99352.

Hydropathy and hydrophobic moment are defined as chemical features of an amino acid sequence. The averaged Chou-Fasman residue structural tendencies, $<P_\alpha>$, $<P_\beta>$ and $<P_t>$, are defined as statistical features. By combining the approach of Chou-Fasman with the sliding window method used by Kyte-Doolittle, we have devised a method for determining the quantitative relationship between any given chemical or statistical feature and protein secondary structure. Rather than grouping amino acids according to residue type, as in the Chou-Fasman approach, in our method we group the amino acids according to the local value of the chemical or statistical feature determined by the surrounding amino acids. We refer to our statistical- or chemical-feature-based relative probabilities as π-alpha, π-beta, π-turn, and π-other for helix, sheet, turn and random, respectively. Here we report the various π-values as functions of the following chemical and statistical features: hydropathy, helical hydrophobic moment, sheet hydrophobic moment, $<P_\alpha>$, $<P_\beta>$ and $<P_t>$. The ranges of the π-structure values are comparable to the ranges of the P-structure values of Chou-Fasman. Graphing the various π-structure values versus the values of the various chemical or statistical features suggests new possibilities for secondary structure prediction algorithms and gives new insight about the effects of chemical and statistical features on protein secondary structure.

M-Pos85 A THEORETICAL STUDY OF TEMPERATURE-DEPENDENT CIRCULAR DICHROISM OF TROPOMYOSIN: BACKBONE AND SIDE-CHAIN CONTRIBUTIONS.

Thomas M. Cooper and Robert W. Woody, Department of Biochemistry, Colorado State University, Ft. Collins, CO 80523.

To interpret the circular dichroism (CD) of tropomyosin, we have performed theoretical modeling of interacting α-helices in coiled coils. We modeled the temperature dependence of the CD of tropomyosin using a Monte Carlo simulation of poly(alanine) with a tyrosine side chain. Strong-coupling exciton theory, with two transitions (amide $n\pi^*$ and $\pi\pi^*$) per peptide residue and four side-chain transitions (L_a, L_b, B_a, B_b) per tyrosine, was used to calculate the CD spectrum. A Monte Carlo simulation of poly(alanine) has been used to calculate the temperature coefficient of backbone and tyrosine CD of a 20-residue helix with one tyrosine side chain. The results can be compared with the experimental temperature dependence of the CD of tropomyosin (A. Holtzer, private communication). The CD temperature coefficient obtained from the Monte Carlo simulation of poly(alanine) with a tyrosine side chain had a backbone and aromatic component. The calculated temperature coefficient for the backbone was found to be 10% that of the experimental value for tropomyosin. The aromatic side chain coefficient was a factor of two larger than the experimental aromatic coefficient. The differences in coefficients imply that tropomyosin undergoes some unwinding to form random coil regions upon warming, while the aromatic side chains reside in a hindered environment. (This work was supported by USPHS Grant GM 22994 and a grant of computer time from The Colorado State University Computer Center.)

M-Pos86 PREDICTING THE SECONDARY STRUCTURE OF GLOBULAR PROTEINS USING NEURAL NETWORK MODELS.

N. Qian and T. J. Sejnowski. Biophysics Department, Johns Hopkins University, Baltimore, MD 21218. USA

We present a new method for predicting the secondary structure of globular proteins based on nonlinear neural network models. The network model learns from existing protein structures how to predict the secondary structure of local sequences of amino acids. We used proteins with known structures as the training set and tested the performance with proteins that had no homologies with those in the training set. The strength of connections between units in the network were derived from the training set using a learning algorithm, and the performance of the network on the testing set was used as an objective measure of the accuracy of the method. The average success rate of our method on the testing set was 64.3% on three types of secondary structure (alpha-helix, beta-sheet, and coil) with correlation coefficients of 0.41, 0.31 and 0.41 for each type respectively. These quality indices are all higher than those of previous methods. The prediction accuracy for the first 25 residues of the N-terminal sequence was significantly better. We concluded from computational experiments on real and artificial structures that no method based solely on local information in the protein sequence is likely to produce significantly better results for non-homologous proteins. The performance of our method on homologous proteins is much better than for non-homologous proteins, but is not at present as good as template matching techniques.

M-Pos87 MONTE CARLO SIMULATIONS OF EQUILIBRIUM GLOBULAR PROTEIN FOLDING OF GREEK KEYS AND α-HELICAL PROTEINS. Jeffrey Skolnick, Andrzej Kolinski, Andrzej Sikorski, and Robert Yaris. Institute of Macromolecular Chemistry, Department of Chemistry, Washington University, St. Louis, MO 63130

Dynamic Monte Carlo Simulations have been performed on lattice models of the six stranded Greek key structure of β-proteins seen for example in the B-domain of pyruvate kinase and of model proteins comprised of a bundle of four α-helices. In all cases the model proteins are allowed to freely hunt through all of phase space, and non native as well as native interactions are allowed. The presence of specific regions along the primary sequence that tend to form bends is found to be a crucial element for the formation of a unique native state. These studies suggest that the bends greatly reduce the allowed regions of phase space which the unfolded protein explores. The gross native topology is subsequently determined by the general pattern of hydrophobic and hydrophilic residues. The resulting "native structure" is then fine tuned by the site specific interactions.

In the case of the six member Greek key, the essential features required for formation of a unique structure are interactions that result in the formation of a very stable "U" shaped core followed by the locking of the configuration by the end β-strand that loops under the bottom of the protein. Extensive data on the thermal transition are presented, and possible modifications of the primary sequence by site directed mutagenesis to test the validity of this class of idealized models are suggested.

Monte Carlo folding studies on a four helix bundle were undertaken. Unlike the Greek key structure, such sequential structures are straightforward to produce. Factors influencing the native structure stability are discussed.

M-Pos88 **TITLE: STRUCTURAL STUDIES OF MODEL TYPE I AND TYPE IV COLLAGENS.**
AUTHORS: Boryeu Mao, Cindy Granatir, Henry H. Shih, and Gabriel Vogeli, Computational Chemistry and Molecular Biology, The Upjohn Company, Kalamazoo, MI 49001.

Collagen, the most abundant protein found in mammals, is a structural protein composed of three polypeptide chains. Each polypeptide chain consists of repeating units of Gly-X-Y tripeptide and is in a local left-handed helical conformation; these three chains form a right-handed supercoiled triple helix. The relationship between the conformation and triple helix stability had been studied extensively theoretically and experimentally. The formation of fibrils from polypeptides of different amino acid compositions had also been studied. In this report, we employed conformational energy calculations to investigate tensile and tangential strengths of model type I and type IV collagen fragments. The implication of the results on these triple helix fragments to mechanical and bio-structural properties of collagen molecules will be discussed.

M-Pos89 THEORETICALLY OPTIMIZED THREE-DIMENSIONAL STRUCTURE FOR BACTERIORHODOPSIN
Haruo Abe*, Richard J. Feldmann, Jia-Lin Syi, Byungkook Lee & Bernard R. Brooks Computer Research and Technology, National Institutes of Health, Bethesda, MD 20892, USA and *Department of Physics, Nishinippon Institute of Technology, Kanda-cho, Fukuoka 800-03, Japan

An important information for a detailed understanding of bacteriorhodopsin's function is the tertiary structure of the protein. Experimental data by electron microscopy are, to date, insufficient to define clearly the tertiary structure. We have developed a model for the three-dimensional structure of bacteriorhodopsin using interactive molecular graphics, energy minimization and molecular dynamics. The modeling procedure is as follows. First, seven segments of the amino acid sequence were selected as being probable transmembrane alpha-helices. Second, the seven helices were positioned according to the locations of the rods of density found by electron microscopy to a resolution of 6.5 A in three dimensions (1) and 3.5 A in projection (2) using the interactive molecular graphics. At the same time, the inside-out regions of helices were determined by a helical wheel analysis using the hydrophobicity of the amino-acid residues (3). Third, after connecting turn regions and terminals, this trial structure was refined using energy minimization and molecular dynamics. Stereoscopic views of this optimized structure are presented and the implications of this structure are discussed.

(1) Leifer, D. & Henderson, R. (1983) J. Mol. Biol., 163, 451-466. (2) Henderson, R., Baldwin, J.M., Downing, K.H., Lepault, J. & Zemlin, F. (1986) Ultramicroscopy, 19, 147-178. (3) Eisenberg, D., Schwarz, E., Komaromy, M. & Wall, R. (1984) J. Mol. Biol., 179, 125-142.

M-Pos90 ELECTROSTATIC INTERACTIONS IN PROTEINS K. Soman, M. Gilson and B. Honig. Department of Biochemistry and Molecular Biophysics, Columbia University, 630 West 168th Street, New York, New York 10032.

Electrostatic interactions are known to play an important role in protein structure and function. In a number of recent studies it has been shown that the Poisson-Boltzmann equation provides a firm basis for treating these interactions. The protein is treated as a low dielectric medium containing real and partial charges whose coordinates are known from x-ray analysis. The solvent is treated as a high dielectric medium which contains a simple electrolyte. Fast computers make it feasible to solve the Poisson-Boltzmann equation numerically and to obtain electrical potentials in and around a protein of arbitrary shape and charge distribution. A program, DELPHI, which calculates electrostatic interactions in proteins has recently been applied to a number of problems where electrostatic interactions appear to play a crucial role. These include the effects of charged amino acids on the pK of the active site histidine in subtilisin, the role of the protein's electrostatic potential in stabilizing the tetrahedral intermediate of trypsin and electrostatic contributions to the binding of Ca++. We have also undertaken a survey of the electrostatic potential around proteins in an attempt to determine whether any general patterns can be identified. Results from these various studies will be presented.
Supported by the NIH (GM-30518) and ONR (n000144-86-K-0483).

M-Pos91 ACTIVATED DYNAMICS OF TRYPTOPHAN-47 IN VARIANT-3 SCORPION NEUROTOXIN. Christopher Haydock and Franklyn G. Prendergast. Department of Biochemistry and Molecular Biology, Mayo Foundation, Rochester, Minnesota 55905.

Tryptophan-47 in variant-3 scorpion neurotoxin is partially buried below the protein's surface. The rotational motions of this tryptophan are restricted by the local packing of amino acid residues. This is confirmed by the presence of large energy barriers in the adiabatic potential surface for rotational isomerization of the indole side chain. These barriers divide the energy surface into several distinct wells. Evidently, several conformations of tryptophan-47 are compatible with the packing requirements of surrounding protein residues. We have computed a more accurate adiabatic mapping to confirm the existence of these conformations and determine their relative stability. The new mapping has also provided a better picture of the energy barriers separating the different conformations. In addition we have estimated the effective mass and viscosity for transitions over these energy barriers. The transition rates are then obtained from both the transition state and Kramers theories of activated processes. Finally, the fluorescence lifetime distribution and emission anisotropy are modeled. This work is supported by NIH grant GM34847.

M-Pos92 **Functional Group Mapping of Binding Sites by Molecular Dynamics and Grid Search Techniques***
A. Miranker, P. A. Bash, M. J. Field, and M. Karplus,
Dept. of Chemistry, Harvard University, Cambridge, Ma. 02138

For the design of novel ligands that bind to specific sites of proteins of known structure, it is useful to determine the parts of the binding site that can interact strongly with a range of functional groups (e.g., hydroxyl, aliphatic, carbonyl). We show how quenched molecular dynamics and grid search techniques can be employed for constructing functional group maps of the binding site. For each functional group, molecular dynamics trajectories at 300° K for 100 independent copies of that group were determined simultaneously[1] in the force field of the receptor binding site of the haemagglutinin glycoprotein HA of the influenza virus[2]; although the present study used a static protein, the internal dynamics of the protein can be included. The trajectories were minimized at 2 picosecond intervals to determine energetically favorable locations for the functional groups. The interaction energy of each type of functional group with the protein was also determined on a 0.25 Å three-dimensional grid covering the binding site. This was accomplished by sequentially fixing the center of mass of the functional group at each grid point and minimizing the sum of the Lennard-Jones and Coulomb interaction energies; rotation of the group was allowed during the minimization. Comparison of the results obtained by the two methods showed good agreement. In the x-ray structure of a ligand bound to the protein only some of the favorable functional group sites are occupied and certain functional groups of the ligand are not near an energy minimum. This suggests that the maps of the binding site obtained with the present techniques can aid in the rational design of more tightly bound inhibitors.

* Supported in part by a grant from the Department of Energy.

1. R. Elber and M. Karplus (to be published).
2. W. Weis, J. Brown, S. Cusack, J. Paulson, J. J. Skehel, and D. C. Wiley (submitted)

M-Pos93 MOLECULAR DYNAMICS SIMULATIONS OF BLOOD GROUP "A" AND "H" OLIGOSACCHARIDES.

C. Allen Bush and **Zhen-Yi Yan** Dept. of Chemistry, Illinois Institute of Technology, Chicago, IL 60616 U.S.A.

Molecular dynamics simulation provides a useful tool for detailed descriptions of fluctuations of individual atoms and of variations with time of structural parameters such as torsion angles and interatomic distances. Although the method has been applied extensively to proteins and nucleic acids, little has been done on MD studies of carbohydrates. NMR and circular dichroism results as a function of temperature and of solvent conditions as well as conformational calculations have suggested that the non-reducing terminal sugar residues of blood group oligosaccharides adopt single, well defined conformations which are independent of solvent. In contrast to the trajectories of peptides whose conformations are generally stabilized by such weak interactions as hydrogen bonding and hydrophobic interactions, the trajectories of blood group oligosaccharides are expected to show minimal conformational transitions. To enhance the understanding of conformational properties, molecular dynamics simulations of Fuc(α-1$\rightarrow$2)-Gal-β-O-Me, Gal(β-1$\rightarrow$3)-Glcβ-O-Me and Gal(β-1$\rightarrow$4)Glcβ-O-Me are carried out using the CHARMM program with the potential energy surface developed by Rasmussen and co-workers. The resulting trajectories, the plots of ϕ, ψ versus time will be discussed with respect to experimental observations.

Research supported by NIH grant GM 31449 and by NSF grant DMB 85-17421

M-Pos94 A SYSTEMATIC APPROACH FOR MODELING HOMOLOGOUS PROTEINS FROM A KNOWN CRYSTAL STRUCTURE FOR EVENTUAL USE IN DRUG DESIGN.

C.A. Schiffer, J.W. Caldwell*, J.S. Finer-Moore**, P.A. Kollman*, R.M. Stroud**. Biophysics Program, *Department of Pharmaceutical Chemistry, **Department of Biochemistry & Biophysics, Univ. of California, San Francisco, California, 94143

We have undertaken a study to develop a systematic algorithm for predicting the structure of a protein for which the crystal structure of a related protein is known. Proteins that have a high degree of sequence homology and are functionally identical often have extremely similar tertiary structures. Modeling proteins in this manner may make it possible to pick out species specific differences in protein structure, and thus useful sites for species specific inhibitors. As a first step, we are modeling the structure of rat trypsin from the crystal structure of bovine trypsin. Both crystal structures are known and have an RMS deviation of the CA backbone of .41A. We started with the bovine crystal structure and exchanged those residues which differed between rat and bovine trypsin to the rat residues, with the model-building program, FRODO, which places the new amino acid side chains in an arbitrary conformation. We search for the lowest energy configuration of each individual side chain using energy minimization within the program AMBER. By going through the protein and picking the lowest energy configuration for each of the exchanged residues, it is possible to obtain a rational model of the desired protein. The accuracy of the model can be assessed by comparing it with the rat trypsin crystal structure.

M-Pos95 LABELING A SPECIFIC SEQUENCE OF CHROMATIN FOR ELECTRON MICROSCOPIC EXAMINATION. John D. Brantley and Michael Beer. Dept of Biophysics, The Johns Hopkins University, Baltimore, Md 21218.

A method for labeling a specific sequence of chromatin for electron microscopy has been developed based on the work of Workman and Langmore (1985). For this study, the oocyte 5S gene of Xenopus laevis was chosen because it exists as a set of tandemly arranged repeating units, separated by a Hind III cleavage site. Chromatin is digested with Hind III for 12 hours. A single stranded tail is produced by limited digestion with T_7 exonuclease. A 15mer oligonucleotide probe complementary to the single stranded tail is synthesized and labeled by addition of biotin-11-dUTP with TdT. The probe is annealed to the chromatin for 4 hours at 4C. 20 nm streptavidin-colloidal gold is allowed to react with the biotin for 1 hour at 4C. The sample is then dialyzed into spreading buffer (1 mM HEPES pH 7.5, 1 mM NaCl, 1 mM EDTA) overnight. EM grade glutaraldehyde is added to a concentration of 0.1% and allowed to fix for at least 12 hours. The chromatin is spread by the droplet method on carbon coated grids made hydrophilic with Alcian Blue (Arcidiacono, 1980). Grids are shadowed at 7° with Pt/Pd and examined in a Philips 420 Electron Microscope. Labeled molecules clearly show a gold particle at one end. Supported by NIH grants RR01214, RR07041-22 and FMC.

Arcidiacono, A., A. Stasink, and T. Koller. 1980. Electron Microscopy 2:516-523.
Workman, J.L. and J.P. Langmore. 1985. Biochemistry.24:7486-97.

M-Pos96 **FOLDING OF CHROMATIN CONTAINING UV-INDUCED PYRIMIDINE DIMERS OR TRIMETHYLPSORALEN CROSSLINKS.** James M. Gale and Michael J. Smerdon, Biochemistry/Biophysics Program, Washington State University, Pullman, WA 99164-4660.

The ability of intact and histone H1 depleted chromatin fibers to fold into higher ordered structures *in vitro* was examined following DNA photodamage introduced by two different agents. (1) 254 nm UV radiation and (2) trimethylpsoralen (plus near UV radiation). Both agents form adducts in DNA with a much higher yield than in proteins (DNA specific) and these adducts are predicted to cause different degrees of bending and unwinding of the DNA helix. UV irradiation at 254 nm primarily induces formation of *cis-syn* cyclobutane dipyrimidines and trimethylpsoralen (plus near UV radiation) forms monoadducts and interstrand crosslinks. The salt induced structural transitions of intact and histone H1 depleted chromatin fibers were monitored by both analytical ultracentrifugation and light scattering. Our results show that even in the presence of extremely large, nonphysiological amounts of photodamage by either agent the ability of chromatin to fold into higher ordered structures was not affected. The compact, 30 nm fiber must therefore be able to accommodate a large amount of DNA photodamage (greater than one UV-induced photoproduct or trimethylpsoralen interstrand crosslink per nucleosome) without measurable change in the overall size or degree of compaction of this structure. These results suggests that gross alterations of chromatin fiber structure are probably not involved in the recognition and repair of DNA photodamage.

M-Pos97 HIGHLY COOPERATIVE BINDING TO DNA BY A HISTONE-LIKE, SPERM-SPECIFIC PROTEIN FROM SPISULA SOLIDISSIMA. Louis J. Libertini, Juan Ausio, and Enoch W. Small, Department of Biochemistry and Biophysics, Oregon State University, Corvallis, Oregon 97331.

The highly condensed chromatin from sperm of the bivalve mollusc, Spisula solidissima, is unusual in that the protein component consists of about 20% histones coexisting with a predominant protein which shares characteristics with both protamines and somatic histones [Ausio and van Holde (1987) Eur. J. Biochem. 165, 363-371]. Efforts to study the binding of this protamine-like protein (PLP) to DNA are complicated by aggregation, particularly when the stoichiometry is close to 1. Labeling the PLP with fluorescein isothiocyanate (PFP-F) in order to permit studies to be done at very low concentrations did not eliminate the problems with aggregation and precipitation.

Instead, we examined the binding by looking at the effect of salt on formation of PLP-F:DNA complexes using protein:DNA ratios below those which lead to aggregation. An approach has been developed to simulate the resulting salt curves using the exact binding isotherm of McGhee and von Hippel [(1974) J. Biol. Chem. 86, 192-200]. With this approach and least-squares fitting of the experimental data to simulations, results indicate that the binding is extremely cooperative (ω as high as 10^6) and, considering the very high overall charge of ~140 on PLP, involves the release of a surprisingly small number of ions (~3-5).

This work was supported by USPHS grants GM25663 and GM22916.

M-Pos98 TOWARDS THE UNDERSTANDING OF THE ROLE OF THE HISTONE "TAILS" ON THE STABILITY AND CONFORMATIONAL CHANGES OF NUCLEOSOMES AT MODERATE IONIC STRENGTHS. J. Ausio, F. Dong, and K. E. van Holde, Department of Biochemistry and Biophysics, Oregon State University, Corvallis, Oregon 97331.

Upon increase of the ionic strength from 0.1 M NaCl to 0.6 M NaCl, nucleosome core particles undergo a conformational transition and an apparent loss of stability [Ausio, J., Seger, D., and Eisenberg, H. (1984) J. Mol. Biol. 176, 77-104; Yager, T. and van Holde, K. E. (1984) J. Biol. Chem. 259, 4212-4222]. A release of the N-terminal regions of the histones has been postulated to account for the conformational changes. In order to test this hypothesis, we have prepared selectively trypsinized nucleosomes by the combined use of immobilized trypsin and appropriate reconstitution and fractionation methods in the presence of urea. The particles thus obtained: $[(H3_T\text{-}H4_T)_2\text{-}2(H2A_T\text{-}H2B_T)]\cdot DNA$; $[H3_T\text{-}H4_T)_2\text{-}2(H2A\text{-}H2B)]\cdot DNA$; $[(H3\text{-}H4)_2\text{-}2(H2A_T\text{-}H2B_T)]\cdot DNA$ (where T stands for trypsinized), together with nontrypsinized controls, have been analyzed using the following techniques: analytical ultracentrifugation, circular dichroism, thermal denaturation, and DNaseI digestion. In disagreement with the current hypothesis, analysis of the data clearly indicates very little role for the histone tails in the conformational changes experienced by the nucleosome particle when the ionic strength is raised. Nevertheless, such data provide very valuable information about nucleosome structure and histone-DNA interaction which in turn may lead to a more complete understanding of the nucleosome stability and conformational changes in solution. Supported by PHS grant No. GM 22916.

M-Pos99 **UV-INDUCED PYRIMIDINE DIMER FORMATION IS MODULATED IN NUCLEOSOME CORE DNA.** James M. Gale and Michael J. Smerdon, Biochemistry/Biophysics Program, Washington State University, Pullman, WA 99164-4660.

We have mapped the distribution of pyrimidine dimers (PD) at the single nucleotide level in nucleosome core DNA from UV-irradiated mononucleosomes, chromatin fibers and human cells in culture using the 3' → 5' exonuclease activity of T4 DNA polymerase. The results show that the frequency of PD formation in nucleosome core DNA is strongly modulated with a 10.3 (± 0.1) base periodicity. This periodicity is identical to the helical periodicity of DNA in nucleosomes. The positions of maximal PD formation map to positions where the DNA strands face "out" of the nucleosome core (i.e., at positions farthest from the core histone surface). Furthermore, the individual intensities of the distribution are modulated in a unique and characteristic manner which reflects core histone-DNA interactions, giving rise to a "photo-footprint" of core histone binding. Quantitation of the levels of PD in each 10.3 base ensemble indicates that this distribution is uneffected by folding of the 10 nm chromatin filament ("beads-on-a-string") to the 30 nm chromatin fiber (solenoid). These latter results suggest that the individual core histone-DNA interactions which direct this nonrandom distribution of PD formation remain unaltered by changes in the structural state of chromatin.

M-Pos100 MAXIMALLY STRETCHED DNA. CJ. Marzec and L.A. Day, Public Health Research Institute, 455 First Avenue., New York City, NY, 10016

A-DNA has a nominal 5.9 A interphosphate distance with C_3–*endo* sugar pucker, whereas B-DNA has a nominal interphosphate distance of 7.0 A with C_2–*endo* configuration; the maximum distance between phosphates along one strand, d_{PP}, has been given as 7.1 A . We have employed the Linked Atoms Least Squares computer program to determine the upper limit to d_{PP} and its relation to sugar pucker, as parametrized by the pseudorotation angle P. For a nucleoside diphosphate or a short, non-helical polynucleotide, the stretched d_{PP} vs. P curve has a maximum d_{PP} value of about 7.75 A, occurring at $P \approx 200°$, a C_2–*endo* configuration. The minimum stretched d_{PP} value is about 7.42 A, for a C_3–*endo* sugar pucker. These extended forms have γ near 170°, the ap configuration about the C_4–C_5 bond; this configuration is observed in nucleotide-protein complexes.

A helically wound, single-strand of DNA has maximum d_{PP} values smaller by a few tenths of an Angstrom. For $P = 162°$, a C_2–*endo* sugar pucker form, the maximum d_{PP} value is about 7.45 A.

The bacteriophage Pf1 has a circular, single-stranded DNA, wound to be *locally* two-stranded but not base-paired, and it has an axial rise in its low temperature form calculated to be as large as 6.2 A . The adjacent figure shows a stereochemically feasible Pf1 DNA, modeled as poly (dG-dC) with $P = 162°$, a C_2–*endo* configuration. The extreme axial rise requires that the bases be directed away from the structure axis, allowing interactions with the protein coat. The d_{PP} value for the model Pf1 DNA is about 7.45 A. Thus, even though it is locally two stranded, the length of the low temperature form of Pf1 DNA is almost the maximum possible for a single strand of DNA having $P = 162°$. We conclude that this Pf1 DNA is maximally stretched.

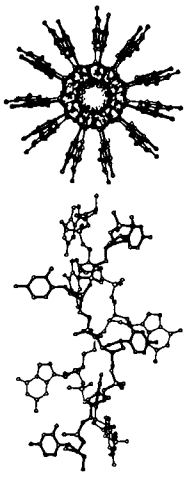

M-Pos101 FLUORESCENCE STUDIES OF SUBUNIT INTERACTIONS IN THE lac REPRESSOR OF E.coli. Catherine A. Royer, Laboratory for Fluorescence Dynamics, Department of Physics, University of Illinois at Urbana-Champaign, Urbana, IL 61801; and Kathleen S. Matthews, Department of Biochemistry, Rice University, Houston, TX 77251.

The lac repressor of E.coli was covalently labelled with 1,5 dimethyl-amino naphthalene sulfonyl chloride. Fluorescence polarization measurements of the dansylated protein indicated that the lac repressor exists as a tetramer above 5 micromolar. No evidence for dissociation upon dilution was observed for fresh samples. However, after several days storage in the cold room, as the protein concentration was diminished (10^{-5} to 10^{-7}M), the steady state polarization decreased, indicating tetramer dissociation, the extent of which depended upon the age of the preparation. Global analyses of the concentration dependence of the fluorescence decay showed that the values of the lifetimes were generally unaffected by dilution. However, there was a concentration dependence of the pre-exponential factors, indicative of a ground state equilibrium, which, like the polarization data, was time dependent. High hydrostatic pressure studies (<2kbar) of fresh dansylated lac repressor polarization showed that the tetramer dissociated to dimer in a concentration-dependent manner. The dissociation constant for the tetramer-dimer transition was 4.6×10^{-8}M, consistent with the dilution studies. The calculated volume change for dissociation was -146ml/mole. At lower concentrations, dissociation was complete to monomer. In all cases, reversibility was partial. Either reassociation was not complete or the reassociated tetramer was in a conformation in which the dansyl moiety had more freedom to rotate. Supported by NIH grants RR03155 (CAR) and GM22441 (KSM).

M-Pos102 SITE-SPECIFIC PROTON-LINKED CONTRIBUTIONS TO THE COOPERATIVE BINDING OF LAMBDA cI REPRESSOR TO O_R. Donald F. Senear and Gary K. Ackers, Department of Biology, The Johns Hopkins University, Baltimore, MD 21218.

The effects of proton activity on the site-specific cI repressor-O_R interactions have been studied using DNase footprint titration. Individual site isotherms were resolved for the binding of repressor to each site of O_R, and of mutant operators in which binding to some sites is eliminated. The Gibbs energies for binding and for cooperativity (in every operator configuration) were determined at each pH (range: 5-8) using a dimer dissociation constant of 20 nM, and with the simplifying assumption of no significant linkage between proton activity and repressor polymerization. The observed effects appear to involve titration of repressor groups that do not actually contact the DNA. More interesting is that the derivitive relationships, $d\ln k/d\ln a_H = \Delta\nu_H$, are significantly different between the three operator sites. While any linkage of proton activity to repressor polymerization will necessarily affect the apparent Gibbs binding energies, it will not change the conclusion that the pH effects are site-specific. Thus, either the array of ionizable groups linked to binding is different at the various operator sites, or the magnitude of the effect on proton binding is different. Either indicates different local electrostatic potentials which can only arise due to induced or pre-existing differences in the conformations of the DNA in the operator sites, a conclusion with broad implications regarding the physical-chemical origins of site specificity. The effect of proton activity on cooperativity is negligible, an unusual observation in light of the prevailing view that cooperativity exclusively reflects protein-protein interactions. (Supported by NIH grant GM-24486).

M-Pos103 GLUTAMATE AS A PLEIOTROPIC EFFECTOR OF PROTEIN ACTIVITY. M.M. Garner, D.S Cayley, and M. T. Record, Jr., Depts. of Chemistry and Biochemistry, University of Wisconsin, Madison, Wisconsin, 53706

The major intracellular small molecule anion of enteric bacteria is glutamate. Timasheff and coworkers have demonstrated that monosodium glutamate has a large negative preferential interaction parameter for proteins, i.e. proteins will be more solvated in glutamate. Native conformations of and protein-ligand complexes should therefore in general be stablized in glutamate (relative to chloride) salts, independent of the enzymatic activities which they exhibit. This laboratory has previously shown that substitution of glutamate for chloride in vitro dramatically strengthens the site-specific binding of gene regulatory proteins. This observation has been extended to a number of other DNA-binding proteins. We will present data showing a large enhancement of glutamate of the end-filling reaction of the Klenow fragment of DNA polymerase, as well as for the nonspecific binding activity of E. coli RNA polymerase. Data from several other enzyme systems unrelated to nucleic acid metabolism will also be discussed.

M-Pos104 **INTERACTION OF THE T7 RNA POLYMERASE WITH ITS PROMOTER: ^{19}F AND ^{1}H NMR OBSERVATIONS**, Martha S. Briggs, William J. Metzler, and Ponzy Lu, Department of Chemistry, University of Pennsylvania,Philadelphia, PA 19104

We have used ^{19}F and ^{1}H NMR to investigate the interactions of the RNA polymerase of coliphage T7 with its 23 bp promoter. 5-Fluoro-2'-deoxyuridine was substituted for thymidine residues in 24 bp synthetic DNA's containing the T7 promoter. Sites of fluorination were chosen for their locations within or outside the region of the promoter contacted by the protein, as determined by DNase footprinting and methylation studies. Control experiments show that the fluorinated promoters are used by the polymerase to initiate transcription. Upon addition of T7 RNA polymerase to the fluorinated promoter, the chemical shifts of the fluorine signals change to varying degrees. These changes are consistent with the fooprinting results. Addition of substrate ribonucleotide triphosphate(s) corresponding to the initial base of the transcript results in further changes in the ^{19}F NMR spectrum, showing that the motion of the protein along the DNA during elongation can be followed by this method. These experiments help to elucidate the means of protein-DNA recognition and the mechanisms of transcription initation; further, they demonstrate the utility of ^{19}F NMR for study of a high molecular weight complex. Although the large size of the T7 RNA polymerase (about 100 kD) makes proton NMR of the protein difficult to interpret, it is possible to use ^{1}H NMR to observe small ligands. We have studied binding of the initiating nucleotide to the T7 RNA polymerase in the absence and presence of a synthetic DNA template. These experiments provide information on the conformation of the initiating nucleotide bound in the complex. (Supported by NCI Postdoctoral grant F32CA08133 to M.S.B, NIH training grant support to W.J.M., and NIH grant GM32,987 to P.L.)

M-Pos105 MOLECULAR DYNAMICS STUDY of LEXITROPSIN-DNA BINDING
S.WANG, G.C.LEVY, P.N.BORER,Intr.by J.C.DABROWIAK, NIH RESOURCE, SYRACUSE UNIV.,SYRACUSE, NY13244-1200

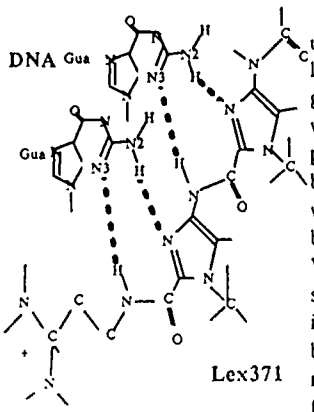

We have studied DNA binding of several oligonucleotides to "lextropsin 371" (lex371) using molecular dynamics calculation (CHARMM,M.Karplus); lex371 is an oligopeptide that is similar to the antibiotic netropsin. The topology of lex371 and its parameters for CHARMM have been generated based on MNDO calculations. The final conformation of several DNA-lex371 complexes was energy minimized using the adapted basis Newton-Raphson algorithm in CHARMM by several pathways to avoid being trapped in local minima. Of the different oligonucleotide sequences that have been generated and docked with lex371, the sequence d(CCGT) + d(ACGG) binds most strongly; which is consistent with foot printing analysis (J.Dabrowiak). The results indicate that the hydrogen bonding mode is different from the one proposed from X-ray analysis of netropsin-DNA complexes. We propose a Guanine hydrogen bond clamp with the complex; the Guanine N2H and N3 of the same base form two H-bonds to lex371. Netropsin binding with its preferred sequences is also studied. The final conformation of the complexes is achieved similar to above procedure. The results will be compared with X-ray crystallography and/or solution NMR data. Further refinement of the 3-dimensional structure of the complex will be carried out by applying proton-proton distance constraints from NMR NOESY data.

M-Pos106 FLUORESCENT LABELLING OF TRANSCRIPTION TERMINATION FACTOR RHO. Steve Seifried, Yan Wang, and Peter H. von Hippel. Institute of Molecular Biology, University of Oregon, Eugene, OR 97403, U.S.A.

E. coli transcription termination protein rho operates in transcript release as an oligomer of six identical subunits. In discharging this release function, rho must bind to the nascent transcript, thus activating an RNA-dependent ATPase. Each rho monomer carries a nucleotide-triphosphate binding site, one (or more) RNA binding sites, and two (or more) subunit interaction sites. Experiments by other techniques suggest that the conformation of the rho monomers, and/or their interactions within the hexamer, are changed as a consequence of rho ATPase activation. We seek additional biophysical probes of the structure and dynamics of the activated rho hexamer in a continuing effort to study the transcript release mechanism catalyzed by rho. To this end we have used the lone sulfhydryl (cys-202) of each rho subunit to attach fluorescent probes (fluorescein and AEDANS). Labelling is specific and greater than 90% complete. Contrary to earlier reports, we find that the chemical modification of rho at cys-202 does not affect the properties of activated rho. Subunit assembly, RNA binding, and poly(rC)-activated ATP hydrolysis are all virtually unperturbed by this modification. The environment(s) of cys-202 in active and inactive rho oligomers have been probed by various fluorescent techniques using this modified rho. We are also initiating measurements of intersubunit distances, subunit exchange, and fluorescent energy transfer between these probes in RNAactivated and in-active rho hexamers. [Supported by USPHS grants GM-15992 and GM-29158 (to PHvH).]

M-Pos107 THE INTERACTION OF E. COLI RNA POLYMERASE WITH LACTOSE PROMOTER DNA. D.D. Lorimer and A. Revzin, Dept. Biochem., Michigan State Univ., E. Lansing, MI 48824.

Many promoters have been found to contain overlapping binding sites for RNA polymerase. We previously showed [Lorimer and Revzin, Nucl. Acids Res. 14, 2921 (1986)] that polymerase will form several stable, mutually exclusive, complexes in vitro on cloned lac DNA fragments. We observed an open, heparin-stable complex at the P2 promoter (which initiates at nucleotide -22), a closed, heparin-sensitive P1 complex (which initiates at +1 in the presence of the catabolite activator protein (CAP)), and possibly a third, heparin-sensitive complex ("P3") about ten base pairs downstream of P1 that competes well with P1 and P2. We are using a two pronged approach to create a lac promoter fragment which may be used to examine the closed P1 complex. As a first step a P2 down mutant was constructed by site specific mutagenesis. Binding studies and run-off transcription experiments have confirmed that a T to A transversion at position -29 abolishes P2 activity without affecting P1 utilization. We had previously determined that cleavage at +36 by the restriction enzyme AluI does not abolish interference by a polymerase molecule bound at P3. In an attempt to eliminate the P3 site we have used Bal31 nuclease to delete DNA sequences downstream of +1. Five deletions terminating at +25, +19, +14, +1 and -7 were subsequently isolated and fused to $P2^-$ lac fragments yielding potential $P1^+P2^-P3^-$ clones. We are currently characterizing these constructs for their ability to bind RNA polymerase and initiate transcription at P1 only. The fragments all contain an intact CAP site and may be used to study the transition of P1 complexes from the closed to open state.

M-Pos108 DNA SEQUENCES TO THE RIGHT OF +1 ARE NOT CRITICAL FOR UTILIZATION OF THE lac PROMOTER. D.D. Lorimer and A. Revzin, Dept. Biochem., Michigan State U., E. Lansing, MI 48824.

The sequences which define E. coli promoters have been well established. Two highly conserved sequences around -10 and -35 have been identified and their roles in RNA polymerase function studied. The importance of the sequences flanking these areas has only recently been given attention. Brunner and Bujard [EMBO J. 6, 3139 (1987)] have shown that in many promoters changing sequences upstream of -35 and downstream of -10 has a substantial effect on transcription. We have constructed a lacUV5 promoter fragment which contains the usual sequence from -59 to +1 but with all the DNA downstream of +1 replaced with non-lac DNA. This fragment binds polymerase well and initiates from +1 at 70% the rate of the normal lacUV5 promoter. We were thus led to examine the downstream sequences of the wild type lactose promoter. Five deletions, to +25, +19, +14, +1 and -7, have been isolated and tested for their ability to interact with RNA polymerase in vitro. Two deletion fragments, ending at +25 and +19, bind polymerase normally at the P1 promoter site, from which initiation occurs at +1, in the presence of the catabolite activator protein. Further deletions are incapable of binding polymerase unless heterologous DNA is added downstream of the deletion, but all five are capable of initiating transcription when some DNA is present there. Thus, wild type sequences beyond +1 are not critical for transcription from the lac promoter. The fact that the deletion that ends at -7 is capable of interacting with polymerase is a surprise since that is the end of the -10 consensus region. However the -7 deletion does not initiate transcription well. Because this may be due to an unfavorable C at +1 in the construct rather than the usual A or G, we are currently testing other heterologous DNAs for their ability to replace normal sequences downstream of -7.

M-Pos109 FLUORESCENCE INVESTIGATIONS ON THE Phe-$tRNA^{Phe}$·EF-Tu·GTP COMPLEX, T.L. Hazlett, A.E. Johnson*, and D.M. Jameson, Dept. of Pharmacology, Univ. of Texas Health Science Center at Dallas, Dallas, TX, 75235. *Dept. of Chemistry, Univ. of Oklahoma, Norman, OK, 73019

Time-resolved fluorescence methodologies were employed to study the hydrodynamics of aminoacyl-tRNA free in solution and bound to elongation factor Tu (EF-Tu). The probes utilized were ethidium bromide and a fluorescein-labeled Phe-tRNA (Phe-$tRNA^{Phe}$-F^s). Dynamic polarization data for ethidium bromide bound to Phe-$tRNA^{Phe}$ (5°C) gave two Debye rotational relaxation times ρ_1=136ns and ρ_2=8ns with amplitudes, r_0, of 0.24 and 0.08, respectively. The former relaxation time is clearly global while the latter may be due to either tRNA structural motion or probe movement within a 'loose' binding site. For the corresponding complex with EF-Tu·GTP relaxation times of ρ_1=195ns, r_0=0.23, and ρ_2=13ns, r_0=0.07 were found. The slow global relaxation time is longer than expected for a sphere of equal volume (145ns) indicating the asymmetric nature of the complex. Analysis of Phe-$tRNA^{Phe}$-F^s data (5°C) yielded two relaxation times ρ_1=103ns, r_0=0.25, and ρ_2=4.8ns, r_0=0.09. The short relaxation time probably represents the probe's structural motion at its point of attachment, the s^4U-8 residue. Analysis of the corresponding EF-Tu·GTP complex also yielded two relaxation times: ρ_1=206ns, r_0=0.24, and ρ_2=4.7ns, r_0=0.10. The global relaxation time of 206ns is consistent with the ethidium bromide results. The fast rotation is similar in size and amplitude to that seen in the free Phe-$tRNA^{Phe}$-F^s, suggesting that the fluorescein is not sterically hindered in the complex. Thus, the EF-Tu does not interact with the tRNA region where the probe is located. Supported by NSF grant DMB8706440 (DMJ) and NIH grant GM26494 (AEJ).

M-Pos110 CONTROL OF THE SWITCH BETWEEN THE E. coli SINGLE STRAND BINDING PROTEIN -ssDNA BINDING MODES. AN INTRINSIC PROPERTY OF THE SSB PROTEIN TETRAMER. W. Bujalowski and T.M. Lohman, Department of Biochemistry & Biophysics, Texas A&M University, College Station, Texas 77843.

We have studied the binding of the oligonucleotides, $d(pT)_{16}$ and $dT(pT)_{34}$, to the E. coli SSB protein as a function of NaCl and $MgCl_2$ concentration (25°C, pH 8.1) by monitoring the quenching of the intrinsic protein fluorescence. We find four binding sites for $d(pT)_{16}$ and two binding sites for $dT(pT)_{34}$ per SSB tetramer. In the case of $dT(pT)_{34}$ there are widely different affinities between the two binding sites depending on the salt concentration. At 200 mM NaCl we observe nearly stoichiometric binding of $dT(pT)_{34}$ to both binding sites within the SSB tetramer. At 1.5 mM NaCl, only a single molecule of $dT(pT)_{34}$ can bind per SSB tetramer, even with a ten-fold molar excess of $dT(pT)_{34}$ over the second binding site. $MgCl_2$ is effective at 100-fold lower concentrations than NaCl in promoting the binding of the second molecule of $dT(pT)_{34}$. In the case of $d(pT)_{16}$ the first two molecules bind with much higher affinity than the third and fourth one. An increase in salt concentration reduces the difference in affinities among binding sites but does not eliminate it. The simplest explanation is that a salt-dependent negative cooperativity exists between DNA binding sites within the SSB tetramer. The binding of $d(pT)_{16}$ can be described very well by a simple, sequential "square" model for ligand binding to tetrameric protein, but not by a "tetrahedral" model. The values of the intrinsic binding constant, K, and negative cooperativity parameter σ have been obtained and they will be discussed. These strong interactions among nucleic acid binding sites within the SSB tetramer also seem to be responsible for the transition between the two SSB-ss polynucleotide binding modes, which cover 35 to 56 nucleotides per tetramer (Bujalowski, W. & Lohman, T.M. (1986) Biochemistry 26, 7799). Extreme negative cooperativity stabilizes the $(SSB)_{35}$ binding mode, in which the SSB tetramer binds tightly to ssDNA using only two of its subunits while the other two subunits remain unbound. This may provide a mechanism by which the SSB protein can bind tightly to ssDNA while interacting simultaneously with other proteins involved in DNA metabolism.

M-Pos111 **EFFICIENCY OF DNA REPAIR SYNTHESIS IN HYPERACETYLATED NUCLEOSOMES.** Brinda Ramanathan and Michael J. Smerdon, Biochemistry/Biophysics Program, Washington State University, Pullman, WA 99164-4660.

Treatment of human fibroblasts in culture with millimolar concentrations of sodium butyrate induces histone hyperacetylation and stimulates DNA repair during early times after UV irradiation (*J. Biol. Chem.* 257, 13441, 1982). Since only a fraction of the total chromatin becomes hyperacetylated during sodium butyrate treatment and only a fraction of the DNA lesions are repaired more efficiently, it was not known if the enhanced repair of these lesions occurred in the hyperacetylated chromatin fraction. To this end, we have fractionated chromatin from sodium butyrate-treated human fibroblasts into different acetylated forms and monitored the level of repair synthesis occurring in each of these forms following UV irradiation. Our results indicate that most (or all) of the enhanced DNA repair synthesis occurring in these cells at early times after irradiation is located in the hyperacetylated chromatin fraction. Nucleosomes from moderately acetylated regions of chromatin contained only about half the level of repair synthesis found in hyperacetylated nucleosomes. These results could be explained by (1) changes in the initial level of UV damage in hyperacetylated chromatin or (2) increased DNA repair efficiency in the hyperacetylated regions of chromatin. To shed light on these possibilities, our current investigations have focused on (a) comparison of the distribution of repair synthesis in the different acetylated forms of nucleosomes and (b) determination of the levels of pyrimidine dimers in these regions both immediately after UV damage and following different extents of repair.

This investigation was supported by NIH grant ES02614 (MJS) and PHS grant CA43079 from the National Cancer Institute (BR).

M-Pos112 EFFECTS OF A FISH OIL DIET ON PLASMA LIPOPROTEINS

Stephen R. Wassall*, Daniel Belcher†, Carol A. Langsford† and William Stillwell†
Departments of Physics* and Biology†, Indiana University-Purdue University at Indianapolis, Indianapolis, IN 46223

The effects of dietary n-3 fatty acids (20% supplement of menhaden oil, a fish oil rich in n-3 fatty acids, vs. hydrogenated coconut oil) on molecular order and dynamics within the outer amphiphilic monolayer of rat HDL (high density lipoprotein) and LDL (low density lipoprotein) were investigated by ESR and fluorescence of intercalated doxyl and anthroyloxy, respectively, labelled stearic acids. Fluorescence polarization of HDL indicates that fluidity in the central region of the acyl chain (positions 6 and 10) is substantially less for the mendaden oil (MO) diet than the hydrogenated coconut oil (HCO) diet. Lower down the chain (position 12), the trend is the same but of smaller extent. Qualitative agreement, although considerably reduced in magnitude, is exhibited by spin label ESR which measured greater order in the central region of the acyl chain (positions 5, 7 and 10) and a smaller restriction in acyl chain mobility lower down the chain (positions 12 and 16). In contrast, negligible difference in order and fluidity throughout the outer monolayer of LDL was seen between MO and HCO diets by either ESR or fluorescence. The results are discussed in terms of a 'hook' conformation predicted by molecular models for n-3 fatty acids.

M-Pos113 ENVIRONMENTAL AND GEOMETRICAL SAMPLING OF ELECTRONIC STATES IN TRYPTOPHAN PEPTIDES. Predrag Ilich and Franklyn G. Prendergast. Department of Biochemistry and Molecular Biology, Mayo Foundation, Rochester, Minnesota 55905.

A comparative theoretical study of indole 3-derivatives of this general formula was accomplished by quantum mechanical calculations. Heats of formation, energies and modes of nuclear vibrations, substituent torsional barriers, and energies and intensities of electronic transitions were calculated for a selection of X,Y and Z fragments representing (i) a flexible, nonpolar, electronically localized substituent, (ii) a rigid, π-electron interacting substituent, and (iii) a short peptide chain. Examples studied were the pair of dipeptides AW and WA for which energy shifts, intensity and transition moments changes for one- and two-photon electronic transitions were calculated for a selection of (i) conformers, (ii) ionization states, and particularly (iii) for a variety of discrete and continuous environments. Supported by NIH grant GM 34847.

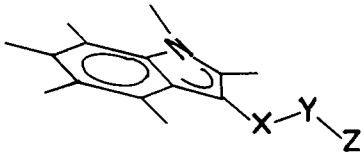

M-Pos114 Identification of Phase Transitions in Frozen Living Wood by Mechanical Analysis and Electron Microscopy

The winter wood of Populus balsamifera, balsam poplar, is capable of withstanding freezing to liquid nitrogen temperatures if the freezing rate is below 0.7°C/min. Dynamic Mechanical Analysis (DMA) scans of poplar twigs frozen at rates below 5°C/min show that in the intracellular fluids several aqueous domains exist which have different glass transition temperatures. Freeze-etch electron microscope analysis supports the hypothesis that these domains are spinodally decomposed regions of the cytoplasm. Thermomechanical Analysis (TMA) implies that the highest temperature glass transition is associated with sugar-protein complexes, whereas the lower transitions are likely to be aqueous protein glasses. The spinodal decomposition observed may explain the deterioration of these very hardy tissues after 8 months of storage at temperatures between -20°C and -80°C.

Authors: Allen Hirsh, Robert J. Williams, Thomas Bent*, and Eric Erbe+,
Jerome Holland Laboratory of The Red Cross, Rockville, MD

*Comsat Corporation, Clarksburg, MD
+USDA ARC Research Station, Beltsville, MD

M-Pos115 QUANTUM EFFECTS IN THE DYNAMICS OF ENZYMATIC PROTON TRANSFER William Bruno and William Bialek, *Departments of Physics and Biophysics, University of California, Berkeley, CA 94720*

Recent experiments on the enzymes plasma amine oxidase and yeast alcohol dehydrogenase (1) have revealed patterns of kinetic isotope effects which are unexpected if one assumes that the proton or hydride transferred during the catalytic step is moving classically over a barrier. These results have prompted us to study several simple dynamical models for 'atom' (hydrogen, proton, or hydride) transfer in the active site of an enzyme in an attempt to determine when the classical picture breaks down and quantum mechanics becomes important. In all these models the atom moves between a donor and acceptor, while the distance between these groups fluctuates as the enzyme 'breathes.' We have found that coupling to the breathing motion tends to reduce the observable kinetic isotope effects and endows even 'pure tunneling' reactions with a sizable activation energy, so that reactions which appear classical by conventional criteria may in fact proceed by tunneling. In some models the classical transition state occurs near the point where the protein fluctuates so much that the barrier to atom transfer disappears — the breathing mode becomes the reaction coordinate. In such cases quantum effects are much stronger than otherwise expected, and the catalytic rate depends on the dynamics of the breathing itself. This situation can arise at physiological temperatures in models using plausible parameters and may have novel signatures in the vibrational spectroscopy of the scissile bond.

(1) J.P. Klinman and co-workers, personal communication.

This work is supported in part by the National Science Foundation.

M-Pos116 EVIDENCE FOR THE INTERACTION OF TERMINAL COMPLEMENT COMPLEXES WITH CYTOSKELETAL COMPONENTS OF ERYTHROCYTES. Zi-Yao Liu, Marty Sanders*, and Valerie W. Hu, Dept. of Biochemistry, Uniformed Services University of the Health Sciences, Bethesda, Md. 20814-4799 and *Immunology Branch, National Cancer Institute, Bethesda, Md. 20205.

The lateral mobilities of erythrocyte membrane proteins and terminal complement complexes were measured on complement-treated erythrocyte ghosts by the technique of fluorescence recovery after photobleaching (FRAP). Results showed that the lateral diffusion coefficient of the bulk membrane proteins decreased with the assembly of the terminal complexes on the membrane and was significantly reduced with assembly of the C5b-9 complex. These changes in the mobilities of the endogenous proteins may reflect interaction of the terminal complexes with the spectrin network since the diffusion coefficients of the complement complexes themselves are characteristic of anchored proteins ($D = 1.18 \times 10^{-11}$ cm^2/sec for the C5b-9 complex). Spectrin-depletion of the complement-lysed erythrocytes results in 25- and 45-fold increases in the diffusion coefficients of the membrane proteins and the C5b-9 complex, respectively. Conversely, oxidative crosslinking of spectrin by diamide reduced the diffusion coefficients of both membrane and complement proteins. These results suggest that the lytic complexes of complement interact in some manner with the erythrocyte cytoskeleton. This cytoskeletal interaction may provide another means through which complement might exert its pathological effect on cells.

M-Pos117 CRYSTAL STRUCTURE AND CONFORMATION OF FRENTIZOLE, A NOVEL IMMUNOMODULATING AGENT. T. Srikrishnan, Center for Crystallographic Research, Roswell Park Memorial Institute, Buffalo, New York 14263.

Frentizole, [1-(6-methoxy-2-benzothiazolyl)-3-phenylurea] (F) is a new immunoregulatory agent which inhibits both humoral and cellular immune response in mice. This drug was selected from among a large series of heterocyclic urea compounds on the basis of both high immunosuppressive activity and low acute toxicity and has been employed to modulate the immune response in human to rheumatoid arthritis and systemic lupus erythematosus. Crystal structure of F has been undertaken to study the conformation of the molecule in the solid state as a first step in the investigation of the structure-activity relationship of immunomodulators. Crystals of F (ethanol/water) are monoclinic, space group $P2_1/c$, with a=11.187(4), b=7.392(2), c=32.727(6)Å, β=92.77(2), V=2703Å^3, Z=8, D_o=1.47 g/c.c, D_c=1.472 g/c.c. The structure was solved with CAD-4 data (4725 reflections, 1875 >3σ), by the multisolution techniques to a final R value of 0.061. There are two independent molecules in the crystallographic asymmetric unit with very different conformations. In molecule A the urea group is in the plane of the benzothiazole ring (dihedral angle 0.9°) whereas in the molecule B the angle is 4.4°. The dihedral angle between the planes of the phenyl group and the benzothiazole ring are 157° and 12° respectively in molecules A and B. The molecules are linked by a pair of N-H...N hydrogen bonds involving the urea nitrogens and two other N-H...N bonds involving the urea nitrogen and the nitrogen of the benzothiazole group. Thanks are due to Eli Lilly Co. for a gift of the sample. Work supported by ACS-IN54W8, NYS State Dept. of Health and in part NIH GM-24864.

M-Pos118 REACTIVE FLUX CORRELATION THEORY OF DIPEPTIDE "HELIX-COIL" TRANSITION Huan Xiang Zhou, (Intr. by S. Gruner, Department of Physics, Princeton University) Department of Physics and Atmospheric Science, Drexel University, Philadelphia, PA 19104.

The reactive flux theory of activated processes (D. Chandler, 1978, J. Chem. Phys., **68**, 2959) is generalized to two dimensions. In two dimensions, the transition state is identified as the intersection of the 'reactive path' and the 'basin boundary'. The probability that the system is in the transition state is calculated as the probability of the system being at the basin boundary. The reactive flux is obtained by calculating the dynamics of the transition state trajectories. As a model system of the helix-coil transition, the van der Waals potential of a dipeptide, N-methyl alanyl acetamide, is calculated. The generalized method is applied to the transition from the state representing the extented conformer to the state representing the helical conformer. The transition rate found (1.4×10^9 sec^{-1}) is compatible with previous experiments for the helix-coil transition ($1.0 \times 10^6 sec^{-1}$ to 1.0×10^9 sec^{-1}, quoted by J. A. McCammon et al, 1980, Biopolymers, **19**, 2033).

M-Pos119 NMR RELAXATION STUDIES OF OXYGEN MIGRATION THROUGH PROTEINS. Y. Feng, H. Roder and S.W. Englander. Department of Biochemistry and Biophysics, University of Pennsylvania, Philadelphia, PA 19104.

The entry of oxygen into proteins provides evidence for the dynamic nature of protein structures. Fluorescence quenching studies provide information on the timescale of such events, but the spatial resolution is limited. We are using conventional and two-dimensional ^1H NMR relaxation methods to obtain a detailed structural picture of the motions that permit molecular oxygen to migrate through proteins. Since O_2 has an electronic spin S=1, it acts as a paramagnetic relaxation probe and enhances the nuclear relaxation of nearby protons. In a protein with known ^1H assignments, the effect of dissolved O_2 on spin-lattice relaxation provides a measure of the local oxygen concentration at many points throughout the protein.

Initial results on the basic pancreatic trypsin inhibitor (BPTI) and cytochrome c show that O_2 reaches every proton in the two proteins to some extent. Even the most deeply buried protons in both proteins experience at least 20% of the O_2 enhanced relaxation relative to bulk water. Larger effects are observed for exposed groups at the protein surface. The O_2-induced relaxation of several exposed methyl groups in BPTI is larger than the value measured for water in the same sample, indicating preferential association of oxygen with apolar groups on the protein surface. No correlation was found between the oxygen accessibility and the distance of a proton from the protein surface. The present results suggest that oxygen is able to diffuse throughout the interior of globular proteins.

M-Pos120 Photodynamics of Ru^{II}(CO)Octaethylporphyrin, Ru^{II}(CO)Mesoporphyrin, and Ru-Porphyrin Reconstituted Horseradish Peroxidase and Myoglobin.

B.A. Crawford, R.G. Alden, M. Lu, and M.R. Ondrias
Department of Chemistry, University of New Mexico, Albuquerque, NM 87131

Comparison of the photodynamics of metalloporphyrin model complexes to those of metalloporphyrin reconstituted heme proteins offers insight into the specific heme-protein interactions at the active site. Ruthenium porphyrin reconstituted proteins provide useful analogies for understanding protein influences upon π-cation radical formation and π-ligand photolysis at the active sites of native, iron-containing systems such as horseradish peroxidase and myoglobin. Transient resonance Raman spectra of Ru^{II}(CO)Octaethylporphyrin, Ru(CO)Mesoporphyrin IX and reconstituted horseradish peroxidase and myoglobin were obtained under equilibrium conditions and within 10 nanoseconds of porphyrin photoexcitation. The equilibrium Ru^{II}(CO) porphyrin models show a strong influence of CO π-back donation in their spectra. However, the characteristics of the photoexcited species are quite dependent upon their initial coordination state. The 6-coordinate species undergoes irreversible CO photolysis. The 5-coordinate species retains the CO-ligand and forms the π-cation radical. Preliminary results indicate that both the Ru-reconstituted myoglobin and Ru-reconstituted horseradish peroxidase do not undergo photolysis. Instead, these proteins exhibit unique behavior subsequent to photoexcitation that may be indicative of protein regulation of excited-state deactivation in Ru^{II} porphyrins. Supported by the NIH (GM33330), the Petroleum Research Fund, and the Associated Western Universities.

M-Pos121 The Photodynamics of Nickel Corphinoid and Salt Extracted F_{430}.

B.A. Crawford[1], J.A. Shelnutt[2], E.W. Findsen[1], and M.R. Ondrias[1]
[1]Department of Chemistry, University of New Mexico, Albuquerque, NM 87131 and Process Research Division 6254, Sandia National Labs, Albuquerque, NM 87185.

A nickel containing macrocycle known as F_{430} has recently been identified as the active site of methyl-coenzyme M methyl reductase, one of the enzymes responsible for methane production from carbon dioxide and hydrogen in Methano bacterium thermoautotrophicum. Recently, a nickel corphinoid model was synthesized, which serves as an analog to the F_{430} reaction center. Equilibrium resonance Raman and 10 nanosecond transient Raman spectra have been obtained of both the nickel corphinoid models and salt extracted F_{430} corphinoid derivatives at room temperature and 77 K. These data illustrate the differences in photodynamic behavior between the highly reduced nickel corphinoids and nickel porphyrins. In particular, the net d-d transition of nickel evident in the transient spectra of 4-coordinate nickel porphyrins and the ejection of ligands from excited state 6-coordinate species is not observed. Instead, photolysis of only weak field axial ligands is observed in the corphinoid models. Preliminary studies indicate that the salt extracted F_{430} center shows analogous behavior. The results suggest that the corphinoids may form a functionally distinct class of enzyme prosthetic group. Differences in both the dynamic motion resulting from macrocycle flexibility and electronic structure produced by ring reduction may contribute to their unique photodynamic properties. Supported by the NIH (GM33330), the donors of the Petroleum Research Fund, The Associated Western Universities, the DOE, and the Gas Research Institute.

M-Pos122 THE PLANCK-BENZINGER THERMAL WORK FUNCTION IN RIBONUCLEASE REFOLDING.

P.W Chun, Dept. of Biochemistry and Mol. Biol., University of Florida, Gainesville, FL 32610.

In re-examining the thermodynamic parameters of the protein refolding of ribonuclease systems over the temperature range of 220-360°K, based on the Nernst heat theorem, we found that at the temperature $\langle T_s \rangle$, the thermodynamic quantities $\Delta G^\circ \langle T_s \rangle$ and $\Delta H^\circ \langle T_s \rangle$ are of the same magnitude, while $T\Delta S^\circ \langle T_s \rangle$ approaches zero. Based on the Planck-Benzinger thermal work function, $\Delta W^\circ(T) = \Delta H^\circ(T_o) - \Delta G^\circ(T)$, a reasonable *a priori* estimation of $\Delta H^\circ(T_o)$ can be made at $\langle T_s \rangle$. The most striking element of this state function is the symmetry exhibited by $\Delta W^\circ(T)$ and $\Delta G^\circ(T)$. Values for $\Delta H^\circ(T_o)$ at $\langle T_s \rangle$ were determined to be 34.05 ± 1.30 and 19.49 ± 0.42 Kcal/mole in 20-S_1 [I] and 14-S_1 [II] complementation reactions, respectively, and 59.0 Kcal/mole in the ribonuclease A conformational transition as a function of pH.

The Planck-Benizinger thermal work function, $\Delta W^\circ(T)$, is an effective measure of the energy potentially available for any interaction to take place. $\Delta H^\circ(T_o)$, a temperature-invarient quantity, is a primary source of the chemical bond energy essential for any reaction to proceed in a biological system, and is indispensable in any consideration for any reaction to proceed in a magnitude of $\Delta H^\circ(T_o)$ values for 20-S_1 [I] and 14-S_1 [II] is an effective measure of the ease with which these molecules can be refolded to resemble native protein structure, with greatest ease of folding at the lowest chemical bond energy.

The application of the Planck-Benzinger thermal work function to evaluate the chemical bond energy has great potential for studies on the catalytic efficiency of enzymes, because it permits a site-directed, mutagenic approach to the examination of structure-function problems. (Supported by NSF Grant DMB 83-12101-(02)).

M-Pos123 LOW FREQUENCY DYNAMICS AND RAMAN ACTIVE NORMAL MODES OF A-DNA, B-DNA, AND Z-DNA CRYSTALS

Om P. Lamba and George J. Thomas, Jr., Division of Cell Biology and Biophysics, School of Basic Life Sciences, University of Missouri-Kansas City, Kansas City, MO 64145.

The Raman spectra of crystals of A-DNA, B-DNA and Z-DNA in the frequency region 300-4000 cm^{-1} have been reported and the data interpreted in terms of the molecular structures known from single-crystal X-ray diffraction analyses.[1] Here we report low frequency vibrations, in the region between 20 and 300 cm^{-1}, for the same A [r(GCG)d(CGC)], B [d(CGCAAATTTGCG)] and Z [d(CGCGCG)] structures examined previously. The low frequency bands can be understood in terms of external lattice phonons (optical modes) associated primarily with the skeletal dynamics (librations) of the purine and pyrimidine bases. Although complete assignment to normal modes is not possible for any of the crystals, assignment of the more prominent bands, centered in each crystal near 26, 36, 45 and 53 cm^{-1}, appears to be straightforward. A self-consistent assignment scheme which accounts for the observed Raman intensities is proposed. This approach assumes that the low local symmetry of the ribose-phosphate moiety, and the low polarizability changes associated with its librations, cannot account for the intense Raman scattering in the frequency interval of interest. A remarkable feature of the data is the close correspondence between low frequency modes in the three canonical DNA secondary structures. The results indicate a similar local environment for the base residues irrespective of the oligomer sequence or secondary structure. (Supported by N.I.H. Grant AI18758.)

[1]Thomas, G.J., Jr. and Wang, A.H.-J. (1988). In Nucleic Acids and Molecular Biology, Vol. 2, Eckstein, F. and Lilley, D.M.J., Eds., Springer-Verlag, Berlin.

M-Pos124 THE ROLE OF SOLVENT VISCOSITY ON PROTEIN STRUCTURAL MOTIONS. King Man Ng, Bela Somogyi* and Andreas Rosenberg. University of Minnesota Medical School, Minneapolis, MN 55455. *Debrecen Medical University, Debrecen, Hungary.

One can argue convincingly that protein structural fluctuations play an important role in enzyme reactions. However, the experimental details of such movements within the protein matrix are, in general, not very well understood. One of the experimentally more accessible approaches is to consider whether the bulk viscosity is coupled to the internal motions, and/or modifies the microenvironments during enzyme reactions. All rate mechanisms predict a linear dependence of log k against log η with the slope indicating the degree of coupling to the solvent viscosity. We have studied the hydrogen isotope exchange and acrylamide fluorescence quenching reactions of the indole sidechain of proteins in two different cosolvents, glycerol and ethylene glycol. These have the advantage that we can independently study the reactions both in the indole as well as in the protein matrix. Hydrogen exchange reactions have a high activation energy, require transient hydration beforehand and usually take place in the μsec to msec range. Fluorescence quenching has a very low activation energy, thus is typically diffusion limited and of the nsec time-scale. By comparing the results and hence the mechanisms of the two reactions, it is possible to establish a relationship between viscosity of the bulk phase and internal motions within the protein matrix. Our data show a clear difference in the response of the two reactions to the cosolvents, with hydrogen exchange fitted very well by Kramers model. The results also imply a different degree of coupling in the different time windows of the observed protein fluctuations. (Supported by NSF DMB-8704740 and NIH 5R01-GM35384.)

M-Pos125 THE CONFORMATIONAL AND DYNAMIC RESPONSE TO HYDRATION: PROTEINS AND CARBOHYDRATES. R.G. Bryant, C. Jackson, T.M. Eads, and S.D. Kennedy. Departments of Chemistry and Biophysics, University of Rochester, Rochester, NY 14642.

The structural and dynamical response of macromolecules to the addition of solvent may differ significantly depending on their structural type. The solid state NMR experiment provides a detailed probe of local structural features and their fluctuations in time as a function of perturbants such as solvent. The enzymic proteins such as lysozyme appear to fall into the class of macromolecules that respond to increasing hydration by relaxing from a significant distribution of local structures, reported through the carbon-13 or cadmium-113 NMR spectrum, to a narrow distribution of local structures. Beyond a critical level, additional hydration does not affect the structure, though some aspects of local structural fluctuations may change further with increasing hydration. By contrast casein or glycogen, which is highly branched, respond to hydration by rapidly increasing motion that leads to loss of local structure and liquid-like resolution in the NMR spectrum at water contents of approximately 70% by weight.

M-Pos126 EFFECTS OF HYDRATION ON MOTIONS IN HOMOPOLYPEPTIDES. S.D. Kennedy, S.D. Swanson, R. G. Bryant, University of Rochester, Departments of Chemistry and Biophysics, Rochester, NY 14642.

The carbon-13 NMR experiment conducted on immobilized materials provides a report on the motional and structural changes that attend perturbations by solvent or other molecular co-factors. We have completed studies on type I and type II polyglycine, the sodium salt of the beta sheet form of poly-L-glutamic acid, and poly-L-lysine. The structures of polyglycine are compact and show little dynamical change on hydration, though there is evidence for some very slow motions on the ms range. By contrast, poly-L-glutamic acid and poly-L-lysine show dramatic water induced dynamical changes. Motions in the side chains are the most affected, while little effect is apparent in the backbone. The carbon-13 CP-MASS spectrum shows that the secondary structure of these polymers is maintained at humidities less than about 70%, which is consistent with the infrared and x-ray diffraction data. The NMR data demonstrate that while there is some distribution of local conformation at low water contents, the structures become considerably more uniform at higher hydration levels. The side chain carboxyl in poly-L-glutamic acid fluctuates rapidly through an angular excursion of approximately -+45° with fluctuations ortnogonal to the side chain axis in the range of about +-20°. The side chain motions of hydrated poly-L-lysine become progressively larger from the beta carbon to the epsilon carbon reaching very large angular excursions at the terminus.

M-Pos127 **Diffusion Models of Ion Channel Gating and the Origin of Power Law Distributions from Single-Channel Recording.** G.L. Millhauser*, E.E. Salpeter† and R.E. Oswald*, *Department of Pharmacology, NYSCVM and †Newman Laboratory of Nuclear Studies, Cornell University, Ithaca, NY 14853.

The lifetimes of unitary currents from ion channels, as revealed from single channel recording, are traditionally thought to follow exponential or multi-exponential distributions. The interpretation of these event-time distributions is that the gating process follows Markov kinetics among a small number of states. Recent evidence suggests, however, that certain systems exhibit distributions that follow power laws of the form t^{-a} or functions related to power laws. Likewise, it has been suggested that data sets which appear to be multi-exponential may be fit to simple power laws as well. In this work we propose a different view of ion channel gating kinetics that is consistent with these recent observations. We retain the Markovian nature of the kinetics but, in contrast to the traditional models, we suggest that ion channel proteins have a very large number of states all of similar energy. Gating, therefore, becomes a diffusion process. We show that our simplest one-dimensional model exhibits power law behavior with exponents that approximately span the range of current experimental observation. Our model is also suggests a basis for the recently proposed fractal scaling schemes. We believe that our approach is consistent with modern views of protein dynamics and, thus, may provide a key to the molecular details of the gating process.

M-Pos128 **SOLITONS IN ALPHA HELICES.**

Anthony Nicholls, Institute of Molecular Biophysics, Florida State University, Tallahassee, Fl.

It has been suggested that alpha helices may be conduits of vibrational energy, via the mechanism of soliton production. If this were true, it would have implications for the interpretation of structure and function of most proteins. Two such proposals are models by Davydov, and by Scott, Careri et al.

The derivation of the equation of motion for an excitation on the helix, in both models, rests on an assumption as to the nature of quantum mechanical correlation within the system. It can be shown that this supposition is incorrect. As a consequence, when certain parameter limits are chosen, neither system will exhibit soliton motion, although it is still predicted by both theories.

Finally, for the Scott model, a theory has been developed which allows the computation of the dynamics of the system for parameter values normally suggested. Such simulations clearly show no soliton motion.

Based on these results, the concept of the molecular soliton seems inappropriate for the alpha helix.

M-Pos129 TIME DEPENDENT FLUCUATIONS OF TUNA CYTOCHROME c : EFFECT OF DIELECTRIC FUNCTION.

John J. Wendoloski and James B. Matthew, E. I. du Pont de Nemours & Co., Inc., Central Research and Development, Experimental Station, Wilmington, DE 19898.

Molecular dynamic simulations have been carried out for 125 picoseconds using the program AMBER (Weiner et al. 1984, JACS 106, 765) implemented on an ST-100 array processor. Trajectories were computed with five dielectric functions included in the nonbonded electrostatic term (9.5 A cutoff radius). The dielectric formalisms, in order of increasing effective dielectric, were: dielectric set equal to R and 4R (where R is the charge separation distance), constants of 50, 80, and 6400 and dielectric of one with the inclusion of 800 explicit water molecules (TIPS3P). Average structures were calculated from the coordinates sets collected along the trajectory between 25ps and 125ps. RMS differences for alpha carbon positions between the average structures and the X-ray structure varied from 0.93 to 1.87 A, while the RMS differences between the average structures varied from 1.1 to 2.1 A. More variability is seen in the behavior of the charged sidechains. Calculated radii of gyration for the simulations increased from 12.6 to 13.0 A with increasing dielectric. In the low dielectric cases, R and 4R, the Lys and Arg residues fold back on the protein surface to form fourteen ion pairs with all the carboxyl functions. This also reduces the calculated protein surface area from the X-ray structure value of 5900 A to a value that fluctuates between 5000 and 5300. In the higher dielectric simulations (50, 80, and solvated) ion pairs decreased to six, four, and two, respectively, and the average surface areas increased to 5500, 5600 and 6000 A. The effect of these rearrangments on predicted electrostatic potentials and counterion distribution about the protein will be presented.

M-Pos130 STRUCTURAL AND CHEMICAL DIVERSITY OF THE FILAMENTOUS BACTERIOPHAGES
Sarama Bhattacharjee, Marc J. Glucksman* & Lee Makowski
Dept. of Biochemistry & Molecular Biophysics, Columbia Univ. P&S, New York, NY 10032

The class I filamentous bacteriophages are rod-like, flexous particles 60A in diameter and 9000A in length. In M13, and the very closely related f1, and fd, a single-stranded loop of DNA runs along the filament axis and is ensheathed by about 2700 copies of a small, predominantly alpha-helical, 50 amino acid protein. These coat proteins are arranged on a helical lattice with a five-fold rotation axis and a two fold screw. The pitch of the screw axis is 33A. M13 and fd differ only in position 12 of the protein sequence, where there is an ASN or ASP respectively. X-ray diffraction data have been collected on M13, fd and on mutant, fd24f, (kindly provided by Dr.S.J.Opella, U. Penn.) which differs from native fd with a PHE in position 24 instead of TYR. Data have been collected to a resolution of 4A at pH2 and pH 8 (pKa=4.3) for native and for two heavy atom derivatives (iodine and mercury). A simple amino acid change in fd vs. M13 yields alterations in the helical symmetry. One factor in the control of the symmetry appears to be the charge on amino acid 12. At pH 2 and pH 8, M13 exhibits an integral, two-fold screw. fd (or fd24f), at pH 2 demonstrate the same symmetry as M13, but at pH 8 the two-fold screw becomes non-integral, concomitant with the ionization state of ASP 12. The structural change represents a change in the tilt of the alpha-helical segments. When fd or fd24f are iodinated at pH 8, the symmetry is integral as in M13. Currently the fiber diffraction data to 7A spacing are being phased using a combination of model building and isomorphous replacement techniques. This should establish the conformation of the coat protein on the intact virion.

M-Pos131 THE RELATIONSHIP OF THE THREE-DIMENSIONAL STRUCTURE OF HEXON TO ITS ROLE AS THE MAJOR COAT PROTEIN OF ADENOVIRUS. Francis K. Athappilly, Zhaoping Cai, Alex P. Korn, Ramachandran Murali and Roger M. Burnett. Department of Biochemistry and Molecular Biophysics, Columbia University, New York, New York 10032.

Hexon is the principal component of the adenovirus virion, with 240 copies accounting for 62% of the particle mass (150×10^6 daltons). We have determined the crystal structure of the 967 residue polypeptide, developed an architectural model for the arrangement of hexons in the virion, and used electron microscopy to determine precisely their relative positions. We are currently refining the molecular model and investigating the molecular properties important for hexon's role as a coat protecting the protein-covered core containing the DNA. The hexon trimer has a pseudo-hexagonal base formed from six beta-barrels, two in each subunit, and acts as a "tile" in the close-packed p3 array on each facet of the virion. Hexon tops, formed by interwoven loops rising from the barrels, define the outer surface of the virion. The initial hexon model, based on MIR phases, has been refined using PROLSQ on a STAR array processor. After several cycles, the R value for 19657 reflections in the resolution range 5.0 - 2.9 Å dropped from 48.6% to 32.7%. The model phases were combined with MIR phases and used to calculate a new map in which the model was rebuilt. The extraordinary stability of the molecule arises from an extensive intersubunit interface, and the unusual entanglement of surface loops and the N-terminus. The subunit interface is dominated by highly hydrophobic contacts and contains few charged residues. We are currently analyzing the hexon-hexon capsid contacts. (Supported by NIH Grant AI 17270 and NSF Grant PCM 84-18111).

M-Pos132 RELATIONSHIP BETWEEN STACKED DISK AGGREGATES OF TOBACCO MOSAIC VIRUS PROTEIN (TMVP) IN SOLUTION AND DIMERS OF BILAYER DISK AGGREGATES IN CRYSTALLINE STATE. K.Raghavendra, J.A. Kelly and T.M. Schuster, Molecular & Cell Biology, U-125, University of Connecticut, Storrs, CT06268.

Klug and coworkers have shown that TMV protein crystallizes as dimers of cylindrical bilayer disk aggregates (4 layers of subunits) from solution (0.3M $(NH_4)_2SO_4$ in I=0.1M Tris/HCl, pH 8.0, room temperature) for a protein concentration of 8.0 mg/mL. We have used varying salt concentrations (0.1, 0.2 and 0.3M) of $(NH_4)_2SO_4$ and developed protocols to identify solution aggregates involved in the crystallization process. We have found that 28S aggregates, observed as coaxial dimers of cylindrical bilayer disk aggregates (4 layers of subunits) in electron micrographs, readily form at 20°C in crystallizing buffers and correspond to about 25% of the total protein in 0.1M, 85% in 0.2M and 100% in 0.3M $(NH_4)_2SO_4$, respectively. When 0.2M and 0.3M solutions are left at room temperature for 2-3 weeks, single crystals of the protein grow by the bulk crystallization method. The protein crystals have identical unit cell dimensions as those reported earlier for the dimers of bilayer disk aggregates by Klug and coworkers. Protein also crystallizes from 0.1M $(NH_4)_2SO_4$ solutions only after adding poly ethylene glycol and using the hanging drop method. We have not observed isolated bilayer disk aggregates in solution before crystallization nor do the metastable stacked disks reported by Raghavendra et al. (Biochemistry, 1986, 25, 6276) lead to crystal formation. We conclude that 28S aggregates in solution crystallize as dimers of bilayer disk aggregates. We have evidence to show that the bilayer disks are not the nucleating species in the in-vitro TMV assembly and there is no direct switch in subunit packing between the cylindrical bilayer disks and the short helical aggregates, the nucleating species in the virus assembly; the switch is mediated only through the dissociation to protein subunits. (Supported by the NIH grant AI-11573 to TMS)

M-Pos133 POSSIBLE AMINO ACID SEQUENCE HOMOLOGY BETWEEN HUMAN IMMUNODEFICIENCY VIRUS gp41 AND THYMOSIN β4. Anna Fang Wu and Tai Te Wu, Northwestern University Medical School, Chicago, IL 60611, and Northwestern University, Evanston, IL 60201.

Complete genomic sequences of eight related types 1, 2 and III human immunodeficiency viruses, HXB2, ROD, BH10, BRU, ELI, MAL, H9 and SF2/ARV-2, are available from GenBank. On aligning the translated amino acid sequences of their env-proteins, we noticed one invariant hexapeptide, Gly Ile Val Gln Gln Gln, and two invariant pentapeptides, Leu Thr Val Trp Gly and Gln Gln Glu Lys Asn, in the extra-membrane portion of gp41, and one invariant hexapeptide, Arg Arg Ile Arg Gln Gly, near its C-terminal intra-membrane portion. These peptides are not found in the NBRF protein sequence data bank. Only their constitutive tetrapeptides are present in many different proteins. One of them, Gln Glu Lys Asn, appears in thymosin β4, a ubiquitous protein of 43 amino acid residues with no known function. This tetrapeptide is located in one of the two antigenic epitopes of thymosin β4, residues 22 to 32:

THR GLN GLU LYS ASN pro leu pro ser lys GLU

where important antigenic amino acid residues are capitalized. Type III viruses, for example, have a corresponding sequence of

gln GLN GLU LYS ASN glu gln glu leu leu GLU

This fortuitous amino acid sequence similarity suggests that there is a remote possibility of their sharing the same receptor. If this happens to be the T4 glycoprotein of helper T-cells, it may be worthwhile to investigate whether thymosin β4 can be used as a therapeutic agent.

M-Pos134 STRUCTURE OF THE COVALENT DNA ADDUCTS OF 9,10-EPOXY-7,8,9,10-TETRAHYDROBENZO(A)PYRENE AND 1-OXIRANYLPYRENE AS PROBED BY OPTICAL DETECTION OF MAGNETIC RESONANCE. H. C. Brenner and V. Kolubayev, Department of Chemistry, New York University, New York, NY 10003.

Structural differences in the epoxide derivatives of polycyclic aromatic hydrocarbon carcinogens can have profound effects on their reaction mechanisms with DNA and on the ultimate structure of the covalent adducts formed. These differences may also be quite important in determining the carcinogenic and mutagenic activity of these compounds. For these reasons, we have studied the covalent DNA adducts of 9,10-epoxy-7,8,9,10-tetrahydrobenzo(a)pyrene (BaPE) and 1-oxiranylpyrene (1-OP), which differ from the highly carcinogenic benzo(a)pyrene diol epoxide in their lack of 7,8 hydroxyl groups (BaPE) and 7,8 carbon atoms (1-OP). In optical detection of magnetic resonance, the phosphorescence of the pyrenyl chromophore of the bound carcinogen is monitored while pumping its zero field splittings (zfs) with resonant microwaves. The zfs are notably sensitive to environment, and have been used in previous applications to distinguish between solvent exposed and "quasi-intercalative" binding sites, in which there is appreciable interaction with the DNA bases. In the case of the BaPE-DNA adduct, the ODMR frequencies are lowered, and the pyrenyl phosphorescence red shifted, relative to the 9,10 diol derivative of BaPE in the same solvent, which is our model for a solvent-exposed chromophore. Enzymatic digestion to mononucleoside adducts shifts the spectral parameters to agree with the diol. By contrast, the phosphorescence and ODMR of the 1-OP covalent adduct is only slightly red shifted from that of the diol derivative of 1-OP, and blue shifted relative to physical, intercalative complexes of the diol with DNA. The ODMR results are thus consistent with quasi-intercalative binding in the case of BaPE, but show very little base interaction in the 1-OP adduct. Work supported by DHHS-NCI Grant CA-20851.

M-Pos135 IMAGE PROCESSING OF THE SIDE VIEW OF ANDROCTONUS AUSTRALIS HEMOCYANIN

N. BOISSET (1), J.C. TAVEAU (1), R. WADE (2), J. FRANK (3), J. LAMY (1)
(1) Université François Rabelais, TOURS (France), (2) CENG, GRENOBLE (France), (3) N.Y. State Department of Health, ALBANY, N.Y.

The 4x6-meric hemocyanin of the scorpion Androctonus australis observed produces in the electron microscope three different views called "top view", "45° view", and "side view", respectively.

Though the top and the 45° views have been extensively studied, the side view has never been investigated by image processing. In this poster, the side view has been submitted to the correspondence analysis (CORAN) method of image processing (van Heel and Frank, 1981, Ultramicroscopy, 6, 187-194) under different conditions: (1) after negative staining with uranyl acetate, and (2) in frozen hydrated specimens. For comparison, a carbon film was used in the two set of grids.

The results obtained with negatively stained molecules show small details in the interdodecamer bridge area and a meniscus effect related to deviations from a perfectly vertical orientation. The preferential staining of the molecule portion in contact with the film allows a discrimination between the two flat faces of the molecule seen in the top view.

Side views from frozen hydrated specimens showed no difference between the flat faces. However, small nuclei of material were distinctly and constantly found in the average maps computed from clusters of images separated by CORAN. Though in most cases the disposition of these nuclei was difficult to interpret in term of molecular architecture, their reproducible positions with respect to the contour of the side view suggest that they represent authentic architectural details.

M-Pos136 CHARACTERIZATION OF A SINGLE OXYGEN BINDING DOMAIN OF OCTOPUS DOFLEINI HEMOCYANIN.
K. I. Miller, K. E. van Holde, A. Toumadje, W. C. Johnson, Jr., and J. Lamy*
Department of Biochemistry and Biophysics, Oregon State University, Corvallis, OR 97331 USA
*Université Francois Rabelais, Tours, FRANCE

Octopus hemocyanin consists of 51S whole molecules (MW - 3.6×10^6) which dissociate into 10 identical 11S subunits (MW = 3.6×10^5). The polypeptide chain of the subunit can be cleaved proteolytically into seven immunologically distinct globular oxygen binding domains (1). The C-terminal domain (Od-1) has been purified from a partial tryptic digestion. It is a 3.8S globular protein (MW = 4.9×10^4; $f/f_o = 1.23$). Circular dichroism measurements show similar secondary structure when compared with the whole subunit, but there are substantial differences in amino acid composition when compared with the whole subunit. It does not self-associate in the presence of $MgCl_2$, as the subunit does, nor does it prevent association of subunits to whole molecules, but it does appear to bind to the 51S molecule, altering the sedimentation coefficient significantly. It has an absorbance spectrum similar to other molluscan hemocyanins and binds oxygen reversibly. It has a small normal Bohr effect ($-\Delta\log p50/\Delta pH$ - 0.3) and shows increased oxygen affinity in the presence of $MgCl_2$. Though less pronounced than the similar responses of the whole molecule, these results demonstrate some control of oxygen binding behavior by ion binding sites on the isolated domain, independent of interactions between allosteric units.
Supported by NSF DMB 85 17310 (KI and KEvH) and CNRS RCP 080816 (JL) and USPHS GM-21479 (WCJ).
(1) Lamy, J. et al., 1987, Biochemistry 26, 3509.

M-Pos137 THE STRUCTURAL BASIS FOR THE ION SPECIFICITY OF MONENSIN.
G. David Smith and Walter A. Pangborn, Intr. by William L. Duax. Medical Foundation of Buffalo, Inc., 73 High Street, Buffalo, NY 14203

Monensin is a linear, polyether monocarboxylic acid that exhibits specificity for sodium ion over that of lithium or potassium ion. The structures of three different sodium ion complexes of monensin have been determined by crystallographic techniques and have shown that the conformations of the monensin ions are nearly identical although the crystal packing and solvent content in the three crystal forms are quite different. In each case, the sodium ion has distorted octahedral coordination. The structure of a lithium ion complex of monensin has also been determined and is quite different from that of the sodium ion complex. Because of the reduced size of the lithium ion, it can occupy only a portion of the binding cavity of the ionophore and is bound to only four monensin oxygen atoms and one water molecule. As a result, the conformation of monensin ion in the lithium ion complex is more like that of the free acid form of the ionophore than other complexed forms. In contrast, potassium ion is too large to optimally bind to the monensin ion. Crystallographic studies on the potassium form have shown that as a result of the larger size of the potassium ion, a small distortion is introduced into the spiro ring system. Molecular mechanics calculations have been carried out on this moiety and show qualitatively that the spiro ring distortion is of higher energy than other known conformations of monensin. Thus, this ring strain, induced by the coordination of the larger potassium ion, can be used to explain the selectivity of monensin for sodium ion. Research supported by Grant GM32812 awarded by the National Institutes of General Medical Sciences, DHHS.

M-Pos138 C-DNA CLONING AND SEQUENCING OF THE C-TERMINAL DOMAIN OF OCTOPUS DOFLEINI HEMOCYANIN.
W. H. Lang and K. E. van Holde, Department of Biochemistry and Biophysics, Oregon State University, Corvallis, Oregon 97331.

The 11S subunit of Octopus dofleini has been shown to be a single polypeptide chain (M_r= 3.5×10^5), containing seven oxygen binding domains. One domain can be cleaved off very easily upon limited proteolytic digestion. This domain was shown to be the C-terminal domain.

A cDNA library was constructed using poly-A^+ RNA purified from Octopus dofleini branchial gland, which is the site of hemocyanin synthesis in cephalopods. The library was screened with a oligonucleotide probe derived from a portion of the partially known sequence of the C- terminal domain of Paroctopus dofleini dofleini. The clone with the longest insert was sequenced and used for Northern blotting.

The cDNA insert (1157 bp) contained an open reading frame of 1071 bp coding for 357 amino acids. Approximately 35 amino acids from the N-terminal end of the C-terminal domain are missing. By comparing our sequence with Helix pomatia β_c-hemocyanin unit D, we found 43.5% identical and 11.7% similar residues. Supported by NSF grant DMB 85-17310.

M-Pos139 STRUCTURE OF EUKARYOTIC FLAGELLAR COMPONENTS BY CRYO-ELECTRON MICROSCOPY. John M. Murray and R. Ward (Intr. by Rick S. Hock), Dept. of Anatomy, Univ. of Pennsylvania, Philadelphia, PA 19104-6058.

Various subfragments of eukaryotic flagella can be prepared by disrupting the crosslinks holding outer doublets and central pair singlet microtubules together. Electron microscopy of frozen hydrated, unstained, unfixed flagellar subfragments reveals well preserved structure and the presence of periodic attachments. The central pair complex has a repeat distance of 33.5 nm. The isolated peripheral doublet microtubules have lateral attachments with periodicity of 24 nm when viewed in one projection, and the characteristic triplet radial spoke pattern of 96 nm repeat when viewed in the orthogonal projection. 3D reconstruction requires orienting multiple views of a component with respect to each other, which is complicated by the low overall symmetry. To solve the orientation problems, we have developed methods to acquire multiple images of a single particle, using very low electron dose and low magnification. Presently we collect up to 20 images having a resolution of approximately 3 nm.

M-Pos140 SPATIALLY NONUNIFORM POLYMERIZATION AND ALIGNMENT OF SICKLE HEMOGLOBIN Frank A. Ferrone, Jin Tong Wang, Huan Xiang Zhou, Michael Cho, and Soumen Basak* Department of Physics and Atmospheric Science, Drexel University, Philadelphia, PA 19104.

Using laser photolysis to create and indefinitely maintain the deoxy derivative, we have monitored the time evolution of the spatially non-uniform polymerization of sickle hemoglobin. We find that polymerization, as observed by light scattering, initially occurs with circular symmetry in almost gaussian profiles. The growth can be well represented by a straightforward model of two-dimensional polymerization and proliferation. The apparent width of the profiles accelerates, due to the flattening of the gaussian curves. A decrease in the scattering signal is seen which is rationalized as the result of polymer elongation. Alignment occurs subsequent to polymer formation, as inferred from the fact that birefringence appears later than the scattering. We show that the birefringence can also be explained by the lengthening of polymers if we make the added assumption that entanglement selects for the radial direction. This assumption allows us to formulate a simple model which explains the unusual shape of the birefringence progress curves. Finally, we predict and observe diffusion of monomers into the immobilized polymer mass which increases the total heme concentration in the photolyzed region. Further tests of this description are provided by depolymerization experiments, which will also be discussed.

*present address: Saha Institute of Nuclear Physics, Calcutta, India.

M-Pos141 COLLAGEN FIBRIL SPACING IN CORNEA STROMAS FROM A VARIETY OF DIFFERENT SPECIES: A SYNCHROTRON X-RAY DIFFRACTION STUDY.
T.J. Gyi, K.M. Meek, G.F. Elliott, The Open University, Oxford Research Unit, Boars Hill, Oxford.

The low-angle equatorial X-ray diffraction pattern from the corneal stroma has been used to measure the mean collagen interfibrillar spacing (centre to centre) in fresh specimens from a variety of different vertebrate species. Differences in measured spacings allowed species to be grouped; the marine animals (trout, salmon, herring, whale and dolphin) gave an interfibrillar spacing of <50nm; the mammals (including cow, wallaby and man) 50-70nm; and the coypu, guinea pig, squirrel and mouse gave a diffuse diffraction pattern suggesting a range of spacings which extends beyond that of the other mammals. These results show that the collagen interfibril spacing in certain species is less regular than that described in the classical version of the lattice theory of transparency (Maurice, 1957) and is more compatible with the modifications of that theory to include limited order (Hart & Farrell, 1969) or the absence of scattering centres (Benedek, 1971). These results also do not exclude theories based on uniform refractive index (Smith, 1969).

Maurice, D.M. (1957) J. Physiol., 136, 263-286.
Hart, R.W. & Farrell, R.A. (1969) J. Opt. Soc., 59, 766-774.
Benedek, G.B. (1971) Appl. Opt. 10, 459-473.
Smith, J.W. (1969) Vis. Res., 9, 393-396.

Supported by MRC, U.K. and NIH grant EY05405.

M-Pos142 THE EFFECTS OF PHOSPHATE BUFFER ON THE REAGGREGATION OF PURIFIED ALPHA-CRYSTALLIN ISOFORMS. Lynnell W. Radlick*, Jane F. Koretz*, and Robert C. Augusteyn#, *Center for Biophysics and Biology Dept., RPI, Troy, NY 12180-3590 and #Biochemistry Dept., Univ. of Melbourne, Parkville, 3052, Victoria.

Alpha-crystallin, the major protein component of the crystalline lens in vertebrates, exhibits two isoforms, A and B. The ratio of the two in situ is species-specific; for most studies, the protein is obtained from bovine lenses, where A:B is 3:1. Each isoform can by phosphorylated at one (or perhaps more) site(s), and the phosphorylated and non-phosphorylated forms separated and concentrated. Since this protein has no known enzymatic activity, it was considered possible that phosphorylation might affect its aggregation behavior. To test this, each of the two isoforms, phosphorylated and non-phosphorylated, was allowed to reaggregate in Tris buffer, pH 8.0. In all four cases, the resultant particles exhibited a mean diameter of about 9.5 nm; the only difference observed was that the phosphorylated isoforms showed a much broader diametric distribution than the non-phosphorylated. Reaggregation into phosphate buffer, however, resulted in four unique populations, the only one of which was similar to the Tris reaggregates being the non-phosphorylated B form. It is highly likely that adsorption of phosphate molecules by the hydrophilic regions of the alpha-crystallin subunits caused these aggregate changes; such an effect has been seen in other aggregating systems in vitro, most notably alpha-paramyosin (Munson and Krause, Biophys. J., 37:48a, 1982).
Supported in part by grant EY02195 from NIH.

M-Pos143 SPONTANEOUS INTERBILAYER TRANSFER OF GALACTOSYL CERAMIDES. Jeffrey D. Jones and T.E. Thompson. Department of Biochemistry, University of Virginia, Charlottesville, Virginia 22908.

The spontaneous interbilayer transfer of galactosyl ceramides from 1-palmitoyl-2-oleoyl phosphatidylcholine (POPC) bilayers has been examined at 45°C. The transfer of bovine brain phrenosin (galactosyl-N-2-D-hydroxyl acyl sphingosine) and kerasin (galactosyl-N-n-acyl sphingosine) exhibit biphasic kinetics. For both compounds about 20% of the lipid moves with a half-time of 12h and the remaining 80% with a half-time of 100 days. These results are consistent with the presumptive phase structure of bilayers composed of these lipids in POPC. In contrast to these results, the semi-synthetic N-palmitoyl dihydrogalactosyl ceramide in the same matrix phospholipid transfers with a single half-time of approximately 12h. This strongly supports the conclusion that this glycolipid is molecularly dispersed in the POPC bilayer at 45°C. These data suggest that the length of the N-acyl group of galactosyl ceramide appears to be an important factor in determining the phase structure of POPC bilayers containing these glycosphingolipids. Transfer kinetics were determined by two methods. In the one, small unilamellar vesicles containing 5% glycolipid were incubated with an excess of large unilamellar acceptor vesicles. Separation was achieved by passing alliquots of the vesicle dispersion over a gel filtration column at appropriate time intervals. Transfer was calculated by determining the movement of tritiated glycolipid relative to that of a ^{14}C cholesterol oleate nonexchangeable marker. In the other method, a negatively charged lipid was included in the donor vesicles and separation was achieved using DEAE sephacel mini columns. (Supported by USPHS Grant GM-23573).

M-Pos144 THE EFFECT OF THE GANGLIOSIDE GM_1 ON THE KINETICS OF THE SPONTANEOUS EXCHANGE OF CHOLESTEROL BETWEEN PHOSPHATIDYLCHOLINE BILAYERS. L. Bar, Y. Barenholz and T.E. Thompson (Introduced by P.W. Holloway). Department of Biochemistry, University of Virginia, Charlottesville, Virginia 22908.

We have extended our investigation of the kinetics of the spontaneous interbilayer transfer of cholesterol in 1-palmitoyl-2-oleoyl phosphatidylcholine (POPC) bilayers to bilayers containing ganglioside as well. This study was prompted by the fact that gangliosides are often components of the plasma membranes of mammalian cells. Since GM_1 alone in aqueous dispersons forms micelles not bilayers, a phase diagram of this ternary lipid system in excess water was experimentally determined at 37°C. The diagram delineates regions in which either micelles or bilayer vesicles exist alone and a region in which both structures coexist. It is interesting to note that the range of concentration of these components occurring in plasma membranes falls well within the region in which only vesicles are present. The kinetics of cholesterol exchange between small unilamellar vesicles were investigated at various compositions of GM_1, cholesterol and POPC in the vesicle region of the phase diagram. The exchange rate was found to decrease with increasing concentration of GM_1. At concentrations of GM_1 less than 10 mole %, about 20% of the total cholesterol is non-exchangeable in the 8h time frame of the experiments. This is close to the value of the non-exchangeable pool found in the absence of GM_1 in previous studies (L.K. Bar et al., Biochem. 25, 6701, 1986). However, at concentrations of GM_1 greater than 10 mole % all of the cholesterol is exchangeable. In the biological concentration range, GM_1 modifies the phase structure of phosphatidylcholine bilayers containing cholesterol. (Supported by USPHS Grants GM-14628 and HL-17576).

M-Pos145 STRONG ATTRACTION INDUCED BETWEEN LIPID BILAYER MEMBRANES BY NON-ADSORBING POLYMERS. D. Needham* and E. Evans+ *Mechanical Engineering and Materials Science Duke University, Durham, N.C. +Pathology and Physics, University of British Columbia, Vancouver, B.C. Canada

The weak attraction operating between lipid bilayer membranes resulting from intrinsic colloidal forces is augmented by the presence of non-adsorbing polymers. Micromechanical experiments on lipid bilayer vesicles allow direct measurements to be made of free energy potentials for assembly of two bilayers to adhesive contact in aqueous salt solutions and in concentrated solutions of water soluble polymers. We have examined the effects of dextran, poly(ethylene oxide) and two plasma proteins - albumin and fibrinogen. The measured free energy potential for adhesion progressively increases with increasing macromolecule concentration, even for large volume fractions (0-0.1). The results are consistent with a thermodynamic model based on a depletion of polymer from the contact zone. For equilibrium exchange of polymer between the gap and bulk regions, the added attraction is shown to be simply the osmotic pressure difference between the bulk polymer concentration and the depreciated value at the mid-point of bilayer separation. For the random coil polymers in "good" solvent a self consistent mean-field theory predicts, i) the measured concentration dependence of adhesion energies between neutral lipid surfaces for all molecular weights studied, ii) that no polymer remains in the gap at equilibrium separation (~ 24Å), iii) the observed attenuation of adhesion energy for electrical double-layer repulsion between charged bilayers in concentrated polymer solutions. For the more rigid plasma proteins, mixing of solvent and protein in a narrow gap depends on the reduction in entropy caused by steric elimination of orientational states, resulting in an exclusion of protein, osmotic pressure difference and augmented attraction.

M-Pos146 THE STABILIZATION OF A POLYMERIZABLE LECITHIN WITH CARBOHYDRATES. Alan S. Rudolph, Joel M. Schnur, Alok Singh. Biomolecular Engineering Branch, Code 6190, Naval Research Laboratory, Washington, DC, GeoCenters Inc., Newton Center, MA.

We will report on the water-free stabilization of monomeric 1,2,-bis(tricosa-10,12-diynoyl)-sn-glycero-3-phosphocholine ($DC_{8,9}PC$), a phosphatidylcholine with diacetylenic moieties at the C10 and C12 positions, using disaccharides such as trehalose. This sugar has been shown by a number of laboratories to interact with phospholipids, maintaining the lipids in a liquid-crystalline like phase in the absence of water. The result is the stabilization in the dry state of phospholipid assemblies with retention of their contents. In the present work, we examine the effect of trehalose on the phase behavior of $DC_{8,9}PC$. Dry mixtures of trehalose-$DC_{8,9}PC$ (lyophilized from SUVs) show a reduction in the gel to liquid-crystalline phase transition temperature to the temperature of the hydrated transition temperature (42°C). Higher concentrations of sugars (.25M) result in the loss of any detectable gel to liquid-crystalline transition. This suggests that the diacetylenic lipid is maintained in a liquid-crystalline or glass-like phase in the absence of water. We are currently examining these preparations using raman and infrared spectroscopy to determine the phase characteristics of these mixtures. In addition, we are examining the effect of carbohydrates on the polymerization efficiency of this lipid, and the stabilization of tubular microstructures (and other morphologies) formed from $DC_{8,9}PC$.

M-Pos147 STRUCTURAL PARAMETERS AFFECTING THE LAMELLAR TO REVERSED HEXAGONAL TRANSITION TEMPERATURES OF PHOSPHATIDYLETHANOLAMINES AND MONOGLYCOSYL GLYCEROLIPIDS. R.N.A.H. Lewis, D.A. Mannock and R.N. McElhaney, Department of Biochemistry, University of Alberta, Edmonton, Alberta; D.C. Turner and S.M. Gruner, Department of Physics, Princeton University, Princeton, New Jersey.

The lamellar (L_α) to hexagonal (H_{II}) phase transition of a number of phosphatidylethanolamines (PE) and monglycosyl glycerolipids (MGDG) was examined by Differential Scanning Calorimetry, X-Ray diffraction and ^{31}P-NMR spectroscopy. The L_α-H_{II} transition temperatures (T_H) of the PEs are very sensitive to changes in the length and chemical structure of the hydrocarbon chains. With the PEs, T_H decreases with increasing hydrocarbon chain length and for any given chain length, tends to occur at a constant temperature interval above the main chain melting phase transition temperature. In contrast, the L_α-H_{II} transition temperatures of the MGDGs are relatively insensitive to length and chemical structure of the hydrocarbon chains. Instead their L_α-H_{II} transition temperatures are more sensitive to the nature of the glycosidic linkage between the glycerol and sugar moieties. Thus, although both groups of lipids readily form non-bilayer structures and possibly fulfill similar functional roles in biomembranes, their different sensitivities to the above structural parameters may be indicative of some fundamental differences in the principles underlying their so called 'non-bilayer forming tendencies'. (Supported by the Medical Research Council of Canada and the Alberta Heritage Foundation for Medical Research).

M-Pos148 DSC AND ^{31}P-NMR SPECTROSCOPIC STUDIES ON THE THERMOTROPIC PHASE BEHAVIOUR OF A HOMOLOGOUR SERIES OF UNSATURATED PHOSPHATIDYLCHOLINES. R.N.A.H. Lewis, B.D. Sykes and R.N. McElhaney. Department of Biochemistry, University of Alberta, Edmonton, Alberta, Canada.

The thermotropic phase behaviour of dioleoyl phosphatidylcholine and six of its longer chain homologues was studied by differential scanning calorimetry and ^{31}P-NMR spectroscopy. All of the lipids studied exhibited single transition endotherms on heating, and their transition temperatures were considerably lower than those of their linear saturated acyl chain counterparts. Upon cooling, these lipids exhibit multiple transition exotherms which were observed at temperatures below those of their heating endotherms. Both the heating and cooling behaviour showed signs of hysteresis and were very sensitive to the composition of the bulk aqueous phase. ^{31}P-NMR studies indicated that the observed behaviour of these lipids was the result of net interconversions between the liquid-crystalline state and a condensed subgel-like phase. These studies suggest that while the presence of cis-double bonds in a lipid bilayer does result in relatively low gel/liquid-crystalline phase transition temperatures, its presence does not preclude the formation of highly ordered gel states and at reduced temperatures, results in a reduction of the degree of disorder in the liquid-crystalline state.

(Supported by the Medical Research Council of Canada and the Alberta Heritage Foundation for Medical Research).

M-Pos149 PHOSPHOLIPID DISTRIBUTION AND HEADGROUP MOTION IN PHOSPHATIDYLCHOLINE LIPOSOMES OF DIFFERENT SIZE. V. V. Kumar and Wolfgang J. Baumann, The Hormel Institute, University of Minnesota, Austin, Minnesota 55912.

1-Palmitoyl-2-oleoyl-sn-glycero-3-phosphocholine (POPC) liposomes were prepared by sonication or extrusion. POPC (0.15 mmol) was hydrated by vortexing in 2.5 ml buffer (150 mM NaCl, 20 mM Tris or Hepes, pH 7.4, in D_2O). The dispersions were repeatedly frozen and thawed before passing through polycarbonate membranes (Nucleopore, 200 to 30 nm; Lipex Biomembranes Extruder, 800 psi). The liposomes were characterized by freeze-fracture electron microscopy. Both sonication and extrusion through filters of up to 100 nm produced small unilamellar vesicles (SUV). Vesicle diameter ranged from 22 ± 3 nm for sonicated SUV to 80 ± 18 nm obtained by extrusion through 100 nm filters. With the smaller size filters (30 and 50 nm), the vesicles were somewhat larger (48 ± 12 and 58 ± 13 nm) than the respective pore size; with the larger filters (80 and 100 nm), the opposite was observed (71 ± 13 and 80 ± 18 nm, respectively). Vesicles extruded through 200 nm filters contained some multilamellar structures. Phosphorus-31 NMR (32.2 MHz) in the presence of Pr^{3+} (3 mM) showed that the ratio of POPC in the outer versus the inner vesicle leaflet ($R_{o/i}$) decreased from 1.9 for 22 nm vesicles to 1.0 for 80 nm SUV. Ion leakage did not occur. While 22 nm SUV gave rise to a sharp phosphorus signal near 40 ppm ($\nu_{1/2}$ 8.5 Hz), half-height linewidth significantly increased with increasing vesicle size ($\nu_{1/2}$ 43 Hz for 80 nm SUV). The decrease in observed T_2^* values indicates a considerable decrease in headgroup motion, which can be attributed to a decrease in vesicle rotational motion due to an increase in vesicle size. (Supported by NIH Grant HL 08214 and the Hormel Foundation).

M-Pos150 THE CRYOPRESERVATIVE ACTON OF SYNTHETIC GLYCOLIPIDS. RAYMOND P. GOODRICH AND JOHN D. BALDESCHWIELER. CALIFORNIA INSTITUTE OF TECHNOLOGY, DEPARTMENT OF CHEMISTRY AND CHEMICAL ENGINEERING, NOYES LAB,127-72,PASADENA,CA 91125.

We have previously described the capacity of a series of synthetic glycolipids to modify the phase behavior of vesicles composed primarily of phosphatidylcholines or phospahatidylethanolamines. Through the use of resonance energy transfer,dynamic light scattering, and electron microscopy, the cryopreservative action of these compounds has been further characterized. Small unilamellar vesicles composed of egg PC or POPC:PS (9:1) undergo significantly reduced amounts of fusion upon freeze/thawing or dehydration/rehydration in the presence of various amounts of the carbohydrate derivatives. This effect is dependent upon the presence of carbohydrate and its structure. The effect is eliminated with blockage of the -OH groups of the carbohydrate through acetalation or exchange in D_2O. The capacity of these derivatives to reduce damage to membranes via fusion is believed to be related to the ability of the bound carbohydrate to interact with the lipid head groups. This work was supported in part by a National Research Service Award (T32 GM07616) from the National Institute of General Medical Sciences, grant no. DAAG-29-83-K-0128 from the ARO, and a gift from Monsanto.

M-Pos151 MONTE CARLO SIMULATION OF CONCENTRATION DEPENDENT LATERAL DIFFUSION RETARDATION REQUIRES INTERMOLECULAR PROTEIN-LIPID INTERACTIONS. Patricia K. Donaldson and Watt W. Webb, Applied Physics, Cornell University, Ithaca, NY 14853.

We have run monte-carlo lattice simulations of protein and lipid lateral diffusion for protein area fractions up to 0.5, in the presence of nearest neighbor intermolecular forces. We compared the resulting diffusion coefficients with experimental data on the effects of bacteriorhodopsin concentration (Peters and Cherry, PNAS 79, 4317, 1982) or gramacidin C concentration (Tank et al., Biophys. J. 40, 129, 1982) in lipid multibilayers. Protein diffusion data could be fit by assuming either an attractive interaction between proteins, as in Pink et al. (BBA 863, 9, 1986), or a repulsive interaction. Both protein and lipid diffusion data could be fit simultaneously by including an additional interaction between proteins and lipids. The nearest neighbor interaction energy between molecules could be included explicitly, as a Boltzmann factor in the hopping probability, or indirectly, by increasing the size of proteins to take into account bound lipid. The size of the lipid boundary layer necessary to fit the data was consistent with the calorimetric estimate of Chapman et al. (J. Mol. Biol. 113, 517, 1977).

This work was supported by NSF grant DMB 8609084 and the Cornell Biotechnology Program. Computations were performed on the Cornell National Supercomputer Facility.

M-Pos152 THE EFFECT OF LITHIUM ON PHOSPHATIDYGLYCEROL AND PHOSPHATIDYLSERINE BILAYERS: NMR AND DSC RESULTS. J.F.M. Post* and D.A. Wilkinson^, *Department of Human Biological Chemistry and Genetics, University of Texas Medical Branch, Galveston, TX, and ^Medical Physics, Allegheny-Singer Research Institute, Pittsburgh, PA.

Lithium is widely used in the treatment of manic-depressive illness. Its mode of action is not well understood, but it is postulated to occur via an interaction with nerve membranes. Our calorimetry (DSC) and Li-NMR studies show that this interaction is very small in the case of DPPC and DPPG. The slight increase seen in the DPPG chain meeting transition temperature (3-4°C) and enthalpy (20%) in Li compared to Na or K is consistent with a partial dehydration of the glycerol headgroup. However, both concentrated DPPC and DPPC-DPPG (4:1) dispersions showed equal quadrupolar splittings of 4.5 kHz at room temperature indicating the lack of effect of surface charge on direct lithium binding. The phase behavior of DMPS in the presence of lithium depends critically on hydration conditions. A reproducible endotherm at 40.6°C (ΔH = 7.1 kcal/mol) can be obtained by hydrating the lipid in LiCl at 90°C. Hydration at 55-60°C produces a presumably less-hydrated lipid species melting at 81°C. The lithium spectrum showed a single line (350 Hz wide) with no visible quadrupolar fine structure within a spectral width of 100 kHz. There may be a distribution of quadrupolar splittings causing the typical quadrupolar spectrum from bound ion to broaden beyond recognition.

M-Pos153 FLUORESCENCE EVIDENCE FOR ETHANOL-INDUCED BILAYER TO INTERDIGITATED GEL TRANSITION IN PC'S.

Parthasarathy Nambi[1], Elizabeth S. Rowe[1] and Thomas J. McIntosh[2], [1]VA Medical Center, Kansas City, MO 64128 and the University of Kansas Medical School, Kansas City, KS; and [2]Department of Anatomy, Duke University Medical Center, Durham, North Carolina 27710.

It is now well established that a number of amphiphilic molecules, including ethanol, can induce the formation of the interdigitated gel phase (I) in PC's. We have shown earlier that ethanol induces biphasic melting behavior in PC's [E.S. Rowe, Biochemistry, 22, 3299 (1983)]. From the work of Simon and McIntosh [BBA, 773, 169 (1984)] it is now recognized that ethanol-induced biphasic melting behavior is a consequence of acyl chain interdigitation. We have found that the fluorophore 1,6-Diphenyl-1,3,5-hexatriene (DPH) can be used to detect the transition from the bilayer gel phase (B) to the I phase. We show that the B to I change can be induced by increasing the temperature. This conclusion is supported by x-ray diffraction experiments. Using fluorescence we have investigated the temperature, alcohol concentration, and lipid chain length dependence of the B to I transition. (Supported by the Veterans Administration and by NIAAA).

M-Pos154 Measurement of Liposome Particle Size by DLS and Light Microscopy, Martin C. Woodle and Francis J. Martin, Liposome Technology, Inc., 1050 Hamilton Court, Menlo Park, CA 94025

A variety of studies have brought to light the realization that the behavior of liposomes can vary dramatically with particle size. Controlling particle size in parenteral formulations is also very important from the point of view of safety.

Accordingly, considerable effort has been applied developing methods for measuring particulates in parenterals and liposome size distributions. Unfortunately, no single method presently exists which is capable of measuring liposome size and distribution (by either mass or number) over the entire range needed. Furthermore, by virtue of the unique nature of liposomes, every available method has problems that must be considered when interpreting results on liposome samples.

Dynamic Light Scattering (DLS), also known as PCS and QELS, has been used extensively to characterize liposome size particularly in the low end of the range (sonicated and other SUV preparations). In this work, a study of the range and resolution of DLS applied to liposomes will be reported. A critical comparison of DLS methodology and recommended modifications for application to liposomes will also be presented.

At the other size extreme (particles > 1 micron), light microscopy is very important in the analysis and characterization of liposome formulations. A computerized video system for enhancing the use of microscopy and quantifying the results will be described including recommendations for further enhancements.

M-Pos155 METASTABLE BEHAVIOUR OF PHOSPHATIDYLETHANOLAMINES (PE) AND PHOSPHATIDYLCHOLINES (PC).

D. Bergstrome, L. X. Finegold, and M.A. Singer. Dept. of Medicine, Queen's University, Kingston, Ontario, Canada K7L 3N6.

Aqueous dispersions of C10PE, C12PE, C14PE and C16PC were prepared and then incubated at 0.1°C, 5°C, 15°C and 25°C for variable periods of time. The thermal properties of these preparations were measured with a Mettler model 2000 B, differential scanning calorimeter. C16PC developed a subtransition at about 18°C; this transition had an optimal incubation temperature of 0.1°C, appeared within 12 hours of incubation, and displayed maximum growth of enthalpy over the first 72 hours. PE dispersions showed variable patterns of metastable behaviour and unlike C16PC, the new transitions in these lipids did not display smooth growth kinetics with incubation time. C12PE preparations had an optimal incubation temperature of 5°C and showed multiple new transitions above the gel to liquid crystal transition temperature (Tc). C14PE preparations displayed multiple subtransitions most consistently when incubated at 0.1°C. C10PE behaved like C12PE and developed several new transitions above the Tc when incubated at 0.1°C. Binary mixtures of C12PE and C14PE displayed metastable behaviour characteristic of the predominant lipid whereas mixtures of intermediate molar concentrations did not form any metastable phases. In contrast to the above results, hydrating C14PE dispersions below the Tc resulted in the appearance of a new transition above the Tc which was replaced by the subtransitions described above when the sample was subsequently incubated at 0.1°C. In summary, PE dispersions show variable new transitions either above or below the Tc dependent upon hydration temperature and incubation conditions. These new transitions display discontinuous growth rather than the kinetics characteristic of C16PC.

M-Pos156 ^{2}H NMR AND HIGH PRESSURE FTIR STUDIES OF THE LOCATION AND PRESSURE-INDUCED EXCLUSION OF THE LOCAL ANESTHETIC TETRACAINE IN MODEL AND NERVE MEMBRANES. I.C.P. Smith*, M. Auger*, H.C. Jarrell*, P.T.T. Wong*, D.J. Siminovitch* & H.H. Mantsch*. *Division of Biological Sciences, *Division of Chemistry, National Research Council of Canada, Ottawa, Ontario, Canada K1A 0R6.

The location of the local anesthetic tetracaine in multilamellar dispersions of 1,2-dimyristoyl-sn-glycerol-3-phosphocholine (DMPC) in the presence and absence of 30 mole % of cholesterol, and in nerves, was determined by deuterium NMR (^{2}H NMR) and high pressure Fourier transform infrared (FTIR) spectroscopy. ^{2}H NMR spectra of specifically deuterated tetracaine indicate that the location of the anesthetic in DMPC bilayers differs in cholesterol-containing DMPC bilayers; in the latter system, the anesthetic is located closer to the aqueous interface of the lipid bilayer. An increase in temperature results in a deeper penetration of the anesthetic into the bilayer. Infrared spectra were measured in a diamond anvil cell at 28°C as a function of pressure up to 25 kbar for the model membrane systems and for two different nerves, the myelinated frog sciatic nerve and the unmyelinated nerve from the lobster walking leg. The results reveal a correlation between the location of the anesthetic in model membranes and that in nerves. They also indicate that tetracaine is expelled by pressure from both model and nerve membranes, and that for model membrane systems, low pH or cholesterol will assist pressure in squeezing the anesthetic out of the bilayer.

M-Pos157

THE THERMOTROPIC PHASE BEHAVIOR OF DIELAIDOYLPHOSPHATIDYLETHANOLAMINE AND THE EFFECT OF n-ALKANOLS. **Jeffrey A. Veiro, Elizabeth S. Rowe. Intr. by Harvey F. Fisher. The University of Kansas Medical School and the V.A. Medical Center, Kansas City, MO.**

An optical density, P-31 NMR and freeze-fracture electron microscopy study of the thermotropic phase behavior of dielaidoylphosphatidylethanolamine (DEPE) is reported. Changes in optical density are observed at the temperature of the main gel to liquid crystalline, and bilayer to inverted hexagonal phase transitions of DEPE. It is shown by both optical density and NMR that the n-alkanols stabilize the bilayer arrangement relative to the inverted hexagonal phase of DEPE and also promote the transition from the bilayer gel to liquid crystalline phase. The structural transition between the bilayer and inverted hexagonal phase of pure DEPE was also investigated by P-31 NMR. A sharp isotropic component in the typical bilayer and inverted hexagonal P-31 NMR spectra was observed on cycling through this transition. The magnitude of the isotropic component was solely a function of the number of cycles through the transition, and it was stable in both the liquid crystalline lamellar and inverted hexagonal states. Freeze-fracture electron micrographs of samples containing the isotropic P-31 NMR resonance showed the presence of an inverted cubic-like phase.
Supported by the Veterans Administration and the National Institute of Alcohol Abuse and Alcoholism.

M-Pos158 pH-SENSITIVE LIPOSOMES: PHASE CHARACTERIZATION AND CORRELATION WITH LIPID MIXING AND CONTENT LEAKAGE. David Collins and Leaf Huang, Department of Biochemistry, University of Tennessee, Knoxville, TN 37996-0840.

We and others have shown that liposomes composed of dioleoylphosphatidylethanolamine (DOPE) and either oleic acid (OA) or palmitoylhomocysteine (PHC) become unstable and fusion active at acidic pH. Such pH-sensitive liposomes are able to mediate the cytoplasmic delivery of encapsulated contents, probably by fusing with the membranes of endocytic vesicles. DOPE alone will not form stable bilayers at neutral pH but will form extensive aggregates characteristic of hexagonal (H_{II}) phase. When a second stabilizing component such as OA or PHC is added to DOPE, stable liposomes can be formed. Fusion of the liposomes can be induced by addition of protons or divalent cations and may involve a transition of the lipids into non-bilayer phases. Since cytoplasmic delivery by pH-sensitive liposomes seems to involve an acid induced fusion with the cellular endosome, an understanding of the phase behavior of pH-sensitive liposomes is important. We have investigated the phase behavior of pH-sensitive liposomes using light scattering to monitor the phase transition. We have also investigated the temperature dependence of leakage and fusion for the two types of liposomes. Our light scattering data suggests that pH-sensitive liposomes undergo a transition from bilayer ($L\alpha$) to H_{II} phase and that the $L\alpha$-H_{II} transition is reflected in the fusion and leakage behavior of the liposomes. Liposomes composed of DOPE:PHC are more stable than DOPE:OA liposomes, requiring higher temperature and/or lower pH values to form H_{II} phase. The greater stability of DOPE:PHC liposomes may indicate that their mechanism of delivery may differ from that of DOPE:OA liposomes. We are currently investigating this possibility. Supported by NIH grant CA 24553.

M-Pos159 THE PHYSICAL PROPERTIES OF THE GANGLIOSIDE GM_1: SINGLE AND MIXED SYSTEMS WITH PHOSPHATIDYLCHOLINE (PC). R.A. Reed and G.G. Shipley, Biophysics Institute, Boston University School of Medicine, Boston, MA 02118

Gangliosides have been shown to function as cell surface receptors, as well as participating in cell growth, differentiation and transformation. Although information concerning their biological functions is plentiful, little is known about their physical properties in membrane systems. The thermotropic and structural properties of GM_1 in single and mixed systems with PCs have been investigated by differential scanning calorimetry (DSC), microcalorimetry (MC) and x-ray diffraction. By DSC and MC, hydrated GM_1 undergoes a broad endothermic transitions T_M=26°C (ΔH=1.7 Kcal/mol GM_1). X-ray diffraction below and above this transition (0 and 33°C) indicated a micellar structure with changes occurring only in the wide angle region (sharp reflection at 1/4.13Å at 0°C; diffuse reflection at 1/4.41Å at 33°C). In hydrated binary mixtures with dipalmitoyl PC (DPPC), GM_1 was shown to decrease the enthalpy of the DPPC pre-transition at low molar compositions (0-20 mol% GM_1) while increasing the T_M of both the pre- and main transition over this range. Between 35 and 85 mol% GM_1 two transitions were observed, and at greater than 85% GM_1 the phase behavior was dominated by the properties of GM_1. X-ray diffraction indicated a single bilayer phase from 0-28 mol% GM_1, with the formation of two separate phases (bilayer and possibly micellar) at greater than 28 mol% GM_1. A hydration study at low GM_1 compositions (5.7 mol%) indicated a conversion of the DPPC bilayers to an infinitely swelling system in the presence of GM_1. The properties of GM_1 were also investigated in the presence of palmitoyl-oleoyl PC and egg yolk PC.

M-Pos160 STABILIZATION OF H_{II} PHASES BY LOW LEVELS OF DIGLYCERIDES & ALKANES: AN NMR, DSC & X-RAY DIFFRACTION STUDY -D.P. Siegel, J. Banschbach[1], and P.L. Yeagle[2]; [1]Procter & Gamble Co., Cincinnati, OH 45247, [2]Dept. of Biochemistry, School of Medicine, SUNY Buffalo, NY 14214

Small amounts (2-5 mole %) of hydrophobic molecules like diglycerides [1] and alkanes [2] greatly reduce the L_α/H_{II} transition temperature (T_H) of phospholipid membranes. Important properties of membranes, including susceptibility to fusion [3], change near T_H. The T_H of biomembrane lipids, and hence these properties, might be modulated by metabolic production of such molecules (e.g., diglycerides by PI hydrolysis). To determine the environment of hydrophobic molecules in H_{II} phases and infer how trace levels of them stabilize H_{II} phases, we obtained ^{2}H-and ^{31}P-NMR spectra of monomethylated dioleoyl-PE (DOPE-Me) systems containing 2-8 mole % of perdeuterated alkanes or dipalmitin. Kirk & Gruner proposed that alkanes partition into the interstices between H_{II} tubes, reducing an unfavorable chain-packing contribution to the H_{II} free energy [4,6]. The ^{2}H-NMR data are consistent with this interpretation. ^{2}H-NMR spectra of the L_α phases indicate that alkanes reside near the bilayer midplane with chains roughly aligned with the phospholipids, as others suggested [5]. There is a dramatic reduction of alkane orientational order in the H_{II} phase, implying an interstitial location. The ^{2}H-NMR linewidths at various alkane contents and the consistent decrease in T_H with increasing alkane content show that these signals do not arise from phase-separated alkane. In contrast, the dipalmitin data are most consistent with diglyceride localization at the lipid-water interfaces in both phases, with the dipalmitin chains parallel to those of DOPE-Me. This implies that diglyerides lower T_H by reducing the spontaneous radius of curvature of the lipid/water interfaces, R_o [6]. X-ray diffraction data also support this interpretation. -(1) Biophys.J. 51:355a; (2) ibid., 26:231; (3) Biochem. 25:4141; (4) J. Physique 46:761; (5) Chem. Phys. Lip. 35:259; (6) PNAS 82:3665.

M-Pos161 CRYO-TRANSMISSION ELECTRON MICROSCOPIC STUDY OF LIPOSOMAL DISPERSIONS UNDERGOING THE LAMELLAR/INVERTED HEXAGONAL (L_α/H_{II}) PHASE TRANSITION

Y. Talmon[1], D. Siegel, J. Burns, and M. Chestnut[2]; [1]Dept. Chem. Enging., Technion, Haifa 32 000, Israel; [2]Procter & Gamble Co., Cincinnati, OH 45247.

We are using Cryo-Transmission Electron Micrsocopy (CTEM [1,2]) to study the first events occurring between unilamellar liposomes during the L_α/H_{II} phase transition. CTEM is desirable because (a) the procedure freezes ca. 0.5 μm-thick films of the sample on sub-millisecond time scales (fast enough to image intermediate structures [3]); (b) no perturbative staining or freeze-fracture techniques are necessary; and (c) the samples are viewed in the transmission mode at temperatures $<108^oK$, allowing imaging of entire hydrated aggregates rather than single fracture planes. We have studied DOPE dispersions prepared via high-pressure filtration at pH 9.9. We trigger the L_α/H_{II} phase transition just prior to rapid freezing by mixing the sample solution with a buffer of pH ≤ 8 on the microscope grid. Under these circumstances, the sample is extensively aggregated within seconds. No H_{II} phase formation occurs on isolated unilamellar structures in these preparations, and domains of what appear to be H_{II} phase are observed only within aggregates of liposomes. This indicates that the transition requires close apposition of bilayers in order to proceed, and that the intermediates in the transition are probably inter-lamellar structures, as has been suggested [e.g., 3]. We will also describe some curious liposome morphology observed even when the L_α phase is the equilibrium phase. The present resolution is ca. 25Å, but a search for L_α/H_{II} intermediate structures at higher resolution (5Å) is planned. (1) J.R. Bellare, et al., this volume; (2) J.R. Bellare, et al., J. EM Tech. (in press); (3) D.P. Siegel, Biophys. J. 49:1155 (1986).

M-Pos162 MULTIFREQUENCY CALORIMETRY OF PHOSPHOLIPID BILAYER MEMBRANES. O. L. Mayorga, J. L. Lacomba and E. Freire. Department of Biology, The Johns Hopkins University, Baltimore, MD 21218

A newly developed multifrequency calorimeter has been used to study the gel-liquid crystalline transition of phosphatidylcholine bilayers. This instrument has been designed to measure the amplitude and time regime of the enthalpic fluctuations associated with structural transitions in biological macromolecules. The heat capacity function is directly proportional to the magnitude of the enthalpic fluctuations in a system. At the transition region, macromolecular systems exhibit relatively large enthalpy fluctuations that give rise to the characteristic peaks observed by conventional differential scanning calorimetry. The multifrequency calorimeter developed in this laboratory has been designed to measure the frequency spectrum of the enthalpy fluctuations, thus allowing us to estimate relaxation times and amplitudes in order to dynamically characterize energetic processes within a macromolecular system. This information is obtained from the attenuation in the amplitude and phase angle shift of the response of the system to a periodic heat wave. The frequency-temperature response surface for large dimyristoyl phosphatidylcholine (DMPC) vesicles has been measured and is consistent with a relaxation time in the order of 80 ms at the midpoint of the main gel-liquid crystalline transition. (Supported by NIH grants GM-37911 and NS-24520.)

M-Pos163 INTERACTION OF WATER WITH A LIPID MOLECULE. Irina Vayl and David Busath. Section of Physiology and Biophysics, Brown University, Providence, R.I. 02912.

As a first step in the study of the structure of a lipid bilayer and mechanism of its formation in water solution we calculated using Charmm the electrostatic and Van-der-Waals energy of interaction between a lipid molecule and a water molecule, placing it around the lipid molecule from head to tail.

The VDW attractive energy exceeds the electrostatic repulsion by approximately two times near the hydrocarbon chain of the lipid and is ten times less than the electrostatic energy in the area of the head group.

The calculations involving the energy minimization allowed us to find more favorable positions for the water molecule relative to the lipid. Analyzing these data together with data from calculations of the lipid monolayer and bilayer structure and water-water interactions we can better understand the process of diffusion of water molecules from bulk water into the lipid membrane.

M-Pos164 DETERMINANTS OF MISCIBILITY OF DIACYL PHOSPHATIDYLCHOLINES AND 1,3 DIOLEIN IN MONOLAYERS AND BILAYERS. B. A. Cunningham, J. M. Smaby and H. L. Brockman, Hormel Institute, University of Minnesota, Austin, Minnesota 55912.

The miscibility of 1,3 diolein (DO) with dimyristoyl, 1-palmitoyl-2-oleoyl, dioleoyl, and diphytanoyl phosphatidylcholine (PC) was studied at the argon-buffer interface. The surface pressure-area isotherms for the pure PC's were parallel with approximately equal collapse pressures. Molecular areas at collapse ranged from 47.6 to 69.0 $Å^2$ and for the first three PC's varied linearly with the fraction of cis-unsaturated chains. Isothermal phase diagrams for the PC-DO mixtures at 24°C exhibited PC-DO complex formation with a region of PC and complex coexistence and a region of complex and DO miscibility. The areas of the PC-DO complexes paralleled the PC's alone, but the mole fractions (MF's) of DO in the complexes (X_c's) are constant at 0.21 ± 0.03. Thus, X_c is determined by head group interaction (i.e., dehydration), not by acyl group structure. The miscibility of DO and 1-stearoyl-2-oleoyl PC dispersed in excess buffer was determined using high resolution differential scanning calorimetry. For all PC-containing mixtures, the temperature-composition phase diagram exhibits a transition centered around 9°C, presumably due to the melting of mixed bilayers. Above 0.25 MF of DO there is a second transition centered at 23°C which corresponds to the chain melting of pure DO. The magnitude of the second peak is zero at 0.25 MF of DO and increases linearly with increasing MF. That the X_c's for bilayers and monolayers are nearly the same indicates that the miscibility of DO with PC in both systems is governed by the same interactions. (Supported by NIH grants HL 07311 and HL 08214 and the Hormel Foundation).

M-Pos165 **EXCHANGE AND SHUTTLING OF ELECTRONS BY NITROXIDE SPIN LABELS**

David O. Nettleton, Harold M. Swartz, and Philip D. Morse, II
University of Illinois College of Medicine and Illinois ESR Research Center, Urbana, IL 61801

Nitroxides are able to exchange electrons with hydroxylamines, resulting in reduction of the nitroxide to a hydroxylamine and oxidation of the hydroxylamine to a nitroxide. A positively charged nitroxide, Cat_1 (4-trimethyl amino 2,2,6,6-tetramethyl piperidine 1-oxyl), when encapsulated within liposomes, is not reduced by externally added ascorbate. If the permeant nitroxide Tempone (4-oxo-2,2,6,6-tetramethyl piperidine 1-oxyl) is now added, the Tempone is reduced to the corresponding hydroxylamine by the external ascorbate and. eventually, the Cat_1 is also reduced. The rate at which Cat_1 is reduced is proportional to Tempone and Cat_1 concentration, but is independent of ascorbate concentration. Similar results were found using Tempone and Cat_1 in TB cells. The only hypothesis consistent with these observations is that Tempone acts as an electron shuttle, transferring electrons from ascorbate, across the lipid bilayer, to Cat_1. 5-doxyl stearate also promotes the reduction of Cat_1 in much the same way, except that it is restricted to flip-flop motion from one side of the bilayer to the other and the resultant relative reaction rate is slower. When reduced ^{15}N-PDT (^{15}N perdeuterated Tempone) is mixed in solution with Cat_1, electron transfer from the reduced ^{15}N-PDT to Cat_1 is observed directly by monitoring the decrease in Cat_1 ESR signal and the concomitant increase in signal intensity from ^{15}N-PDT. The equilibrium constant for this latter system is Keq = 2.18. We conclude that membrane-permeable nitroxides can act as electron shuttles and reduce otherwise inaccessable nitroxides in liposomes.

Supported by NIH grants RR 01811, GM 35534, GM 34250, and CA 09067.

M-Pos166 **THERMOTROPIC BEHAVIOR OF MIXTURES OF GLYCOSPHINGOLIPIDS AND PHOSPHATIDYLCHOLINE: EFFECT OF MONOVALENT CATIONS ON SULFATIDE AND GALACTOSYLCERAMIDE, DAVID A. RINTOUL, RUTH WELTI, AND WENXIA SONG, BIOLOGY DIVISION AND BIOCHEMISTRY DEPARTMENT, KANSAS STATE UNIVERSITY, MANHATTAN KS 66506**

The thermotropic behavior of both sulfatide (3-sulfogalactosylceramide) and galactosylceramide in dielaidoylphosphatidylcholine (DEPC) liposomes was studied using steady-state fluorescence polarization of parinaric acid and parinaric acid-labeled lipids. The glycosphingolipid (GSL) concentration of the liposomes was varied from 0 to 100%, and phase diagrams were constructed. These data indicate that sulfatide and DEPC are immiscible in the gel phase at sulfatide mole ratios of less than 0.30. Above this ratio, the lipids are miscible in the gel phase. The temperature of onset of the gel-liquid crystalline phase transition is higher in K^+-containing buffer than in osmotically equal Na^+-containing buffer; the end point of this transition is not altered. Similar measurements, using galactosylceramide, a neutral GSL, indicated that this lipid and DEPC were immiscible in the gel phase at galactosylceramide mole ratios of less than 0.40. Above this level, the lipids were miscible in the gel phase. In contrast to the results obtained using sulfatide, onset temperatures in mixtures of DEPC and galactosylceramide were identical in Na^+ or K^+-containing buffers. These observations indicate that monovalent cations might affect motion and distribution of sulfatide in biological membranes, and further implicate this GSL as an important determinant of function of the Na^+, K^+-ATPase.

M-Pos167 MODULATION OF METASTABILITY IN DIUNDECANOYL PHOSPHATIDYLETHANOLAMINE BILAYERS. Hui Xu, Frances A. Stephenson, and Ching-hsien Huang, Department of Biochemistry, University of Virginia Sch. of Med., Charlottesville, VA 22908.

High-resolution differential scanning calorimetry (DSC) and ^{31}P NMR spectroscopy have been used to study the thermal history of aqueous C(11):C(11)PE dispersions. The lipid dispersions were treated in two different ways. One involved the sonication of cold samples, called nonheated samples, and the other involved the intermittent sonication of the dispersion at 55°C, called the heated sample. The nonheated sample exhibits a single sharp endothermic transition centered at 38.4°C, and a shift in T_m to 18.6°C is observed if the sample is subjected to an immediate second heating scan. The thermograms for heated samples, however, are characterized by two sharp endothermic transitions centered at 18.3 and 37.9°C, respectively, and a relatively broad exothermic transition which occurs between the two endothermic transitions. The relative peak intensity of the two endothermic transitions observed for heated samples depends on the incubation time allowed at 4°C. Similar DSC experiments have been performed with N-monomethyl-C(11):C(11)PE. In this case, both heated and nonheated samples exhibit identical thermotropic behavior with a single endothermic transition at 9°C. A total elimination of the bilayer metastability of C(11):C(11)PE by monomethylating the lipid headgroup suggests that the headgroup-headgroup interaction may take place between the lipid lamellae, and the lipid metastable behavior may be attributable to the headgroup-headgroup interaction. Supported by NIH Grant GM-17452.

M-Pos168 DRY DIPALMITOYLPHOSPHATIDYLCHOLINE AND TREHALOSE REVISITED. Lois M. Crowe and John H. Crowe, University of California, Davis, CA 95616.

We have reinvestigated the interactions of the disaccharide, trehalose, with bilayers of dipalmitoylphosphatidylcholine (DPPC) in order to rectify some of the unavoidable experimental defects of the original study (Crowe *et al.*, Science 223, 1984). Specifically, our mixtures of lipid and carbohydrate have been formed from an aqueous rather than organic medium and the mixtures have been kept as dry as possible at all stages to eliminate the effects of slight and unquantified hydration. Unilamellar vesicles were formed from DPPC by sonication (av. diameter, 25 nm) or by extrusion (av. diameter, 90 nm) and then either lyophilized (gel phase) or dried over anhydrous $CaSO_4$ at 60°C (liquid crystalline phase), followed by exposure to vacuum. The effects of trehalose on the gel to liquid crystalline transition were even more striking than in our previous study: at a 1:1 mass ratio, trehalose decreased T_m of *dry* DPPC approximately 80 °C (from 105 °C to 24 °C. The effect of trehalose on T_m depended on the amount of trehalose present and whether the sample was dried from above or below T_m. The effect of storage at low temperature was also studied: samples stored at 4-6 °C for about 4 weeks showed a reversion to a higher transition temperature, i.e. they packed as if they had been dried in gel phase. A phase diagram for dry DPPC/trehalose is presented. Results indicate that the PC headgroups require the expanded liquid crystalline spacing for maximum interaction with trehalose, as previously suggested by Gaber *et al.* (Biophysical J. 49, 435a, 1986) for DMPC. (Supported by grant DMB 85-18194 from NSF).

M-Pos169 BILAYER MEMBRANES CONTAINING POSITIVE LIPIDS. J. Cui*, S. McLaughlin*, G. Ljunger, R. Pashley. Dept. Physiology & Biophysics, HSC, SUNY, Stony Brook* and Dept. Chemistry, ANU, Canberra, Australia.

Double-chained quaternary ammonium surfactants form positively charged bilayer membranes. The electrostatic surface potential deduced from force measurements between these bilayers adsorbed onto mica sheets (Mara, 1986; Pashley et al., 1986), and from NMR, fluorescence, conductance, mobility (Winiski et al., 1986) and EPR (Hartsel & Cafiso, 1986) measurements can be described by Gouy-Chapman-Stern theory. All available measurements suggest that anions bind to the surface in the sequence $F, OAc < Cl < Br, NO_3$. However, the intrinsic binding constants for Cl (10 M^{-1}) and Br (100 M^{-1}) deduced from force measurements are an order of magnitude higher than those deduced from the other measurements. We wondered if ions bind more strongly to adsorbed than to free bilayer membranes. To test this possibility, we measured the electrophoretic mobility of multilamellar bilayer vesicles formed from mixtures of a zwitterionic and positive lipid and also the mobility of monodisperse silica spheres coated with a bilayer of positive lipid. We obtained similar results with the free and adsorbed bilayers, which rules out this possibility. If the hydrodyanamic plane of shear is 0.2 nm from the surface, the data can be described by assuming the intrinsic binding constants of F, OAc; Cl; Br, NO_3 are of order 0; 1; 10 M^{-1}. We will discuss possible explanations for the small difference between the electrostatic potentials deduced from force and mobility measurements.

M-Pos170 THE PROFILE OF THE ELECTROSTATIC POTENTIAL ADJACENT TO CHARGED BILAYER MEMBRANES. M. Langner and S. McLaughlin. Dept. Physiology and Biophysics, HSC, SUNY, Stony Brook, NY 11794

The Poisson-Boltzmann equation predicts how the electrostatic potential should depend on the distance from a charged bilayer membrane. Marra (1986), Pashley et al. (1986) and Evans & Parsegian (1986) tested this prediction by measuring the force between charged bilayer membranes. We measured the potential both at the surface and 1 nm from the surface of charged membranes using fluorescent probes. We formed lipid bilayer membranes with charge at the surface (5:1 PC:PS and PC:PI) and with charge 1 nm from the membrane surface (5:1 PC:G_{M1}). We estimated the potential 1 nm from the surface by attaching fluorescent probes to the sialic acid residue of G_{M1}, incorporating this molecule into vesicles, and quenching the fluorescence with the cations thallium or tempamine (Wininski et al., Biochemistry, in the press). We used a similar technique to estimate the potential at the surface of the vesicles, and obtained results that agreed with other measurements of the surface potential. The potential 1 nm from the surface of the PC:PS and PC:PI membranes agreed with the prediction of Gouy-Chapman theory. The potential 1 nm from the PC:G_{M1} bilayer agreed with the prediction of the more general, but still highly oversimplified, Poisson-Boltzman eqation. Supported by NIH grant GM24971, NSF grant BNS 8501456 and a post-doctoral fellowship from the Anna Fuller Fund.

M-Pos171 THE ELECTROSTATIC POTENTIAL DUE TO A SINGLE FIXED CHARGE AT A MEMBRANE-SOLUTION INTERFACE. R. T. Mathias, S. McLaughlin, G. Baldo, and K. Manivannan, Department of Physiology & Biophysics, HSC, SUNY, Stony Brook, N.Y. 11794.

We present expressions for the potential produced by a single fixed charge q at a membrane-solution interface. We simplify the problem by ignoring the finite thickness of the membrane, confining the electrolyte to the aqueous phase, and making all the assumptions inherent in the simplest form of the Debye-Huckel theory. Thus the problem is reduced to solving the Laplace equation for the membrane phase and the linearized Poisson-Boltzmann equation for the aqueous phase. When the dielectric constant of the aqueous phase, ε_a, is much greater than the dielectric constant of the membrane phase, ε_m, the potential in the aqueous phase is given approximately by: $\psi_a \cong 2q\exp(-\kappa r)/(4\pi\varepsilon_o\varepsilon_a r)$. This equation, which has been used previously by other investigators without derivation (e.g. Cole, 1969; Nelson and McQuarrie, 1975), is twice the Debye-Huckel expression for the potential produced by a charge q in a bulk aqueous solution. The equipotential curves are continuous at the interface, but protrude farther into the membrane than the aqueous phase. The curves in the membrane exhibit a bulge near the interface because the field lines bend back towards the counterions in the aqueous phase. The shape of these curves depends on the ratio $\varepsilon_m/\varepsilon_a$. The average potential in the aqueous phase due to a number of discrete charges fixed at the interface is independent of ε_m, however, and is identical to the potential obtained from linearized Gouy-Chapman theory, in which the fixed charges are assumed to be uniformly smeared over the membrane-solution interface with a density σ: $\langle\psi_a(z)\rangle = (\sigma/\varepsilon_o\varepsilon_a\kappa)\exp(-\kappa z)$.
NIH GM24971, NSF BNJS8501456, NIH EY06391, NIH HL36075.

M-Pos172 CRYOPROTECTION OF PHOSPHOLIPID MEMBRANES BY AMINO ACIDS
T. Anchordoguy, S.H. Loomis, J.F. Carpenter, and J.H. Crowe
University of California, Davis

The abilities of eleven amino acids to inhibit fusion between liposomes during freeze/thaw were assessed by resonance energy transfer. Small unilamellar vesicles were frozen in liquid nitrogen and thawed at room temperature in a variety of amino acid solutions. In addition to amino acids, some of the solutions contained 350mM NaCl. The presence of salt transformed some fusogenic amino acids, e.g. glutamine (90% probe intermixing at 100mM), glycine (77%), and alanine (82%), into effective cryoprotectants, (5%, 12%, 15%, respectively). We suggest that this effect is due to electrostatic interaction between the salts and ionizable sites on the amino acid or the phospholipid. However, the salt had no effect on other fusogenic amino acids with similar structures, e.g. glutamate, aspartate, leucine, isoleucine, and valine (approx. 90% intermixing at 100mM). Futhermore, certain amino acids, e.g. arginine, histidine, and lysine, minimized probe intermixing regardless of the presence of salt (5% intermixing at 100mM). The latter three amino acids all have a secondary amino nitrogen in their side chain. We believe that this nitrogen interacts directly with membrane phospholipids, and we will present results of experiments that test this hypothesis.

M-Pos173 PREVENTION OF HEXAGONAL PHASE TRANSITIONS IN PHOSPHATIDYLETHANOLAMINE. Christina Aurell Wistrom, Lois M. Crowe, John H.Crowe, Department of Zoology, Univ. of California, Davis, CA 95616.

Some phosphatidylethanolamines (PE) are known to form non-bilayer phases such as inverted hexagonal tubules or lipidic particles under physiological condition. These non-bilayer structures are formed by destabilization of the bilayer and are supposed to responsible for damage to biological membranes containing PE during conditions such as freezing or dehydration, causing leakage of cytoplasmic contents or fusion of cell membranes. The thermotropic phase behavior has been studied in hydrated L-α-dioleoylphosphatidylethanolamine (DOPE) in presence of trehalose (a disaccharide) and other carbohydrates, with Fourier transform infrared spectroscopy (FT-IR), differential scanning calorimetry (DSC) and electron microscopy. FT-IR of hydrated DOPE showed the thermotropic transition temperatures for the gel to liquid crystalline (LC) phase to about -8 oC and for the LC to H_{II} phase at 8 ^{o}C. In presence of trehalose 1:4 (mol lipid/mol trehalose) no H_{II} transition could be seen in the symmetric CH_2 stretching vibration (2850 cm $^{-1}$) in the acyl chain region. Results from DSC scans of hydrated DOPE with various concentrations of trehalose up to 4.0 mol/mol lipid have been recorded. At concentrations of 0.3 mol/mol a H_{II} transition was detected and at 0.4 mol/mol and above no transition could be found up to 60 ^{o}C, the limit of the scan. A preliminary binary phase diagram of hydrated DOPE in presence of different mol fractions of trehalose was constructed based on results from DSC. Electron micrographs support the above results suggesting that trehalose interacts with the lipid and prevents the H_{II} transition in DOPE. (Supported by grant DMB 85-18194 from NSF).

M-Pos174 GEL TO LIQUID CRYSTALLINE PHASE TRANSITIONS ARE RESPONSIBLE FOR LEAKAGE FROM DRY POLLEN DURING REHYDRATION. J. H. Crowe, F.A. Hoekstra, and L.M. Crowe. University of California, Davis, and Agricultural University, Wageningen.

When dry pollen or seeds are imbibed they leak their cytoplasmic contents. This leakage has been hypothesized to be due to the presence of hexagonal II (H_{II}) phase lipids in the plasma membrane of the cell. Many investigators have searched for non-bilayer phases in membranes of such organisms, without success, a potential explanation for which is presented elsewhere at these meetings (poster by Aurell Wistrom *et al.*). We present evidence here that the leakage is due to a gel to liquid crystalline phase transition during imbibition. Using Fourier transform infrared spectroscopy it was possible to record spectra in the CH_2 stretching region in intact pollen of *Typha*. The vibrational frequency of the CH_2 groups abruptly increases with temperature, thus providing an estimate of the transition temperature (T_m). T_m changed with hydration state, from $0o^{C}$ in hydrated pollen to 33^{o}C in dry pollen. Concurrent studies on purified phosphatidylcholine (PC) from the same pollen were consistent with this change in T_m with hydration state. Further, studies with the isolated PC showed that sucrose, found at high concentrations in the pollen, depresses T_m, and probably does so *in vivo*. When the pollen was imbibed at various temperatures viability increased with temperature coincidentally with the increase in vibrational frequency of the CH_2 groups. In fact, viability of the pollen is linearly and directly related to this vibrational frequency while leakage is inversely related to it. We interpret these findings as consistent with the hypothesis that leakage is due to a gel to liquid crystalline phase transition during imbibition. (Supp. by grant DMB 85-18194 from NSF).

M-Pos175 STRUCTURE OF FULLY HYDRATED LIPID BILAYERS

M. C. Wiener, R. M. Suter and J. F. Nagle. Department of Physics, Carnegie Mellon University, Pittsburgh, PA 15213.

Traditional methods of obtaining electron density profiles for lipid bilayers use the interlamellar repeat diffraction intensity data, which is sometimes supplemented by measuring the interlamellar repeat distance D as a function of water content to obtain n_W, the number of water molecules per lipid in the fully hydrated bilayer. In a previous abstract [Wiener et al. (1986) Biophys. J. 51:159a], we showed that volumetric data obtained in our lab could be usefully combined with wide angle x-ray data, the D spacing, and n_W. However, that analysis did not use the low angle intensities. In this presentation, all the relevant data are employed, including new low angle x-ray data obtained for DPPC using a diffractometer equipped with a rotating anode source, graphite crystal monochromator, and scintillation detector. The analysis represents the electron density profile as a constant density for the interlamellar water, a constant density for the methylene hydrocarbon region, a negative Gaussian for the terminal chain methyls and one or more Gaussians for the headgroup region. This representation, which is similar to the strip model representation [Worthington (1969) Biophys. J. 9:222], is more definitive in describing the different regions of the bilayer than the traditional Fourier representation. The analysis also yields the area per lipid molecule and the chain tilt for phases with essentially all-trans chains. The analysis does not require solution of the phase problem but predicts phases in good agreement with those given in the literature.

M-Pos176 NEW LOW TEMPERATURE PHASE IN DPPC/WATER DISPERSIONS

C. P. Yang, M. C. Wiener, and J. F. Nagle. Department of Physics, Carnegie Mellon University, Pittsburgh, PA 15213.

Dispersions were formed by hydrating, in excess cold (5°C) water, DPPC that had been freshly lyophilized from chloroform at 5°C. With no further incubation at low temperatures these preparations exhibit sharp endothermic DSC peaks at temperatures between 21 and 26°C, depending upon scanning rate, that could be confused with the subtransition. The transition enthalpy (9 kcal/mole) is larger than that of the subtransition (4.1 kcal/mole, Tristram-Nagle et al., Biochemistry, 26, 4288 (1987)), although this difference might be attributed to imperfect formation of the C phase in the previous work. The true transition temperature was determined by equilibrium dilatometry to be about 19°C compared to 14°C for the subtransition, strongly indicating that the new transition is not the same as the subtransition. The volume change at the transition (0.025 ml/g) is only slightly larger than the subtransition volume change (0.017 ml/g), so the ratio of volume change to enthalpy change is 50% smaller than for the subtransition and the main transition, and similar to that of the pretransition. The X-ray diffraction pattern of this low temperature phase has strong reflections corresponding to 64.9, 15.3, 9.19, 4.23, 3.82 Angstroms, as well as a number of weaker reflections. This pattern is unlike that of the usual C phase or the usual gel phase and does not have a characteristic lamellar repeat pattern, indicating that the low temperature phase is a new nonlamellar phase.

M-Pos177 DISPROPORTIONATION IN PHOSPHOLIPID-DETERGENT SYSTEMS: COEXISTENCE OF VESICLES AND MICELLES.

G. Strauss[a], F. Alhaique[b], A. Memoli[b], E. Santucci[b], and F.M. Riccieri[b], [a]Dept. of Chemistry, Rutgers University, Piscataway, NJ 08854, and [b]Institute of Pharmaceutical Chemistry, University of Rome 00185, Italy.

Small unilamellar zwitterionic and anionic phospholipid vesicles were equilibrated with ionic single-chain detergents, bile salts, and blood plasma. Particle size distributions were assessed by dynamic light scattering and turbidity. Loss of vesicle integrity was measured by release of self-quenched carboxyfluorescein (CF) from vesicle cores. Some of these detergents at low mole fractions produced enlarged vesicles but no micelles. At higher detergent/phospholipid ratios, micelles coexisted with vesicles for 24 hours or longer. Vesicle and micelle sizes changed only slightly with increasing detergent/lipid ratio, but the mass ratio of micelles to vesicles increased until only micelles remained. The decline of CF retention with increasing detergent/lipid ratio was much steeper than the decline in the number of vesicles. This showed that the bilayers were disrupted by detergents even when no micelles were present.

Differences between measured micelle/vesicle ratios and overall detergent/phospholipid ratios demonstrated that the reaction mixture disproportionates, forming mixed vesicles containing detergent, and mixed micelles containing phospholipid. This occurs at detergent concentrations below the CMC for that detergent as measured in the absence of phospholipid. Disruption of bilayers by detergents is a function of the critical packing parameters ($V/\ell A$) of the interacting molecules and also depends on the creation of discontinuities.

M-Pos178 [^{3}H]RYANODINE BINDING TO SARCOPLASMIC RETICULUM Ca^{2+} RELEASE VESICLES.
GERHARD MEISSNER, JEFFREY La DINE AND JOHN SUTKO*. Department of Biochemistry, University of North Carolina, Chapel Hill, NC 27599 and *Department of Pharmacology, University of Nevado, Reno, NV 89557.

Ryanodine, a plant alkaloid isolated from the wood of Ryania speciosa, modifies the conductance and gating behavior of the skeletal and cardiac sarcoplasmic reticulum (SR) Ca^{2+} release channels by inducing the formation of a long-lasting subconductance channel state [Rousseau *et al.*, 1987, *Am. J. Physiol.* 253, C368]. Binding of [^{3}H]ryanodine to the membrane bound and detergent solubilized skeletal SR Ca^{2+} release channel was determined in the presence of the protease inhibitor DIFP and assayed by centrifugation and absorption to glass fiber filters soaked in polyethyleneimine. Both the rate of association and dissociation were dependent on free Ca^{2+}, Mg^{2+} and adenine nucleotides. Under optimal conditions in the presence of micromolar Ca^{2+} and millimolar adenine nucleotide, the presence of a single high-affinity receptor site was observed with a K_D in the 4-10 nM range and B_{max} values of 0.1, 25 and 600 pmol/mg protein for whole rabbit skeletal muscle homogenates, Ca^{2+} release vesicles and the purified receptor, respectively. Reduction of free Ca^{2+} to [nM] reduced the association rate and affinity of ryanodine binding to the membrane-bound channel, whereas omission of nucleotide affected only the association rate. The slow rate of [^{3}H]ryanodine dissociation from its binding site ($\tau_{1/2}$> 10h at 37°C) in the presence of μM Ca^{2+} and mM nucleotide was accelerated 10-100 fold by addition of Mg^{2+} or by decreasing free Ca^{2+} to [nM]. [^{3}H]ryanodine binding and activation of Ca^{2+} release correlated with a majority of SR junctional-derived vesicles containing 3-10 Ca^{2+} release channels/vesicle.

Supported by NIH grants AR 18687 and HL 27470 and MDA.

M-Pos179 IMMUNOLOGICAL STUDY OF CA^{2+} RELEASE COMPONENTS OF SARCOPLASMIC RETICULUM
Mario S. Rosemblatt[a,c], Maria Eugenia Cifuentes[a], and Noriaki Ikemoto[a,b] a Dept. Muscle Res., Boston Biomed. Res. Inst., Boston, Mass. 02114; b Dept. Neurol., Harvard Med. Sch.; c Lab. Biol. Cell. Immunol., Univ. Chile

We have been searching monoclonal antibodies (mAb) that have definitive effects on Ca^{2+} release from SR. One of our SR-specific mAbs, mAb 6/29, was found to be such a mAb. Incubation of SR with the mAb shortened the holding period of the maximal level of active Ca^{2+} uptake, and increased the rate of the subsequent spontaneous Ca^{2+} release with no appreciable effect on Ca^{2+}-ATPase activity. These effects were completely blocked by several uM ruthenium red, suggesting that the mAb binds to Ca^{2+} release components rather than to the Ca^{2+}-ATPase. The rate of passive $^{45}Ca^{2+}$ efflux was approximately doubled after the mAb treatment as determined by rapid filtration. The mAb had no appreciable effect on the $[Ca^{2+}]_o$-dependence of passive efflux as shown by stopped-flow studies with chlorotetracycline. At [mAb] that yields the maximum effect (e.g. 1:25 mAb:SR protein, w/w), the amount of mAb 6/29 bound was not more than 3 ug/mg SR, indicating that the antigen is a minor component of SR. The antigen concentration was significantly increased upon purification of the 'junctional face membrane' fraction containing proteins with M_r (in kDa) of 350, 160, 30 and calsequestrin. These results support the view that the Ca^{2+} release machinery is localized in the junctional face membrane region of SR. Further characterization of the antigen is in progress. (Supported by grants from NIH and MDA)

M-Pos180 CHARACTERIZATION OF CA^{2+} RELEASE COMPONENTS OF SARCOPLASMIC RETICULUM WITH POLYAMINES
Maria Eugenia Cifuentes[a], Michel Ronjat[a], and Noriaki Ikemoto[a,b] a Dept. Muscle Res., Boston Biomed. Res. Inst., Boston, Mass. 02114; b Dept. Neurol., Harvard Med. Sch.

Some polyamines are potent inhibitors of release of actively loaded Ca^{2+} in the presence of pyrophosphate (Palade, P., J. Biol. Chem. 262, 6149, 1987). In an attempt to develop appropriate markers of the key proteins involved in Ca^{2+} release, we reinvestigated the effects of several polyamines on caffeine- and Ca^{2+}-induced Ca^{2+} release in the absence of Ca^{2+}-precipitating reagents. Although neomycin and gentamycin inhibited Ca^{2+} release in agreement with the report, polylysine, protamine and spermine induced rapid Ca^{2+} release at low concentrations (e.g. at 0.6 uM polylysine the maximal release rate = 5.4 s^{-1}). The polylysine-induced Ca^{2+} release was inhibited by the Ca^{2+} release blocker ruthenium red (RR), and the amount of [^{3}H]-polylysine binding was significantly reduced by RR (e.g. from 100 pmol/mg SR to 40 pmol/mg by 2 uM RR). Thus, RR and polylysine bind competitively at least partly to the same site(s). In order to identify the polylysine-binding components, a heavy SR fraction was solubilized with zwittergent 3-14 and passed through a polylysine affinity column (polylysine-Affigel 102). Components with M_r > 300 k and calsequestrin were found to be the major polylysine binding proteins. Further studies with an azido-labeled [^{3}H]-polylysine are in progress. (Supported by grants from NIH and MDA)

M-Pos181 EFFECTS OF MAGNESIUM(II) ON LANTHANIDE(III) IONS AT CALCIUM(II) SITES ON SARCOPLASMIC RETICULUM ATPASE. Eileen M. Stephens and Teresa Zirino, Department of Physiology and Biophysics Program, University of Virginia, Charlottesville, VA 22908.

Magnesium(II) is a essential ion in the transport cycle of Ca(II)ATPase. MgATP is the substrate under physiological conditions, and Mg(II) is required for the rapid breakdown of the phosphorylated intermediate, EP, and the release of calcium ion into the lumen of the sarcoplasmic reticulum. The observation of both high and low affinity sites, and of cooperative binding suggest that magnesium may have other functions in this system.

We have used the paramagnetic and luminescent properties of trivalent lanthanide ions, terbium and gadolinium to monitor the effects of the addition of $MgCl_2$ to mixtures of rabbit skeletal muscle SR vesicles and lanthanide trichlorides. In the presence of 5mM $MgCl_2$ we observe increased occlusion of these ions, as indicated by decreasing hydration and increasing dipole-dipole correlation times. The aqueous medium surrounding the vesicles was removed by pelleting the vesicles. The low water-proton relaxation rate in the buffer solution indicated that no kick-off of paramagnetic ions had occured after the addition of magnesium.

(Supported by NIH grants DK 35865 and 5-SO7 RR05431-28, and by the Muscular Dystrophy Association.)

M-Pos182 CONFORMATIONAL TRANSITIONS IN THE CALCIUM ATPASE IN SKELETAL SR STUDIED BY TIME RESOLVED FLUORESCENCE ENERGY TRANSFER.
Woubalem Birmachu, Franz L. Nisswandt and David D. Thomas, Department of Biochemistry, Univeristy of Minnesota Medical School, Minneapolis, Minnesota 55455.

We have measured the distance between the binding sites of 5-(2-((iodoacetyl)amino)ethyl) aminonaphthalene-1-sulfonic acid (IAEDANS) and fluorescene-5-isothiocyanate (FITC) on the Calcium-ATPase of skeletal muscle under conditions proposed to affect the enzyme's conformation. Fluorescence energy transfer experiments using the single photon counting method has allowed us to resolve two distances between IAEDANS and FITC. When one IAEDANS is bound per Ca-ATPase, 80 $\pm$ 3% of the probes have an excited-state lifetime of 18.70 $\pm$ 0.20 nsec. When FITC is bound to each IAEDANS-labeled enzyme, this IAEDANS lifetime component is resolved into two, indicating two binding sites that result in the same IAEDANS lifetime. 60% of this population has a lifetime of 11.5 $\pm$1.5 nsec, corresponding to an energy transfer efficiency E = 0.40 $\pm$ 0.07 and a donor-acceptor distance r = 52 $\pm$3 Å; 40% of the population is unquenched and has a lifetime of 19.0 $\pm$ 0.5 nsec. Addition of Ca^{++}, or the phosphate analogue monovanadate, and phosphorylation with inorganic phosphate had no effect on the donor-acceptor distance. In comparison, decavanadate, which crystallizes the ATPase, induces a marked decrease in the average distance, and limited proteolysis with trypsin induces a small increase. Thus, while ligands that are proposed to cause conformational changes in the enzyme do not change the detected intramolecular distance, significant changes are induced by physical perturbations of protein structure.

M-Pos183 TIME-RESOLVED PHOSPHORESCENCE ANISOTROPY STUDIES OF THE ROTATIONAL DYNAMICS OF THE SARCOPLASMIC RETICULUM Ca-ATPase IN THE PRESENCE OF SUBSTRATES. Scott M. Lewis and David D. Thomas, Department of Biochemistry, University of Minnesota Medical School, Minneapolis, Minnesota 55455

We used time-resolved phosphorescence anisotropy to study the molecular dynamics of the Ca-ATPase in the microsecond time range. Specific intermediates in the calcium transport cycle have been proposed to change the motion on this time scale. The Ca-ATPase was alternatively labeled with eosin and erythrosin derivatives. Erythrosin-5-iodoacetamide (ERIA) was chosen for the study of ATP and calcium since it preserves transport function. In addition, erythrosin-5-isothiocyanate was chosen for comparison since, while the enzyme does not bind ATP, it interacts with other ligands and its anisotropy decay was large and easily analyzed. Cross-linking reagents greatly increased the anisotropy for both probes, indicating that large-scale rotations are being detected. It was found for ERIA-Ca-ATPase that nucleotides (AMPPNP, ADP) and calcium had little effect on the correlation times or amplitudes of the anisotropy decay. For both probes, decavanadate decreased the mobility on the microsecond time scale, whereas monovanadate had no effect. Under phosphoenzyme conditions, the formation of E_2-P had no effect on the correlation times or amplitudes, however the addition of DMSO, which shifts the equilibrium toward phosphoenzyme formation, decreased the mobility. Under conditions of steady-state calcium transport, there was no change in the correlation times. We conclude that there are no changes in microsecond motions that are attributable to specific intermediates in the transport cycle. These results are consistent with the findings from saturation-transfer EPR spectroscopy.

M-Pos184 EU-4093 does not modify the capacity of calcium uptake by the sarcoplasmic reticulum. A. J. Mijares, A. Gerardi, J. R. López. Centro de Biofísica y Bioquímica, Instituto Venezolano de Investigaciones Científicas, Apartado 21827, Caracas 1010A Venezuela.

Malignant hyperthermia (MH) is a hypermetabolic myoplathy whose pathophysiology is associated to a malfunction of intracellular calcium homeostasis in skeletal muscles (López et al, Muscle Nerve, in press). We have studied the effect of the new muscle relaxant EU-4093 on the capacity of calcium uptake of crude sarcoplasmic reticulum (SR) vesicles prepared from Malignant hyperthermia susceptible (Poland China) and non susceptible swine (Yorkshire). Longissimus dorsi muscle was removed, and inmediately placed in ice. The SR membranes were isolated following the method describe by Martonosi and Feretos (J. Biol. Chem. 239:648, 1964). The calcium uptake was 0.257 $\pm$ 0.02 (μmoles Ca^{2+}/mg prot. x min.) in non susceptible swine and 0.227 $\pm$ 0.01 (μmoles Ca^{2+}/mg prot. x min.) in susceptible. No difference was observed between these two groups of swine in three diferents preparation$_5$(n=5). The incubation of SR vesicles for 5 minutes previous to addition of ATP in EU-4093 up to 10^{-5}M did not modify the capacity of calcium uptake by the SR measured at 2, 5 and 10 minutes in non susceptible and MH susceptible swine. These results suggest that the prophilactic and therapeutic effect of this muscle relaxant on MH susceptible swine is associated to its inhibitory action on calcium release and not to changes in calcium uptake.

M-Pos185 **RYANODINE AFFECTS OPEN Ca^{2+} RELEASING CHANNELS IN THE SARCOPLASMIC RETICULUM (SR) OF SKINNED STRIATED MUSCLE.** Judy Y. Su, Dept. of Anesthesiology, Univ. of Wash. Seattle, WA 98195

Evidence suggests that ryanodine blocks Ca^{2+} releasing channels in the SR, a process which may be associated with muscle depression. In skinned fibers from striated muscle pretreated with ryanodine, removal of the ryanodine did not restore normal tension development upon subsequent stimulation with caffeine (C_2). This effect was dose- and "activity"-dependent (Biophys J 49:569a, 1986). This study was designed to examine whether the "activity"-dependent effect of ryanodine takes place at the pump or at the channel, and to study gating kinetics of the channel. Right ventricular papillary muscle (PM), and skeletal muscle (adductor magnus, AM; soleus, SL) were isolated from rabbits killed by cervical dislocation. Pieces of the muscle were homogenized (sarcolemma disrupted). Fiber bundles from PM, and single fibers from AM and SL were dissected from the homogenate and mounted on photodiode tension transducers. To distinguish ryanodine effects on the pump from effects on the channel, ryanodine was added to the protocol (Pflügers Arch 380:29, 1979) in either of two places. The first was a brief exposure at the beginning of Ca^{2+} loading, the second was a brief exposure at the beginning of the caffeine-induced tension transient. When given at the beginning of Ca^{2+} loading, ryanodine had no effect on C_2. In contrast, ryanodine given during channel activity caused depression of C_2. Tension depression was made more severe with increasing duration of ryanodine exposure. The introduction of ryanodine at varying times after caffeine activation revealed that the longer the ryanodine was delayed after initiation of contraction, the less C_2 was depressed. It is concluded that ryanodine affects Ca^{2+} releasing channels, not the pump, and ryanodine-induced depression results from binding to open channels but not to inactivated channels. Supported by Washington Heart Association, and NIH HL 20754 and HL 01100.

M-Pos186 FUNCTION OF THE 53 KILODALTON GLYCOPROTEIN OF THE SARCOPLASMIC RETICULUM. Howard Kutchai, Kevin P. Campbell, & Jeffrey P. Froehlich. Dept. of Physiology, University of Virginia, Charlottesville, VA; Dept. of Physiology & Biophysics, University of Iowa, Iowa City, IA; and National Institute on Aging, Gerontology Research Center, Baltimore, MD.

When rabbit skeletal muscle sarcoplasmic reticulum (SR) was extracted with cholate at low [KCl], the resulting preparations accumulated Ca++ and hydrolyzed ATP at levels similar to untreated SR. SR extracted with cholate at high [KCl] hydrolyzed ATP at normal rates, but was deficient in accumulating Ca++. The high [KCl]-cholate extracted preparations had diminished levels of the 53-kilodalton glycoprotein (GP-53) of the SR membrane. The transient-state kinetics of cholate-extracted SR was studied with chemical quenching methods. Low [KCl]-cholate-extracted SR had steady-state levels of EP and rates of EP formation and ADP-induced EP decomposition similar to those of SR, and transported Ca++ with an initial burst followed by a steady-state rate of transport. High [KCl]-cholate-extracted SR formed normal steady-state levels of EP, had normal kinetics of EP decomposition, formed EP more slowly than control preparations, and transported Ca++ with an initial burst, but with a greatly diminished steady-state rate. Preincubation of SR with an antiserum (AS) against GP-53 resulted in decreased ATP-driven Ca++ transport by the SR, but had no effect on the rate of Ca-stimulated hydrolysis of ATP. Preincubation with AS did not increase the passive permeability of SR to Ca++. Under our conditions the control coupling ratio of 1.5 mole Ca++/mole ATP was reduced to 0.186 mole Ca++/mole ATP in AS-treated SR. Our results are consistent with the interpretation that GP-53 may be involved in regulating coupling of Ca++ transport to ATP hydrolysis in the SR.

M-Pos187 TRANSVERSE TUBULAR PROTEINS OF THE TRIAD JUNCTION OF SKELETAL MUSCLE. A.H. Caswell, N.R. Brandt and R.M. Kawamoto. Department of Pharmacology, University of Miami School of Medicine, P.O. Box 016189, Miami FL 33101

We have employed three methods to elucidate the T-tubular interaction with the junctional foot protein (spanning protein, ryanodine receptor) of skeletal muscle. 1. The hetero bifunctional cross linking agent, SASD, is first iodinated with ^{125}I and then attached to the spanning protein (SP). The liganded SP is incubated and then photo reacted with T-tubule vesicles. Two protein bands with M_r s of 72,000 and 34,000 are labelled with higher activity than pre-illuminated control. The latter comigrates with glyceraldehyde phosphate dehydrogenase (GAPD). 2. The interaction of the SP with detergent extracted T-tubules has been investigated by attaching the SP to a gel matrix and passing dissolved T-tubules through the column. Retained proteins are eluted by increasing the NaCl concentration. The major retained proteins comigrate with GAPD and aldolase. Purified GAPD is retained by an SP column. An affinity column of GAPD retains the M_r 72,000 protein under identical conditions to those used for the SP affinity column suggesting that GAPD and the M_r 72,000 protein compete for binding to SP. Partially purified M_r 72,000 protein is retained by a SP affinity column. 3. T-tubule gels have been blotted onto a nitrocellulose filter and the filters have been incubated with ^{125}I labelled SP and washed extensively. The major proteins labelled are GAPD and aldolase with minor labelling of other proteins including the M_r 72,000 protein. We conclude that the M_r 72,000 protein of T-tubules and GAPD bind SP competitively. The former protein is the major intrinsic protein of T-tubules and may play a role in triadic electrical transmission. Supported by NIH grant AR21601 and by the American Heart Association (Florida Affiliate). RMK was a postdoctoral trainee on NIH grant HL-07188.

M-Pos188 CHARACTERIZATION OF THE REGION OF PHOSPHOLAMBAN THAT INTERACTS WITH CALMODULIN. T. Hanson, G. Strasburg, and C.F. Louis. Dept. of Vet Biol, Univ. MN, St. Paul, MN 55108.

The cardiac sarcoplasmic reticulum (CSR) protein kinase substrate phospholamban (PL) is phosphorylated at Ser-16 by cAMP-dependent protein kinase (cAMP-PK), or at Thr-17 by calmodulin (CaM) activation of the endogenous CSR calmodulin-dependent protein kinase (CaM-PK) [Fujii et al., BBRC 138, 1044 (1986)]. PL is the major CaM affinity-labeled component in CSR (Strasburg et al. J. Biol. Chem. 1988, in press) suggesting that the activity of endogenous CaM-PK is modulated by the interaction of exogenous CaM with PL. To examine this proposal, CSR was subjected to limited proteolysis, and subsequently either phosphorylated with cAMP-PK or CaM-PK, or affinity labeled with benzophenone-^{125}I-CaM (Bz-CaM). Treatment with trypsin resulted in the loss of both the cAMP-PK- and CaM-PK-catalyzed phosphorylations of PL, as well as the loss of Bz-CaM affinity labeling of PL at identical trypsin:CSR concentrations. In contrast, chymotrypsin (which probably cleaves at Tyr-6 of PL) resulted in a loss of both Bz-CaM affinity labeling and CaM-PK phosphorylation of PL, while the cAMP-PK-dependent phosphorylation was unaffected. Similar results were obtained with endoproteinase Lys-C, which likely cleaves at Lys-3 of PL. These results indicate that trypsin, by cleaving at cytoplasmic PL sites (including Lys 3 and Args 7, 10, 11, 25) causes the loss of both the CaM-binding region, and the cAMP-PK and CaM-PK phosphorylation sites of PL. In contrast, the data with chymotrypsin and Lys-C indicate that removal of a small section of the N-terminal cytoplasmic portion of PL does not affect the ability of cAMP-PK to phosphorylate Ser-16 of PL. These results suggest that both the CaM binding domain of PL, as well as the likely site of interaction of PL with the CSR CaM-PK are formed in part by a small number of residues adjacent to, and possibly including the N-terminus of this protein. Supported by NIH grant HL-25880.

M-Pos189 EFFECTS OF $[Ca]_o$, BAY K, AND RYANODINE ON ATRIAL PEPTIDE SECRETION BY ATRIAL MYOCYTE CULTURES. Hiroshi Iida and Ernest Page, The University of Chicago, Chicago, IL 60637.

Atrial natriuretic peptide (ANP) secretion was determined by radioimmuno assay in 7- or 8-day-old primary cultures of atrial myocytes from adult rats after incubation at 37° C in protein-free Gibco Medium 199 whose ion concentrations were (in mM): Ca 1.8, K 5.4, Na 150, Mg 0.8, Cl 130, HCO_3^- 26, phosphate 1.0, HEPES 10 (pH 7.3). In selected experiments spontaneous contractions were abolished with 10 μM tetrodotoxin (+TTX); and/or Ca^{2+} release by sarcoplasmic reticulum (SR) was modified by 1 μM ryanodine (+Ry), which also abolished contractions. T (total pmoles of ANP secreted in 2 hrs into 2 ml of culture medium by myocytes on 3.5 cm diameter dishes) was averaged for 3 control dishes and compared with other dishes from the same culture subjected to specific experimental perturbations. Basal secretion in quiescent (+TTX) cells in 0.2 mM $[Ca]_o$ (T = 33.4) was not reduced by Ry. It remained unchanged when $[Ca]_o$ was raised to 1.8 mM (T = 33), but rose significantly at $[Ca]_o$ of 5.4 mM (T = 41.8); the increase in T at 5.4 mM $[Ca]_o$ (+TTX) was abolished by Ry. In cultures contracting spontaneously ($[Ca]_o$ = 1.8 mM, no TTX), abolishing contractions with TTX decreased T from 17.6 to 13.1. In a second experiment on a different culture of spontaneously contracting cells ($[Ca]_o$ = 1.8, no TTX), 2 μM BAY K 8644 increased T from 30.7 to 40.6. Conclusions: (a) There is significant ANP secretion (insensitive to 1 μM Ry) in absence of contractions and at the very low resting tension prevailing at $[Ca]_o$ = 0.2 mM; (b) Influx of extracellular Ca by raising $[Ca]_o$ increases ANP secretion through a Ry-sensitive process, possibly Ca^{2+}-induced Ca release from SR. Supported by USPHS HL 10503 and 20592.

M-Pos190 PURIFICATION AND CHARACTERIZATION OF A PHOSPHOLAMBAN Ca^{2+}-CALMODULIN-DEPENDENT PROTEIN KINASE FROM CANINE CARDIAC CYTOSOL. R.C. Gupta and E.G. Kranias, Dept. of Pharmacology and Cell Biophysics, University of Cincinnati College of Medicine, Cincinnati, OH 45267.

Cardiac sarcoplasmic reticulum can be phosphorylated by a calcium-calmodulin(CAM)-dependent protein kinase on phospholamban. Phosphorylation is associated with stimulation of the initial rates of Ca^{2+} transport. We report here the purification of a Ca^{2+}-CAM-dependent protein kinase from canine cardiac cytosol, using phospholamban as substrate. Purification involved sequential chromatography on DE-52, CAM-agarose, DEAE Bio-Gel A, and phosphocellulose. This procedure resulted in 1000-fold purification of the "phospholamban Ca^{2+}-CAM-dependent protein kinase" with a 5.4% yield. PAGE (4%), under non-denaturing conditions, revealed that the enzyme was purified to apparent homogeneity. The purified enzyme had a Mr of approximately 550,000 daltons and exhibited a single protein band of 55,000 Mr on SDS-PAGE. The activity of the purified kinase was dependent on calcium, CAM, and ATP-Mg^{2+} or ATP-Mn^{2+}. Metal ions which could substitute for Ca^{2+} in the presence of Mg^{2+} and saturating CAM concentrations were $Zn^{2+} > Co^{2+} > La^{3+} > Fe^{2+} > Sr^{2+}$. The purified enzyme could be autophosphorylated (6 mol Pi/mol subunit) in a calcium-CAM-dependent manner and this was inhibited by trifluoperazine. Other preferred substrates, besides phospholamban, were glycogen synthase, gizzard smooth muscle myosin light chains and myelin basic protein. Phosphorylase b and cardiac myosin light chains were not phosphorylated by the purified kinase. Thus, based on its substrate specificity and its physical properties, the enzyme appears to belong to a class of multifunctional Ca^{2+}-CAM-dependent protein kinases reported to be present in brain, liver and skeletal muscle (Suppported by HL22619, HL26057 and AHA SW Ohio Chapter).

M-Pos191 **IMMUNOGOLD ELECTRON MICROSCOPIC LOCALIZATION OF PHOSPHOLAMBAN IN NEONATAL SKELETAL MUSCLE.** **D.G. Ferguson*, E.F. Young#, E.G. Kranias#. Depts. of *Physiology & Biophysics; #Pharmacology & Cell Biophysics, University of Cincinnati.**

Phospholamban, an intrinsic protein of cardiac sarcoplasmic reticulum (SR), is the putative regulator of the cardiac isoform of the SR Ca^{2+} ATPase. Phospholamban is present in all fibers which express the cardiac Ca^{2+} ATPase isozyme, including adult slow twitch skeletal muscle (Jorgensen and Jones, J. Biol. Chem., 261:3775, 1986). Immunoblot studies have shown that neonatal skeletal muscle expressed both the cardiac and the fast twitch Ca^{2+} ATPase isozymes (MacLennan et al., Biophys. J., 51:1a, 1987), but the distribution of the isozymes within this tissue remains uncertain. We have used an affinity-purified, polyclonal antibody raised against cardiac phospholamban to immunolocalize phospholamban in gently disrupted neonatal skeletal muscle (quadriceps) from rats. In these preparations most of the fibers were well differentiated and there appeared to be two distinct cell types: Cells which had the ultrastructural characteristics of slow twitch fibers contained phospholamban in the SR and the outer nuclear envelope; cells which had the ultrastructural appearance of fast twitch fibers did not retain any label. Immunofluorescence studies are being carried out to examine the distribution of the two cell types in neonatal rat quadriceps in situ. Supported by NIH grants HL 34979 (DGF); HL 26057 and HL 22619 (EGK).

M-Pos192 CHARACTERIZATION OF PHOSPHOLIPIDS ASSOCIATED WITH PURIFIED Ca^{2+}-ATPase AND PHOSPHOLAMBAN ISOLATED FROM CANINE CARDIAC SARCOPLASMIC RETICULUM. H.W. Kim, G. Jakab, I. Edes, and E.G. Kranias, Dept. of Pharmacology and Cell Biophysics, U. of Cincinnati, Cinti., OH 45267.

The Ca^{2+}-pump in cardiac sarcoplasmic reticulum (SR) is under regulation by a polymeric proteolipid, phospholamban (PLB). Phosphorylation of PLB increases the affinity of the Ca^{2+}-ATPase for Ca^{2+}. A similar increase in the affinity for Ca^{2+} was observed when the Ca^{2+}-ATPase was isolated from canine cardiac SR, essentially free of PLB (EC_{50}: 0.053 μM for pure Ca^{2+}-ATPase and 0.86 μM for SR). Thus, the Ca^{2+}-ATPase activity in native SR membranes may be suppressed by PLB and phosphorylation may relieve this inhibition. The phospholipids of the purified Ca^{2+}-ATPase were identified by two dimensional thin layer chromatography and they were phosphatidylcholine (48%), phosphatidylethanolamine (32%), and phosphatidylinositol (13%). Although the amount of total phospholipid in Ca^{2+}-ATPase (0.60 ± 0.14 μmol lipid P/mg) was similar to that in purified PLB (0.62 ± 0.09 μmol lipid P/mg), the composition of phospholipids was different. The major phospholipids in the purified PLB were phosphatidylserine (34%), phosphatidylcholine (22%), sphingomyelin (17%), phosphatidylinositol (13%), and phosphatidylethanolamine (9%). Phospholipids associated with the pure PLB could be phosphorylated by the catalytic subunit of the cAMP-dependent protein kinase and this was inhibited by the heat-stable inhibitor protein. Phosphatidylinositol 4-monophosphate and phosphatidylinositol 4,5-bisphosphate were the main phospholipids being phosphorylated. Thus, it is interesting to postulate that phospholipid phosphorylation together with protein phosphorylation may be involved in the regulation of the Ca^{2+} pump in cardiac SR. (Supported by NIH grants HL 26057 and HL 22619).

M-Pos193 RAPID FILTRATION MEASUREMENTS OF Ca^{2+} RELEASE INDUCED BY Ag^{+}.

MOUTIN, M.J., ABRAMSON*, J. SALAMA**, G. and DUPONT, Y. Intr. by KIRSCHNER, L. Biophysique Moléculaire et Cellulaire, CEN-G, 38041 GRENOBLE, FRANCE. (*) Dep. of Physics. Portland State Un. (**) Dep. of Physiology, Un. of Pittsburgh.

The effect of Ag^{+} on sarcoplasmic reticulum (SR) vesicles of rabbit skeletal muscle preincubated in millimolar $^{45}Ca^{2+}$ was studied using a Rapid Filtration Technique (Dupont, Y. & Moutin, M.J. (1987) in Method in Enzymology 148, 675-683). With this technique the Ca^{2+} release of SR vesicles applied on nitrocellulose filters can be observed with a time resolution as low as 20 milliseconds.

We show that micromolar concentrations of Ag^{+} (Ca^{2+} = 1nM) trigger a large and rapid Ca^{2+} release from the vesicles. In the presence of 1 mM ATP, the initial rate of Ca^{2+} release reaches its maximal value at around 30 µM Ag^{+} ($K_{1/2}$ = 10 µM). This rapid Ag^{+}-induced efflux presents characteristics very similar to the Ca^{2+}-induced Ca^{2+} release. It is inhibited by ruthenium red (RR) and Mg^{2+} and activated by ATP. Moreover, it is dependent upon the presence of extravesicular K^{+} and influenced by a variation of a K^{+} gradient imposed to the vesicles which is supposed to create a membrane potential.

Higher concentrations of Ag+ produce a partial inhibition of the Ca^{2+} release. The remaining slow Ca^{2+} efflux is not totally inhibitable by RR, in contrast from the rapid Ca^{2+} release observed at lower concentrations. In this high concentration range, Ag^{+} may interact with some other component of the SR membrane than the Ca^{2+} release entity.

In conclusion, we have shown that Ag^{+}, like Ca^{2+}, can both open and close the Ca^{2+} release channel from skeletal SR.

M-Pos194 KINETIC STUDIES OF Ca^{2+} RELEASE FROM SARCOPLASMIC RETICULUM (SR) OF SLOW-TWITCH SKELETAL MUSCLE. Young Sup Lee, Adam J. Duhl and Do Han Kim. (Intr. by D. Chester) Dept. of Medicine, University of Connecticut Health Center, Farmington, CT 06032.

The longer twitch duration of slow twitch skeletal muscle compared to fast twitch skeletal muscle has been correlated with the SR function. Since the contraction time of slow muscle is longer than that of fast muscle, Ca^{2+} release mechanisms in slow muscle presumably differ from those in fast muscle. To define the mechanism of Ca^{2+} release from slow muscle SR, we investigated the time course of Ca^{2+} release from passively-loaded junctional SR of slow-twitch rabbit skeletal muscle (e.g. soleus). Ca^{2+} release was triggered by Ca-jump, caffeine, quercetin, or doxorubicin, and the time course of $^{45}Ca^{2+}$ release determined by rapid filtration or manually. Plots of the rate of Ca^{2+} release from slow muscle SR versus pCa_o show that Ca^{2+}-loaded SR releases Ca^{2+} at low free Ca^{2+} concentrations (e.g. 0.1 µM); in contrast, no Ca^{2+} release was observed in the fast skeletal SR (e.g. 0.1 µM). Addition of 2 mM caffeine, 50 µM quercetin or 50 µM doxorubicin increases the rate of Ca^{2+} release induced by Ca-jump indicating that the drug effects are additive. Ca^{2+} release induced by Ca-jump was inhibited by ruthenium red ($C_{1/2}$= 50 µM), tetracaine ($C_{1/2}$= 0.1 mM) or $MgCl_2$ ($C_{1/2}$= 2 mM), but was not affected by ryanodine (1 - 100 µM). The sensitivity of the slow SR to the various inhibitors was generally similar to that of fast SR, but the rate of Ca^{2+}-jump and caffeine induced Ca^{2+} release by slow SR ($t_{1/2}$= 140 ± 49 ms) appeared to be less than that of fast SR (85 ± 13 ms). These results suggest that a unique Ca^{2+} release mechanism in slow muscle SR may be partly responsible for the longer twich duration. Supported by NIH grant HL 33026.

M-Pos195 EXPRESSION OF THE NEUROSPORA PLASMA MEMBRANE H^+-ATPase IN XENOPUS OOCYTES. N.P. Money (1), L.R. Aaronson (2), C.W. Slayman (1,2) and C.L. Slayman (1), Department Physiology (1) and Human Genetics (2), Yale University School of Medicine.

The structural gene encoding the 100 kDa plasma membrane H^+-ATPase of the fungus Neurospora has recently been cloned, sequenced and a full-length cDNA constructed. In order to express this gene in a heterologous system suitable for future structure-function studies, the ATPase cDNA was transcribed in vitro using the SP6 system and purified mRNA was injected into Xenopus oocytes. Pulse-labelling experiments demonstrated the appearance during a three-day incubation period of a single 100 kDa protein, immunoprecipitable with polyclonal ATPase antibody, in the membrane fraction of the oocytes. Expression of the H^+-ATPase was dependent upon 3′ polyadenylation of the mRNA. Hydropathy analysis of the deduced amino acid sequence of the ATPase suggests that it has 8-10 transmembrane segments organized into discrete 'hairpin' structures. According to the Engelman and Steitz hypothesis, these hairpin structures are the essential elements for the insertion of the ATPase into membranes. We have begun a series of experiments to identify potential membrane insertion signals. A cDNA clone encoding the N-terminal portion of the ATPase extending through the first hairpin region was constructed in an SP6 plasmid. An immunoprecipitable 28 kDa product was expressed in oocytes and inserted into membranes. Deletion of the first 78 amino acids from the N-terminus of this peptide did not impair integration into membranes. These data strongly suggest that an insertion signal resides within the first transmembrane hairpin domain of the ATPase. We would also predict that a 'stop-transfer signal' is localized in this domain since the truncated peptides are anchored in the membranes and not translocated across them.

M-Pos196 INACTIVATION OF H^+,K^+-ATPase BY A K^+-COMPETITIVE PHOTOAFFINITY INHIBITOR. Keith B. Munson and George Sachs, UCLA Department of Medicine & Physiology, Los Angeles, California 90024, and Center for Ulcer Research and Education, V.A. West Los Angeles, California 90072.

A light-sensitive derivative, 2,3-(dimethyl)-8-(4-azidophenylmethoxy)imidazo[1,2a] pyridine (DAZIP) of the drug 3-(cyanomethyl)-2-methyl-8-(phenylmethoxy)imidazo-[1,2a] pyridine (SCH 28080) has been synthesized and shown to be a K^+-competitive inhibitor of gastric H^+,K^+-ATPase in the dark. The apparent dissociation constants calculated for DAZIP at pH 6.4 and 7.4 were 1.8 ± 0.2 and 4.7 ± 1.2 uM , respectively. Inhibition required binding of DAZIP to a luminal-facing site on the enzyme. Irradiation in the presence of DAZIP and 2 mM Mg^{2+} resulted in irreversible loss of ATPase activity which was more than two-fold greater at pH 6.4 than at 7.4 showing the enhanced efficiency of covalent incorporation at the lower pH. Further photolyses were conducted at pH 6.4 in the presence of either CDTA, ATP and CDTA, or MgATP. The specificity of light-dependent,covalent insertion of DAZIP for the site of reversible inhibition was shown both by protection against photoinactivation given by K^+ (the competing ligand) and by the observation that the amount of K^+-protectable photoinactivation approached a maximum limiting value as a function of DAZIP concentration. The effectiveness of K^+ in protecting against photoinactivation was 100-fold greater in the presence of ATP and CDTA than in the presence of either Mg^{2+} or CDTA and suggests the formation of a ternary complex of the apo-enzyme with ATP and tightly bound K^+. The dissociation constant for DAZIP (2 uM) calculated from photolyses in the presence of MgATP without added K^+ agreed with the kinetic experiments and suggests that DAZIP inhibits turnover by binding to E·MgATP.

M-Pos197 INTRACELLULAR Ca (Ca_i)-DEPENDENT VOLUME LOSS IN BARNACLE MUSCLE CELLS. H. Rasgado-Flores and E. M. Santiago (Introduced by M. P. Blaustein) Department Physiology, Medical School, University of Maryland, Baltimore, MD. 21201.

Volume regulation is basic for proper cell function, yet little is known about this process in muscle cells. Serendipitously we found that a rise in Ca_i from 0.01 to 1.0 or 10 uM, under normal isotonic conditions, produced substantial (15-30%) shrinkage in internally perfused barnacle muscle cells. Since these cells lose their ability to contract after 1 hr of perfusion, this effect was not due to contraction. To determine whether Ca_i-induced shrinkage was due to net H_2O transfer across the sarcolemma, H_2O loss was measured by monitoring the effect H_2O extrusion should have on the concentration of the internal perfusate's non-permeant solutes, such as sucrose. To accomplish this, ^{14}C-sucrose was added to perfusates containing 0.01 and 1.0 uM Ca_i and radioactivity was measured in aliquots of these solutions before and after perfusing the cell. After perfusing for 2 hr with 0.01 uM Ca_i, the radioactivity collected from the cell's perfusate reached a steady-state and was similar to that from aliquots taken before perfusion. However, increasing Ca_i to 1.0 uM elicited a reversible increase in aliquot radioactivity which was accompanied by a reversible reduction in the cell volume. In other cells a Ca_i-activated volume reduction has been reported to result from Ca_i-induced loss of K + Cl and H_2O. Therefore, we studied the effect of Ca_i on ^{86}Rb (as a K tracer) efflux and the Cl_i-dependence of the Ca_i- induced volume loss. We observed that Ca_i induced ^{86}Rb efflux and that intracellular replacement of Cl by NO_3 prevented the volume loss. In all cases, the measured and expected volume reductions had very similar values. These results suggest that Ca_i activates loss of K, Cl and H_2O from internally perfused barnacle muscle cells, and that this preparation may serve as a model to study volume regulatory mechanisms in muscle and other cells.

M-Pos198 LYTROPIC IONS ON REACTIVITY OF PHOSPHOENZYME OF SODIUM, POTASSIUM-ATPASE.
Robert L. Post, Department of Molecular Physiology and Biophysics, Vanderbilt University Medical School, Nashville, TN 37232.

The phosphoenzyme of (Na,K)-ATPase is composed of 3 reactive states designated E1P, E*P, and E2P. E1P donates its phosphate group reversibly to ADP; E2P is stimulated by K^+ to donate its phosphate group reversibly to water but not to ADP; and E*P responds either to ADP or to K^+ (Yoda & Yoda, 1987, J Biol Chem 262:110). Enzyme from the outer medulla of dog kidney was phosphorylated from [γ-^{32}P]ATP (20μM) in the presence of Na^+ and Mg^{2+} (10mM) at pH 7.1 and 0 °C for 70 sec. To estimate the composition of the phosphoenzyme it was chased with unlabeled ATP (2mM) with or without added ADP (8mM) or KCl (50mM) or both. The chase was terminated after 4 sec by addition of acid. In 540 mM NaCl equal amounts of phosphoenzyme were insensitive to ADP or to KCl. Replacement of Cl^- with ClO_4^-, a more lyotropic ion, changed the composition principally to E1P. Similarly replacement of Cl^- with acetate$^-$, a less lyotropic ion, changed the composition principally to E2P. A ratio of 5:1 acetate:perchlorate was approximately equivalent to chloride. Replacement with other anions showed a lyotropic series as follows: ClO_4^- > I^- > SCN^- > NO_3^- > Cl^- > sulfate^{2-} > acetate$^-$ = formate$^-$ > citrate^{3-}. Polyvalent ions were compared with monovalent ions at equivalent, not molar, concentrations. Replacement of 1/2 of the Na^+ showed that guanidinium$^+$ was more lyotropic and that N-methylglucamine$^+$ and tetramethylammonium$^+$ were less lyotropic than Na^+. It is proposed that lyotropic ions act primarily on equilibria between conformational states of the enzyme and have only secondary effects on ligand binding. Supported by a grant, HL-01974, from the National Heart, Lung, and Blood Institute of the N.I.H.

M-Pos199 MECHANISTIC STUDIES OF THE GASTRIC H^+,K^+-ATPase -- EVIDENCE FOR THE SIMULTANEOUS BINDING OF ATP AND INORGANIC PHOSPHATE. W.W. Reenstra, J.D. Bettencourt, and J.G. Forte. Department of Physiology-Anatomy, University of California, Berkeley, CA 94720

The gastric H^+,K^+-ATPase, located in the apical membrane of the oxyntic cell, is the ion pump that drives acid secretion in the stomach. During steady-state turnover, a phospho-enzyme intermediate (E-P) is formed from ATP. The level of E-P is maximal in the absence of K^+ and decreased by mM concentrations of K^+. Over the same range, K^+ increases V_{max} for ATP hydrolysis. At both 0 and 10 mM K^+, plots of E-P vs. E-P/[ATP] and v vs. v/[ATP] are concave upward. Over the concentration range of 0.1 to 200 uM ATP, the ratio v/E-P increases 3-fold. At [ATP] below 1 uM, Dixon plots of 1/v vs. [Pi] are concave downward; at saturating Pi, 1/v is independent of [Pi]. At low [ATP], hydrolysis can be explained by the following mechanism:

$$E + ATP \rightleftharpoons E\cdot ATP \longrightarrow E\text{-}P \rightleftharpoons E\cdot Pi \longrightarrow E + Pi$$

The ratio v/E-P will vary with [ATP] only if at high concentrations ATP also binds to an enzyme form that occurs before E-P undergoes an irreversible step. Thus, ATP must bind to either E·Pi which is formed reversibly from E-P or to E-P which then forms E·Pi·ATP. In either case, the data require that both ATP and Pi must bind to the enzyme simultaneously. This is also supoprted by the effects of Pi on ATP hydrolysis which show that ATP can bind to the enzyme at saturating Pi. The ability of ATP to bind to E·Pi or E-P also provides an explanation for the biphasic v vs. v/[ATP] plots. The increase in E-P at high [ATP] demonstrates that in the absence of K^+, dephosphorylation of E-P is not the sole rate limiting step at low ATP. (Supported by PHS Grant AM10141)

M-Pos200 HYDROGEN PEROXIDE EFFECTS ON ISOLATED Na,K-ATPASE AND FUNCTIONAL ACTIVITY IN Na LOADED NEURONS. A.S. Hobbs[1], G.M. Wright[1] and D.R. Livengood[2]. [1]Laboratory of Neurochemistry, NINCDS, NIH, Bethesda, MD 20892 and [2]Department of Physiology, AFRRI, Bethesda, MD 20814.

The effect of H_2O_2 on membrane bound Na,K-ATPase and Na-K pump in intact cells was compared using membranes from eel electroplax and intact cardiac ganglia from lobster. Na,K-ATPase activity was assayed in 50 mM NaCl, 10 mM KCl, 3 mM $MgCl_2$ and 50 mM Tris-HCl at 25° C by measuring inorganic phosphate release or using a coupled enzyme assay to measure ADP release. Inhibition of Na,K-ATPase progressed over time, but did not achieve 100%, with 5 mM H_2O_2 producing about 50% inhibition within 5 min. The time course of inhibition was biphasic. In contrast to the effect of H_2O_2 on the Na,K-ATPase, it stimulated the Na-K pump in Na loaded intact neurons of the lobster cardiac ganglia which were exposed to either 0.35 mM or 3.5 mM H_2O_2 for up to one hour. No statistically significant change was observed in membrane potential with H_2O_2, but a significant <u>increase</u> was observed in pump amplitude in both 0.35 and 3.5 mM H_2O_2 treated preparations at 60 minutes. This apparent increase in pump activity could be accounted for by an increase in Na loading during K-free exposure. I-V curves, however, showed no significant change in I_{leak}. Burst potentials showed a tendency toward disorganization of rhythm with H_2O_2. An increase in Na loading through an increase in nonrhythmic spiking activity cannot be ruled out. However, in one experiment in which all spontaneous activity was blocked with TTX, pump activity showed the same increase with H_2O_2 as previously described. These data suggest that effects of H_2O_2 on Na-K pump in intact cells may be secondary to other membrane changes and that caution should be used in interpreting such results.

M-Pos201 VOLTAGE DEPENDENCE OF STROPHANTHIDIN-SENSITIVE CURRENT OF RANA OOCYTES. **Michael M. Wu and Mortimer M. Civan. Depts. of Physiology & Medicine, Univ. of Pennsylvania, Phila., PA 19104**

Current (I_p) through the Na,K-exchange pump depends on membrane potential (V_m), but the nature of the dependence has been unclear. Measured as glycoside-sensitive current, I_p of Xenopus oocytes has been reported to depend directly on V_m, peak at ≃ 20 mV, but to decline thereafter. Defolliculated oocytes of Rana pipiens were voltage clamped [-150,50 mV] with and without 50 μM strophanthidin. Currents were measured while alternately hyper- and depolarizing the membranes for 500 ms at intervals of 3 s. I_p depended directly on V_m up to a plateau at -30 to 10 mV. With further depolarization, I_p displayed either positive or negative slope conductances. Here (in contrast to measurements at more negative potentials), I_p was highly time-dependent, suggesting that a pathway parallel to the pump contributed to the current response at V_m > 10 mV. We examined this by measuring current in the presence of strophanthidin at K^+ concentrations of 0, 2 and 10 mM. In 3 oocytes, a voltage-activated, external K^+-sensitive current (I^K_{Str}) was noted. I^K_{Str} was outwardly directed in the presence of external K^+, appearing at -10 to 10 mV, and was directly dependent on V_m. I^K_{Str} was 8-13 nA with V_m = 40 mV. In the same oocytes, I_{Str} was 14-28 nA at the plateau. The results confirm previous measurements of the voltage dependence of I_p in amphibian oocytes. In addition, we report a strophanthidin-insensitive current, activated at about the same V_m at which I_p displays a negative conductance. We suggest that blockage of the pump leads to accumulation of K^+ in the external space between the vitelline and plasma membranes, activating a conductive channel in parallel with the pump. We further suggest that current through this channel contributes to the negative conductance reported for pump current at positive membrane potentials.

M-Pos202 EVIDENCE FOR PHOSPHATASE INVOLVEMENT IN Na, K, Cl CO-TRANSPORT IN SQUID AXON. A.A. Altamirano, G.E. Breitwieser and J.M. Russell. Dept. of Physiology/Biophysics, UTMB, Galveston, TX 77550.

Na, K, Cl co-transport in the squid giant axon has an absolute requirement for cellular ATP. This requirement is not secondary to the maintenance of ionic gradients since the technique of intracellular dialysis permits ATP depletion concurrently with the maintenance of ionic gradients. We have demonstrated that the ATP requirement of bumetanide-sensitive 36-Cl influx is concentration dependent with an apparent half-saturation concentration of 86 μM. When an axon is dialyzed with an ATP-free dialysis fluid containing 0.5 mM cyanide, bumetanide-sensitive 36-Cl efflux declined to zero with a time constant of 17 min. We studied the effects of 40 μM vanadate or 5 mM F^-, applied intracellularly on three variables: (i) the 36-Cl influx in the presence of ATP; (ii) rate of decline of 36-Cl influx during ATP depletion and (iii) the residual bumetanide-sensitive 36-Cl influx after 60 min. of ATP depletion. Neither vanadate nor fluoride had a significant effect on 36-Cl influx in the presence of ATP. This rules out an effect by these agents on an ATPase. Both agents significantly slowed the rate of 36-Cl inactivation during ATP depletion. The time constant for inactivation in the presence of vanadate = 45 min. and in the presence of F^- = 37 min. (cf 17 min. for control). After 1 hr. of ATP depletion control axons had 5.8 ± pmol/cm^2.s bumetanide-sensitive 36-Cl influx left; vanadate-and fluoride-treated axons had 17.3 ± 2.4 and 13.2 ± 25 pmol/cm^2.s left respectively. Both vanadate and fluoride are well-known protein phosphatase inhibitors and we propose that the slowing of 36-Cl influx inactivation during ATP depletion is a result of greatly decreased protein phosphatase activity. Thus, Na, K, Cl co-transport would be activated by phosphorylation and de-activation by dephosphorylation. Supported by NIH NS-11946.

M-Pos203 DELIBERATE QUIN2-OVERLOAD AS A METHOD FOR CHARACTERIZING THE ACTIVE Ca^{++} EXTRUSION SYSTEM AND CYTOPLASMIC Ca^{++} BUFFERING CAPACITY: APPLICATION TO THE HUMAN PLATELET.
Jonas S. Johansson and Duncan H. Haynes, Dept. Pharmacology, Univ. Miami, Miami, FL 33101

The objectives of the title were achieved in the following experiment: Platelets were loaded with varying amounts of quin2-AM achieving measured final concentrations between 1.02 ± 0.14 and 3.07 ± 0.29 mmol quin2 per liter of platelet volume. The [Ca^{++}]cyt was rapidly elevated to quin2 saturation levels by adding 2 mM Ca^{++} followed by 1 uM ionomycin. The [Ca^{++}]o was then reduced to ca. 100 nM with the aid of EGTA to prevent further Ca^{++} influx, and the kinetics of the fall in [Ca^{++}]cyt were followed. Control experiments showed that the ionophore did not make a significant contribution to the efflux process which is dominated by the Ca^{++} extrusion systems intrinsic to the platelet. Analysis shows that the observed rates of decline of quin2 fluorescence at a particular [Ca^{++}]cyt are dependent upon (a) the absolute rate of the extrusion system (a function of its Km, Vmax and Hill coefficient (n)), (b) the intrinsic Ca^{++} buffer capacity of the cytoplasm (a function of its Kd and Bmax) and (c) the buffer capacity of the intra-cytoplasmic quin2 (a function of its concentration and Kd). The contribution of (c) was known and varied and was used to determine (b) and (a) as a function of [Ca^{++}]cyt. No special assumptions were necessary. The derived Ca-B vs [Ca^{++}]cyt curve has the characteristics of a single binding site (Bmax = 640 ± 70 uM) with an average Kd of 380 ± 60 nM. The rate of extrusion vs [Ca^{++}]cyt curve can be described by two components: A saturable one with Vmax = 2.0 ± 0.3 nmol min^{-1} $mg\text{-}membrane^{-1}$, a Km = 110 ± 27 nM and a n = 1.5 ± 0.4 and a linear one.
Supported by USPHS HL 07188 and Florida Heart Assn.

M-Pos204 Na-H EXCHANGE ACTIVITY IN BARNACLE MUSCLE INDUCED BY HYPERTONICITY. B.A. Davis, E.M. Hogan and W.F. Boron. Dept. Cell. Molec. Physiol., Yale Univ. Sch. of Med., New Haven, CT 06510.

It is well recognized that the primary intracellular pH (pH_i) regulatory system in barnacle muscle is the Na-dependent, $Cl\text{-}HCO_3$ exchanger . Recently, we demonstrated the presence of a Na-H exchanger activated by internal Li^+. Because Na-H exchange often plays a role in regulatory cell-volume-increases, we now have investigated the effect of hyperosmolarity on Na-H exchange in barnacle muscle. pH_i was measured with a glass microelectrode. Muscle fibers, pretreated with 0.5 mM SITS, were exposed to 0-Na^+ Barnacle Seawater (BSW) and internally dialyzed with a 0-Na/pH-7.2 fluid. When exposed to isotonic (ISO, 975 mOsm/Kg) BSW containing 50 mM Na^+ (50Na-BSW), the fibers exhibit minimal Na-dependent pH_i recovery ($dpH_i/dt=0.02\pm1.5 \times 10^{-4}$ pH/min). However, when fibers are bathed in 50Na-BSW made hypertonic (1600 mOsm/Kg, HYPER) with mannitol, there is a significant Na-dependent pH_i recovery ($dpH_i/dt=29\pm5 \times 10^{-4}$ pH/min). This osmotically activated Na-H exchange activity is inhibited 94% by 1-mM amiloride (AMIL-sensitive component: $27\pm6 \times 10^{-4}$ pH/min). For fibers acid loaded by internal dialysis to a pH_i of 6.8, exposure to ISO 50Na-BSW elicits a Na-dependent recovery rate that is inhibited only 24% by AMIL (AMIL-insensitive component: $30\pm4 \times 10^{-4}$ pH/min). Exposure to HYPER 50Na-BSW elicits a Na-dependent pH_i recovery ($dpH_i/dt=51\pm7 \times 10^{-4}$ pH/min) that is faster than with ISO. Moreover, subsequent exposure to AMIL under HYPER conditions completely blocks the Na-dependent pH_i recovery. This suggests either that HYPER blocks an AMIL-insensitive Na-H exchanger and activates an AMIL-sensitive one, or that HYPER increases the amiloride sensitivity of the Na-H exchanger. These results demonstrate the presence of an osmotically induced Na-H exchanger which may function in cell-volume regulation of barnacle muscle.

M-Pos205 MAPPING AND TOPOGRAPHY OF EPITOPES THAT MARK ISOZYME-SPECIFIC DOMAINS OF THE Na,K-ATPase. Kathleen J. Sweadner, Dan P. Felsenfeld, & Heather Shutt. Massachusetts General Hospital Boston, MA 02114. (Intr. by John W. Peterson)

Three distinct genes are known to code for three different isozymes of the catalytic subunit of the Na,K-ATPase. In the rat, at least two of these isozymes have markedly different affinities for the cardiac glycosides. It is of interest to determine what regions of the protein are responsible for functional differences, particularly which variant amino acids are exposed on the surface of the protein. The sequences of the isozymes are known from cDNA clones (Shull et al., Biochemistry 25: 8125, 1986). Alignment and comparison of the sequences reveals that there are only a limited number of clustered sites where amino acid substitutions predict potential antigenic sites that are different for all three isozymes. Consequently, we have produced isozyme-specific antibodies to use as structural probes.

An antibody specific for the alphal (kidney-type) isozyme, McK1, has been the most extensively characterized. It binds to the Na,K-ATPase both in undenatured form and on blots of SDS gels, suggesting both a surface exposure and the recognition of a determinant that is not dependent on correct tertiary folding. Fine-specificity mapping based on sequences from five species and three isozymes narrows down the possible binding sites to two regions, one close to the N-terminal and the other at about amino acid 500, close to the FITC binding site. Tryptic digestion of the undenatured enzyme, which produces large fragments that have been aligned with respect to the amino acid sequence, reveals that McK1 binds to a site very close to the N-terminal. The predicted binding site is KKSKK. Supported by the American Heart Association and by NIH HL 36271.

M-Pos206 RELAXATION KINETICS OF ION TRANSPORT: DRIVING THE CALCIUM ATPASE WITH BACTERIORHODOPSIN. T.G. Dewey & X.L. Wu, Dept. of Chemistry, University of Denver, Denver, CO 80208.

A new technique is presented for measuring ion transport against a constant chemiosmostic potential. This technique employs phase-lifetime spectroscopy to measure chemical relaxation processes. In initial applications the calcium ATPase and bacteriorhodopsin were co-reconstituted into phospholipid vesicles. Illuminating the bacteriorhodopsin results in protons being pumped into the vesicles and a membrane potential is formed. This membrane potential alters the activity of the internal calcium and perturbs the equilibrium of ATP hydrolysis/synthesis coupled to calcium transport. Mechanically chopping the actinic light provides a periodic perturbation to the system and small response signals can be observed using phase-sensitive detection. Using fluorescent indicators, it is shown that this periodic perturbation occurs about a steady state membrane potential which is independent of chopping frequency. The amplitude dispersion curve for the fluorescence of a calcium indicator was also observed and analyzed in terms of the relaxation time for the ATPase-catalyzed calcium transport. The theoretical analysis of such curves is presented (cf. Biophys. J. 51, 809-815). The calcium ATPase showed a single relaxation time on this time scale. The dependence of this relaxation time on ADP and phosphate concentration was measured and analyzed with a random sequential mechanism. This analysis gave dissociation constants for ADP and phosphate of 3.2 mM and 1.4 mM, respectively. These binding steps are followed by a slow isomerization step with forward and reverse rate constants (in the direction of ATP synthesis) of 67 s^{-1} and 227 s^{-1}, respectively. These results demonstrate that highly accurate kinetic data can be obtained with this modulation relaxation technique.

M-Pos207 PROTONS AS CONGENERS OF SODIUM AND POTASSIUM IN HUMAN RED CELL Na,K-ATPase. C. Polvani and R. Blostein, Departments of Biochemistry and Medicine, McGill University, Montreal, Quebec, Canada.

The role of protons as congeners of Na and/or K in the human red cell Na,K-ATPase was examined using inside-out membrane vesicles (IOV). Na-like effects of protons were reported previously (Proton activated Rb transport: J. Biol. Chem. 260:829, 1985). Further evidence supporting this notion is: in the absence of cytoplasmic Na (Na_o), lowering the pH from 7.4 to 6.2 causes (i) an increase in strophanthidin-sensitive ATP hydrolysis, (ii) appearance of K-sensitive EP and, in the presence of Na_o (iii) a decrease in the Na/ATP coupling ratio. K(Rb)-like effects of protons are evidenced in the following: lowering the pH causes (i) an increase in ATP hydrolysis in the presence of Na_o (K absent) due particularly to intravesicular (extracellular) protons, (ii) an increase in the rate of "uncoupled" Na influx (normal efflux) and (iii) a decrease in the Rb/ATP coupling ratio. To determine whether protons are transported in exchange for Na or K, intravesicular pH changes were monitored using FITC-dextran filled IOV derived from DIDS treated cells. With the initial $pH_i = pH_o = 6.2$, a strophanthidin-sensitive decrease in pH_i was observed following addition of ATP (0.2 mM) provided the vesicles contained K (0.2 mM). This pH gradient was abolished following addition of Na. With alkali cation-free IOV, a strophanthidin-sensitive increase in pH was observed upon addition of both ATP (0.02 mM) and Na (4 mM). The foregoing changes in pH_i were not affected by addition of tetrabutylammonium and were not observed at pH 7.4. These ATP-dependent, cardiac glycoside sensitive proton movements indicate that the Na,K-ATPase mediates Na/H exchange in the absence of extracellular K as well as H/K exchange in the absence of cytoplasmic Na. (Supported by the MRC of Canada).

M-Pos208 SODIUM-CALCIUM EXCHANGE IN MEMBRANE VESICLES FROM BRINE SHRIMP. Joo Cheon and John P. Reeves, Roche Institute of Molecular Biology, Roche Research Center, Nutley NJ 07110 USA

Dried cysts of the brine shrimp *Artemia* (San Francisco variety) were hydrated in ice-cold tap water and incubated in aerated half-strength artificial sea water at 30°C. Hatching of the cysts occured approximately 21 hr. after initiation of incubation. Nauplii were collected at various intervals after hatching and homogenized in 400 mM NaCl/20 mM Mops/Tris, pH 7.4. The homogenate was centrifuged for 40 min. at 200,000 x g; the upper, lighter-colored portion of the pellet was resuspended in 400 mM NaCl and centrifuged for 30 min at 200,000 x g over a cushion of 30% sucrose. Membranes at the interface were resuspended in 160 mM NaCl/20 mM Mops/Tris, pH 7.4 and examined for Na-Ca exchange activity. The vesicles accumulated a total of 20 nmol/mg protein of Ca^{2+} when diluted 50-fold into 160 mM KCl containing 13 μM $^{45}CaCl_2$; Ca accumulation was blocked by external NaCl or by treating the vesicles with the Na-ionophore monensin. These results indicate that the vesicles exhibit Na-Ca exchange activity. The initial rate of Ca^{2+} uptake was stimulated by the K-ionophore valinomycin (0.5 μM), suggesting that the brine shrimp exchange system is electrogenic. K_m and V_{max} values for exchange activity were approximately 20 μM and 13 nmol/mg protein·sec respectively. The specific activities of Na-Ca exchange in vesicles obtained at various intervals after hatching were 1.1, 2.8 and 3.4 nmol/mg protein·sec at 1.5, 6 and 12 through 48 hr, respectively. The results suggest that brine shrimp will provide a useful model for studying the biosynthesis of the Na-Ca exchanger.

M-Pos209 PARTIAL PURIFICATION OF THE SODIUM-CALCIUM EXCHANGER FROM BOVINE CARDIAC SARCOLEMMAL MEMBRANES. John T. Durkin, Diane C. Ahrens and John P. Reeves, Roche Institute of Molecular Biology, Roche Research Center, Nutley NJ 07110 USA

The binding of Na-Ca exchange activity to lectin columns is highly dependent on the choice and concentration of the detergent used for solubilization. This property was exploited in the following study. Cardiac sarcolemmal vesicles were solubilized in 4% cholate/0.5 M NaCl/2 mg/ml soybean phospholipids (Asolectin) and the extract was applied to a wheat germ agglutinin-Sepharose 6MB column. Approximately 70% of the Na-Ca exchange activity bound to the column. A small fraction of the bound glycoproteins could be eluted from the column by changing the detergent to 0.3% polyoxyethylene-9-lauryl ether in 30 mM NaCl/20% (v/v) glycerol; this fraction also contained approximately 25% of the original Na-Ca exchange activity. Exchange activity was enriched 15-20 fold compared to control proteoliposomes reconstituted from the original extract; specific activities of 150-200 nmol/mg protein·sec were obtained. Application of 0.25 M N-acetylglucosamine eluted additional Na-Ca exchange activity but the specific activity was only 3-4 fold enriched over controls. Further purification of the high specific activity fraction was achieved with ion exchange chromatography by FPLC using a Mono Q column. The pooled active fractions contained several polypeptide bands when examined by PAGE but it was not clear which was the exchange carrier. The results are consistent with site-density estimates (cf. Cheon and Reeves, this meeting) indicating that the exchange carrier is a minor component of the membrane with a high turnover rate.

M-Pos210 SITE DENSITY OF THE SODIUM-CALCIUM EXCHANGE CARRIER IN RECONSTITUTED VESICLES FROM BOVINE CARDIAC SARCOLEMMA. Joo Cheon and John P. Reeves, Dept Biochemistry, Roche Institute of Molecular Biology, Roche Research Center, Nutley NJ 07110 USA.

The site density of the Na-Ca exchanger in bovine cardiac sarcolemma was estimated from measurements of the fraction of reconstituted proteoliposomes exhibiting exchange activity. Sarcolemmal vesicles were solubilized with 1% Triton X-100 in the presence of either 100 mM NaCl or 100 mM KCl; after a 20-40 min. incubation period on ice, sufficient KCl, NaCl, $CaCl_2$ and soybean phospholipids were added to each extract to give final concentrations of 40 mM NaCl, 120 mM KCl, 0.1 mM $CaCl_2$ and 10 mg/ml phospholipid. These mixtures were then reconstituted into proteoliposomes and the rate of $^{45}Ca^{2+}$ isotopic exchange was measured under equilibrium conditions. Control studies showed that Na-Ca exchange activity was completely lost if Na^+ was not present during solubilization. The difference in $^{45}Ca^{2+}$ uptake between vesicles initially solubilized in the presence or absence of NaCl therefore reflected exchange activity and corresponded to 3.1 ± 0.3% of the total $^{45}Ca^{2+}$ uptake by the entire population of vesicles, as measured in the presence of the Ca-ionophore A23187. Assuming that each vesicle with exchange activity contained 1 molecule of the Na-Ca exchange carrier, a site density of 10-20 pmol/mg protein for the exchanger was calculated. The V_{max} for Na-Ca exchange activity in the proteoliposomes was ~20 nmol/mg protein·sec which indicates that the turnover number of the exchange carrier is 1,000 sec^{-1} or more. Thus, the Na-Ca exchanger is a low density, high turnover transport system.

M-Pos211 FURTHER PURIFICATION OF THE Na/Ca EXCHANGER FROM CANINE CARDIAC SARCOLEMMA. Kenneth D. Philipson and Robert Ward (Intr. by J.S. Frank). Depts of Medicine and Physiology and the Cardiovascular Research Laboratories, UCLA School of Medicine, Los Angeles, CA 90024.

We are continuing our attempts to purify the Na/Ca exchange protein from cardiac sarcolemma and have improved our techniques towards this goal. As reported previously, alkaline extraction (BBA (1987) 899,59-66) and wheat germ agglutinin (WGA)-agarose chromatography (Biophys. J. (1987), 51, 177a) are useful steps for enriching Na/Ca exchange activity. We have now also developed conditions for the successful use of DEAE chromatography. Fractionation of solubilized exchange activity on DEAE is detergent dependent, and we obtain different fractionation patterns using octyl glucoside, nonyl glucoside, and decyl maltoside. We enrich Na/Ca exchange activity about 3-fold by alkaline extraction, 4-fold by DEAE chromatography, and 4-fold by WGA chromatography. By using these three procedures in series, we obtain a final fraction containing about 15% of the initial solubilized activity. Final specific activity is about 2 μmol/mg protein/s. On reduced, silver-stained, SDS-PAGE, the more pronounced bands are at 120 and 70 kDa. Proteins of these molecular weights might be associated with Na/Ca exchange activity.

M-Pos212 EXPRESSION OF CARDIAC SARCOLEMMAL Na/Ca EXCHANGE ACTIVITY IN XENOPUS LAEVIS OOCYTES. S. Longoni, M. Coady, T. Ikeda, and K.D. Philipson. Depts of Medicine and Physiology and the Cardiovascular Research Laboratories, UCLA School of Medicine, Los Angeles, CA 90024

Identification of the cardiac sarcolemmal Na/Ca exchange protein has not yet been accomplished. We therefore decided to use X. laevis oocytes to elucidate the molecular nature of this membrane transport system. We present preliminary data that indicates expression of Na_i-dependent Ca uptake in oocytes injected with rabbit heart total mRNA. Injected oocytes were first loaded with Na either by incubation with ouabain (0.5 mM) or nystatin (30 μM). In the latter case, $[Na]_i$ could reach values as high as 80 mM (as measured using ^{22}Na and an internal aqueous volume for the oocytes of 0.5 μl). To then measure Na/Ca exchange activity, the Na-loaded oocytes were incubated for 10 min at room temperature in a solution containing 90 mM KCl or NaCl, 10 μM $^{45}CaCl_2$, 5 mM HEPES, pH 7.5. Following Ca uptake, individual oocytes were assayed for ^{45}Ca content (6-10 oocytes per experiment). Three days after injection, water-injected oocytes showed a net uptake (measured as the uptake in the K-medium minus uptake in the Na-medium) of 0.2±0.1 pmol Ca/oocyte/10 min (n=10, ±S.D.), whereas for mRNA-injected oocytes the net uptake was 1.5±0.5 pmol Ca/oocyte/10 min (n=10). If the Na-load step was omitted, no mRNA-induced activity could be detected. Thus, the induced Ca uptake requires an outwardly directed Na gradient. The mRNA-induced Ca uptake could be stimulated by about 100% if the injected oocytes were treated with chymotrypsin prior to the Ca uptake assay. This is also a characteristic of Na/Ca exchange activity in sarcolemmal vesicles. We tentatively conclude that the cardiac sarcolemmal Na/Ca exchanger has been expressed in X. laevis oocytes. Size fractionation of the mRNA will provide an estimate of the size of the Na/Ca exchange carrier.

M-Pos213 INFLUENCE OF LIPID ENVIRONMENT ON CARDIAC SARCOLEMMAL Na-Ca EXCHANGE AND Na,K-ATPase ACTIVITIES. Ramesh Vemuri and Kenneth D. Philipson, Depts of Medicine and Physiology and Cardiovascular Research Laboratories, UCLA School of Medicine, Los Angeles, CA 90024.

We have previously demonstrated a requirement of specific anionic phospholipids (PL) (e.g., phosphatidylserine (PS), cardiolipin (Clp), phosphatidic acid) and cholesterol for obtaining optimal Na-Ca exchange activity in reconstituted sarcolemmal vesicles (Vemuri, R. and Philipson, K.D., BBA, in press). We have now reconstituted sarcolemma using various cholesterol analogues (with modifications in the hydroxyl group, side chain, or ring structure). When the reconstitution mixture was phosphatidylcholine (PC):PS:sterol (30%:50%:20% by weight), optimal Na-Ca exchange activity could be obtained with cholesterol and campesterol (17.4 and 19.2 nmoles/mg/s, respectively), while use of several other sterols resulted in little or no activity. Thus, there are strict structural requirements for those sterols which will support exchange activity in reconstituted vesicles. However, when the solubilized sarcolemma is reconstituted into vesicles containing Clp instead of PS, the requirement for cholesterol largely disappears. High exchange activity can be obtained in PC:Clp proteoliposomes in the presence or absence of sterols.

We have also examined the lipid requirements of the sarcolemmal Na,K-ATPase after solubilization and reconstitution. Again we find specific PL and sterol requirements, but these requirements are different from those of the Na-Ca exchanger. The highest Na,K-ATPase is found in vesicles containing PE, Clp or PI. There is no absolute requirement for an anionic PL as with the exchanger. Na,K-ATPase activity also requires the presence of specific sterols with cholesterol, dehydrocholesterol, and dihydrocholesterol providing optimal environments.

M-Pos214 MEMBRANE POTENTIAL IN THE RECONSTITUTED NAK-ATPASE PROTEOLIPOSOMES. Atsunobu Yoda and Shizuko Yoda, Department of Pharmacology, University of Wisconsin Medical School, 1300 University Avenue, Madison, WI 53706

The NaK-pump is electrogenic. However, the absolute potential levels measured in most experiments using animal cells were below 100 mV, lower than the expected equilibrium potential of 200-240 mV. Recently, Karlish et al. [J. Physiol. (1987) in press] reported that the Na-K exchange generated potentials of up to 200 mV in phospholipid vesicles reconstituted with pig kidney NaK-ATPase, but the Na-Na exchange generated much less potential. We measured the electrogenic potentials of the Na-Na exchange in cholesterol-containing egg phospholipid vesicles reconstituted with electric eel NaK-ATPase (PL) using the method of Karlish et al. ATP activated the Na^+-uptake on the inside-out oriented pumps and generated a potential with positive charge inside. ATP also increased the adsorption of the anionic dye, Oxonol VI, into the lipid bilayer. The potential was calculated from this absorption change measured at 620 nm using the diffusion potential due to the Na^+-ionophore "Hemi-Na^+" as a calibration standard. The ATP-dependent membrane potential of the PL with an extracellular medium of 100 mM NaCl built up to 100 mV, even in the absence of K^+ on both sides. Exhaustion of ATP during the reaction with hexokinase and glucose stopped the potential buildup. Digitoxigenin inhibited not only this buildup of potential but also caused the potential to decrease without Na^+ leakage. (Supported by NIH Grant HL16549)